

DEVELOPMENT OF ROTATION MECHANISM FOR
BEAM-STEERING ANTENNA

JASEM ALSABE

Bachelor of Engineering
Mechanical Engineering Major



Department of Electronic Engineering
Macquarie University

July 14, 2017

Supervisor: Dr. Nazmul Huda



ACKNOWLEDGMENTS

I would like to give my thanks to all of the people who have assisted me in completing this thesis research. Thank you to Dr. Nazmul, for supervising my work and his helpful conceptual suggestions. Dr. Muhammad Afzal, for his guidance and the valuable information he has provided me with the antenna system. Dr. David Inglis, for the electronic work supervising. Finally, my father, who is a mechanical engineer and has encourage me to have a better work results and provided me with invaluable suggestions.

STATEMENT OF CANDIDATE

I, Jasem Alsabe, declare that this report, submitted as part of the requirement for the award of Bachelor of Engineering in the Department of Engineering, Macquarie University, is entirely my own work unless otherwise referenced or acknowledged. This document has not been submitted for qualification or assessment at any academic institution.

Student's Name: Jasem Alsabe

Student's Signature: Jasem Alsabe

Date: April 12, 2017

ABSTRACT

During the last thirty years, antenna application technology has significantly improved. Advances in antenna technology has allowed for an increased reception range for both the internet and mobile phones. Macquarie University has invented a new class of planner high-gain antennas as a solution to get a more efficient mobile phone reception and internet connectivity. The antenna accomplishes this goal by gaining satellite radiation waves at any region on the ground, on water or even in the atmosphere. This type of planner antenna requires a beam steering system to be rotated and aligned in a specific direction, this ensure efficient functionality. In addition, this rotation system requires speed and accuracy to track the satellite radiation waves. Many researchers developed the antenna control systems using a range of different methods to track the signal resource. This thesis presents the control system development within Macquarie's antenna planners. The system development began with four designs. These were produced after examining several antenna mechanism research studies and improved upon by utilising these studies to produce a flexible system free of systemic error. The implementation of worm gears and roller methods to the mechanism are introduced to improve the way the antenna performs. This specific development method is not used in any normal antenna control systems and has been designed especially for Macquarie Universities antenna planner system. The simulation and outcome results show that the methods have eliminates any systemic errors and have been shown to improve the overall performance of the mechanism.

Contents

ACKNOWLEDGMENTS	i
STATEMENT OF CANDIDATE	iii
ABSTRACT	v
List of Figures	xi
List of Tables	xiv
Chapter 1	1
Introduction and Background	1
1.1 Project Goal	3
1.2.1 Scope	4
1.2.2 Time	4
1.2.3 Cost	5
Chapter 2	6
2.1 Existing Rotation System Design	6
2.1.1 Design Principle	6
2.1.2 Function of Units	7
2.1.3 Material Selection	8
2.1.4 Systematic Errors	9
2.1.5 Discussion	9
2.2 Reducing Antenna Positioning Error Research Study	9
2.2.1 Positioning an Antenna System Design	10
2.2.2 Discussion	10
2.3 A Cryogenic Rotation System	11
2.3.1 Mechansim	11
2.3.2 Discussion	12
2.4 Wood Thrust Flat Bearing	12
2.4.1 Discussion	14
2.5 Overview in The Development of Antenna Control System	14
2.5.1 Positioning Antenna Based on Orthogonal Filter	14
2.5.2 Poisoning Using FLC and PID Controllers	15
2.5.3 Full Remote Controlled Positioning	16
Chapter 3	17
3.1 Planner Holder	17
3.2 Gears	17
3.3 Bearings	18

3.4 Rollers	18
3.5 Motors	18
3.6 Microcontroller	18
3.7 Power Source	19
3.8 Shield	19
Chapter 4	20
Concept Development.....	20
4.1 First Concept.....	20
4.2 Second Concept.....	21
4.3 Final Concept.....	22
4.4 Concept Testing.....	24
4.4.1 Rotating Speed Rate Speed.....	24
4.4.2 Friction Test	24
4.4.3 Supplier Test	25
4.5 Final Concept Specifications	26
Chapter 5	27
Engineering Analysis	27
5.1 Bearing Cage.....	27
5.1.1 Rolling Element.....	28
5.1.2 Cage	28
5.1.3 Raceway.....	30
5.1.4 Specifications	31
5.2 Driving Gear	31
5.2.1 Worm Screw Calculations	32
5.2.2 Driving Gear Shaft.....	33
5.3 Driven Planner Antenna Holder Gear	35
5.3.1 Gear Material	35
5.3.2 Tooth Calculation	36
5.3.3 Top and Bottom Driven Gears	38
5.4 Motor Holder.....	38
5.5 Bearing Point.....	39
5.6 Micro-controller	39
5.7 Guard.....	40
Chapter 6	41
Prototyping and Fabrication	41
6.1 3D Printing	41
6.1.1 Bearing Cage	42

6.1.2 Shaft Holder	43
6.1.3 Motor Holder	45
6.2 Workshop Manufacturing	47
6.2.1 Driving Worm Screw	47
6.2.2 Driven Gear	51
6.2.3 Bearing Point.....	58
6.2.4 Shaft	60
6.2.5 Coupling.....	62
6.2.6 Guard	67
Chapter 7	68
Testing and Refinement	68
7.1 3D Printer Dimension Issue	68
7.2 Bearing Cage Dimension Issue	71
7.3 Complete System Testing.....	71
Chapter 8	75
Discussion.....	75
8.1 Achievements.....	76
8.1 Costs	77
Chapter 9	78
Conclusions	78
9.1 Review	78
9.2 Future Work.....	78
9.2.1 Feedback System.....	79
9.2.2 Accurate Angle Rotation	79
9.2.3 Stability	79
9.2.4 Guard.....	80
Appendix A	81
Appendix B	82
Appendix C	83
Appendix D	84
Appendix E	85
Appendix F	86
Appendix G	87
Appendix H	88
Appendix I	89
Appendix J	90
Appendix K	91

Appendix L.....	92
References.....	93

List of Figures

Figure 1:Top and front view of Macquarie university antenna planner [6].	2
Figure 2:Block diagram explain the general functionality of the antenna system [7].	2
Figure 3:Overall view for the existing control system [8].	3
Figure 4:The existing control system design [8].	6
Figure 5:Front view of gears [8].	7
Figure 6:Top view of the antenna shows the magnetic parts within [8].	7
Figure 7: CAD drawing of the existing control system [8].	8
Figure 8: Positioning control system design that operates using an input potentiometer [9].	10
Figure 9: Positioning plan of the antenna [9].	10
Figure 10: Cryogenic half-wave plate rotation system [10].	11
Figure 11: CAD drawing that illustrates the cytogetic half-wave plate rotation system [10].	12
Figure 12: An example of the wood thrust ball bearing experiment [11].	13
Figure 13: Example of the wood thrust bearing experiment using small sized balls [11].	13
Figure 14: The overall control system showing the two different gears axes [12].	15
Figure 15: Diagram explains the positioning system by FLC and PID [13].	16
Figure 16: Rotation of elevation, polarisation, and azimuth axes [17].	16
Figure 17: First concept design.	20
Figure 18: Second design concept.	21
Figure 19: Front view for the second design concept.	22
Figure 20: Final concept design.	22
Figure 21: View for the final concept design shows the bearings and the bottom groove.	23
Figure 22: View for the final concept design shows the gearing system.	23
Figure 23: Dynamically testing the final concept in an initial prototype.	25
Figure 24: Complete mechanism design for the next generation of Macquarie antenna application.	27
Figure 25: Ceramic bearing ball [18].	28
Figure 26: Cage design.	29
Figure 27: The designed cage bore dimension.	29
Figure 28: The cage support part for positioning the height.	30
Figure 29: Worm screw parameter [20].	32
Figure 30: A drawing clarify the centroid of worm gearing system [22].	33
Figure 31: Shows the hollow design pin and how does it fit [23].	34
Figure 32: Highlighting the helical tooth parameter [24].	36
Figure 33: A sample of spun measurement over (K) 3 teeth by using a special tool [27].	37
Figure 34: Bottom driven gear.	38
Figure 35: Shows the power provider for the driver board.	39
Figure 36: Manufacturing drawing of the bearing cage.	42
Figure 37: Printing the bearing by 3D printing.	43
Figure 38: Manufacturing drawing for the bottom gear shaft holder.	43
Figure 39: Manufacturing drawing for the top gear shaft holder.	44
Figure 40: Handle tap.	44
Figure 41: Manufacturing drawing for the bottom gear motor holder.	45

Figure 42: Manufacturing drawing for the top gear motor holder.	46
Figure 43: Printing the supported parts by a 3D printer.	46
Figure 44: Manufacturing drawing of the worm gear.	47
Figure 45: Cutting the rod to 27.5mm diameter by turning machine with a three jaw chock.	48
Figure 46: Measuring the rod diameter by using vernier tooling.	49
Figure 47: Measuring a single screw wheel teeth by a tooth vernier tool.	49
Figure 48: Screw wheel tooth cutting by a threaded milling machining.	50
Figure 49: Manufacturing drawing for the driven gears.	51
Figure 50: Fixing the Acetal disk in the turning machine by using 8 jaws chock.	52
Figure 51: Measuring after each turning cut is very important using the vernier tool.	52
Figure 52: Grounding a special tool cutter with a radius of 4.8mm.	53
Figure 53: Fixing the disk to the centre using the dia indicator tool.	53
Figure 54: Setting the hobbing machine index.	54
Figure 55: Two disk are mounted in in the hobbing machine between loads and the cutter hub is behind them.	55
Figure 56: Marking the cutting dimensions by a height gage.	56
Figure 57: Cutting the gear square hole gradually in a small depth.	57
Figure 58: Driven gear tooth shape while cutting them in the hobbing machine.	57
Figure 59: Manufacturing drawing for the bearing point.	58
Figure 60: Putting some bearing balls and taking the heights measurement.	58
Figure 61: Fitting the deep groove bearing between the circlips.	59
Figure 62: Bearing points after machining them.	59
Figure 63: Manufacturing drawing of the shaft.	60
Figure 64: Final shape for the shaft after machining it.	61
Figure 65: Fixing the roller pin in the worm wheel shaft.	61
Figure 66: Manufacturing drawing of the motor shaft coupling part.	62
Figure 67: Manufacturing drawing of the shaft coupling part.	63
Figure 68: The coupling parts shape after lathe machining.	64
Figure 69: Measuring the drill bit by a micrometer to drill an accurate hole size.	64
Figure 70: Drilling the pin holes by fixing the coupling with three jaws.	65
Figure 71: Grounding the pin head to avoid crashing it with the supported components.	65
Figure 72: Fixing the grub screw in the small coupling parts.	66
Figure 73: Manufacturing drawing for the guard.	67
Figure 74: Macquarie University 3D printer.	68
Figure 75: Drilling a hole to host the shaft, in the left side the parting cut off tool.	69
Figure 76: Cutting the supporting parts by a high speed lathe cutter.	70
Figure 77: Supporting shaft parts after machining them.	70
Figure 78: Fixing the motor with the small coupling in the housing part.	71
Figure 79: Fixing the shaft and the large coupling in theirs housing parts.	72
Figure 80: Measuring and marking the drilling spots.	72
Figure 81: Overall view for the complete system.	74

List of Tables

Table 1: Gantt Chart, showing the project timeline.	4
Table 2: Predicted costs for project.	5
Table 3: Designed bearing specifications.	31
Table 4: Total project cost.	77

Chapter 1

Introduction and Background

The internet has become a fixture in our daily lives. It has become prominent within our lifestyle because of the valuable facilities it provides, including a means of communication, social attributes, research abilities, entertainment and so on [1]. There are many electronic devices that enable us to be able to connect to the internet. However, these electronics require an internet provider to have an internet connectivity.

The development and improvement of communication systems have dramatically increased over the last few decades. As a result of this development, many people from all over the world are able to access the internet. This is due to the improvement of network connections which are delivered to a range of devices either through underground internet cables or through reception towers [2].

However, there are some regions where engineers are still trying to find a better solution to provide a better connectivity. An example of these regions includes; on the ground, there remain some areas where hunters are unable to establish an internet connection due to their location not having any underground internet cables. Certain locations are also hard to access and so reception coverage towers are harder to construct. Another example is on water, people such as commercial fishermen or sailors are sailing distances were already established coverage zones are unable to be accessed. A final example is in the atmosphere, where plane passengers who are traveling for long periods may be out of reach of reception [1].

Engineers have worked for a long time trying to solve these problems. They currently use the satellite antenna connection system as the best solution to cover these global regions. The military was the first to benefit from the smart antenna machine which is connected directly to the satellite and provides the internet connectivity [3].

In 2010 this smart antenna was introduced into a commercial stream by Gogo company. Gogo has an established partnership with around 17 major airlines, these airlines benefited the most from the smart antenna. In that time, the internet has been provided to flight passengers with a speed up to 1Mbps [4]. Today the developed antenna provides a speed up to 10Mbps and engineers are developing the next generation which will be able to provide a speed of up to 200Mbps on aircraft, ships or anywhere on the ground. Recently in March 2017, Virgin airline bought the Gogo antenna service and is now Australia's second airline to have the functionality, after QANTAS who already provides passengers with an inflight

Internet [5].

Antenna technology has been developed for a long time and different types generated. The first antenna system was called a Gimbaled antenna. This antenna is made up of three axes controlled by a stepper motor. However, its disadvantage was its large size. The next generation was the ESA system which consists of a fixed magic flat planner. This flat planner doesn't require any motors to control it, but it fails to provide sufficient tracking. The last generation is the VICTS which consists of the same flat antenna planner with a motor control system to improve its tracking requirements [4].

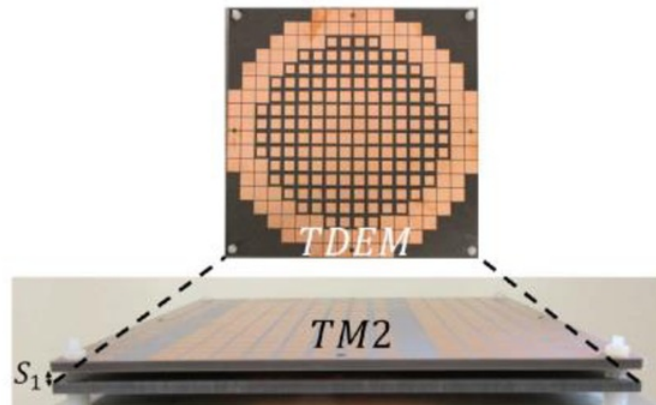


Figure 1: Top and front view of Macquarie university antenna planner [6].

In 2016, Macquarie University developed a revolutionary antenna technology and demonstrated a new high-gain antenna similar to the VICTS [6]. It is made up of two planner plates as shown in the above figure. These require a mechanical control system to serve as a rotation to the antennas planner. Each planner needs to be able to rotate independently.

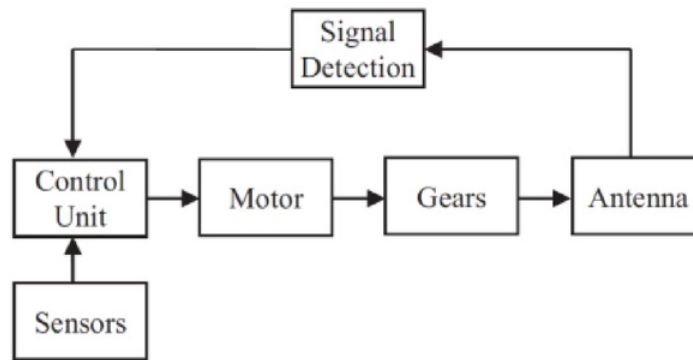


Figure 2: Block diagram explaining the general functionality of the antenna system [7].

The above block diagram explains the general functionality of the antenna system [7]. Starting with the sensor which sends and receives the satellite radiation waves. The control unit, which controls the motors to rotate the antenna by gears. The antenna planner, which

is the platform between the satellite and the sensor. Its function is improving transmitting these satellite radiation waves.

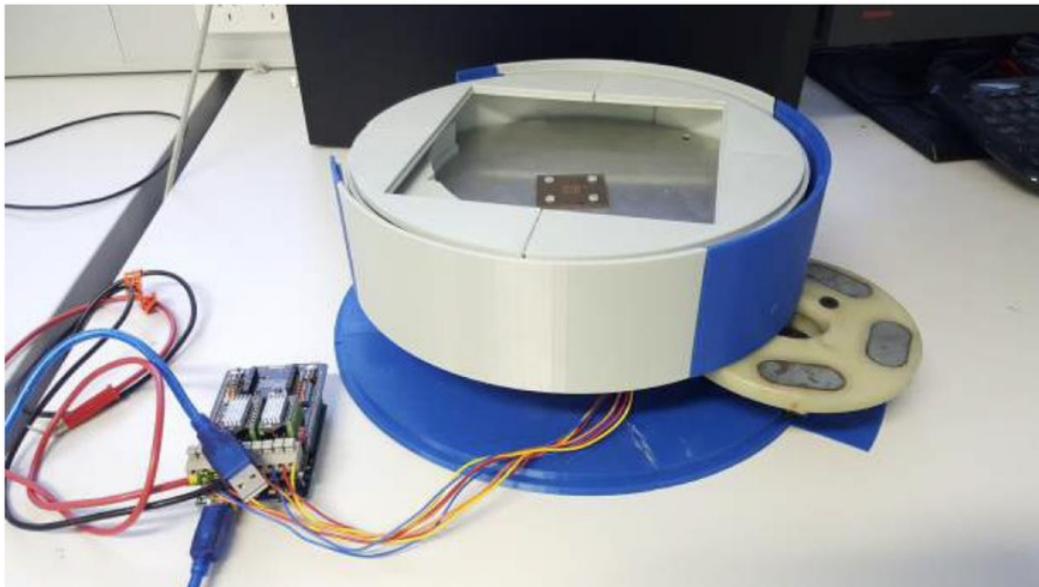


Figure 3: Overall view for the existing control system [8].

The above figure is for the existing control system which was made in 2016 [8]. The system designed to rotate the antenna planner in a magnetic method. However, the mechanism has experienced some issues and the university in the process of resolving these issues and coming up with an updated version which is expected to be done in this research thesis [8].

1.1 Project Goal

The aim of this project is to design a control system that will enable the rotation of two antenna plates. Macquarie's antenna planners are designed to be fitted horizontally and require a control unit which enables them to be able to rotate up to 360° . To operate, the antenna planner requires a control unit to steer its beam, permitting it to track the satellite radiation waves while in motion [6]. To design the control system, a plan is made to organize the work which will lead to the achievement of this goal.

1.2 Project Planning

Providing a success plan helps to ensure efficient and effective planning for a successful project. In project management, planning is an important stage, especially in any engineering related project. In this project, three parameters are considered in planning, these are scope, time and cost.

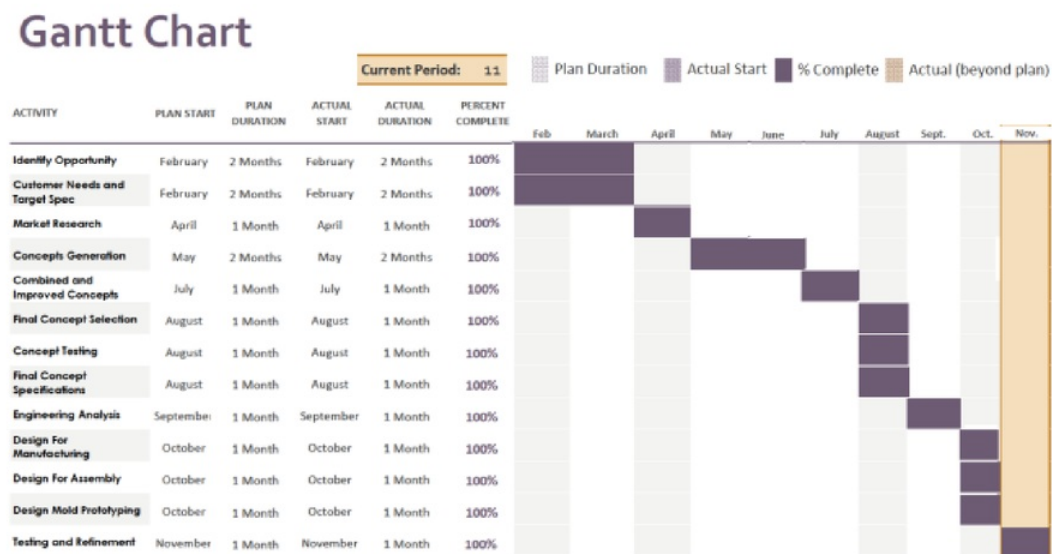
1.2.1 Scope

The general scope was stated in the first section 1.1. The following dot points specify this project design scope:

- To optimise the existing magnetic rotation design.
- To develop the accuracy of antenna plates steering or rotating angles with the desired speed rate.
- To design a low profile system, as it is important to consider the thickness in this particular antenna application.
- To choose the appropriate materials which will be able to resist environmental impacts.
- To make sure nothing jams between the sensor head and the antenna planner.
- Using insulators or non-magnetic elements as much as possible, especially around the planner as they affect the radiation waves transmission.
- To be able to operate the system vertically and horizontally, as this antenna application will experience motion.

1.2.2 Time

Table 1: Gantt Chart showing the project timeline.



To achieve the specified goal and make sure the project will be completed on time, a project management study was made earlier this year. The study was supervised and approved by Dr. Nazmul Huda. The result of this planning is provided in the above updated Gantt chart in Table 1.

The project was launched at the beginning of the year (2017) as the above timeline indicates and it is planned to be completed by the end of the year. The work is divided into four stages consisting of:

1. Planning (February–April): by identifying the opportunity, customers' needs, target specifications and market research.
2. Concept Development (May–August): by designs or concepts generation, combine and improvement, final concept selection, concept testing and final concept specifications.
3. Detail Design (September–October): by doing an engineering analysis, design for manufacturing, design for assembly and design mould prototyping.
4. Testing and Refinement (November): by testing the prototype and refine it if required.

1.2.3 Cost

Minimising the cost is a challenge for the engineers as they need to keep the level of quality while they are saving some budget. The estimated budget for this project is given in the following table.

Table 2: Predicted costs for project.

Antenna driven and driving gears	\$200
Battery	\$150
Thrust ball bearings	\$80
Stepper motors	\$60
Shield	\$40
Dual microcontroller	\$20
Bolts and nuts	\$0
Total estimate	\$550

Chapter 2

Related Work

To have a better-constructed methodology and approach, reviewing applications in the same antenna area will be useful for this project. Reviewing and studying similar applications will provide a better understanding of the concept. This leads to the proposed approach. As the antenna application designs are not published for copyright reasons, the studies made on similar mechanical rotation systems or components and established based on Macquarie antenna control system needs.

2.1 Existing Rotation System Design

The main requirement of this research thesis was to focus on optimising the existing Macquarie rotation system. It is fortunate that there is an existing design to base the study on, enabling the ability to explore its already experienced issues and find a solution for these issues.

2.1.1 Design Principle

Macquarie's existing rotation system project was launched in the beginning of 2016 by a mechanical engineering student. The product was completed by the end of that year. The system consisted of a new rotary method in the antenna field. This method included rotating the antenna planners by magnetic gears.

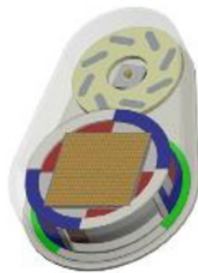


Figure 4: The existing control system design [8].

The design consists of two circular holders [8]. These hold the antenna planner in place. At the base, there are two stepper motors fixed vertically. One of the motors is connected directly with the top inner holder plate whilst the other motor is connected with the outer magnetic driving gear as its shown in right side of the below figure 5.

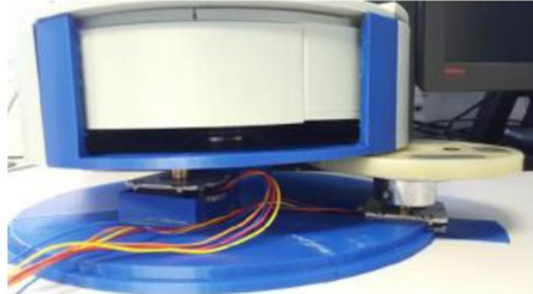


Figure 5: Front view of gears [8].

Inside the outer magnetic driving gear located at the right side, there are a couple of magnetic parts. By driving this gear, it will rotate the inner bottom antenna planner, which is matching the outer magnetic driving gear with magnetic parts as it is shown in the below figure.

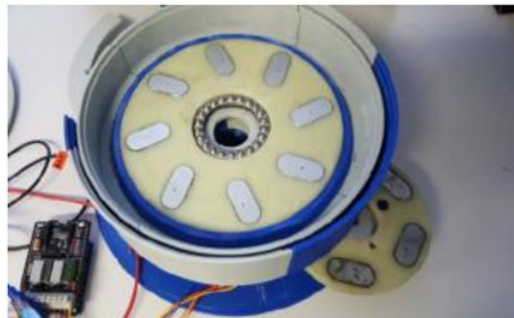


Figure 6: Top view of the antenna shows the magnetic parts within [8].

From here, the motors can rotate each antenna planner independently. The reason for choosing this magnetic rotating method is to be able to operate and rotate the antenna planner with less noise and less vibration.

2.1.2 Function of Units

This section describes each function of the existing design and provides a clear picture of the system operation. The system functions include:

- Two stepper motors: These are fixed vertically within the bottom of the product. One will control the top inner antenna holder whilst the second motor will control the outer magnetic driving gear.

- Two thrust ball bearings: Are fixed in the centre of the driving and driven magnetic gears. The bearing function is required to reduce the friction and hold the axial loads.
- Two antenna holders: the first one holds the top antenna planner while the second one holds the bottom antenna planner.
- A shield: around the antenna holders to protect them from slipping horizontally.

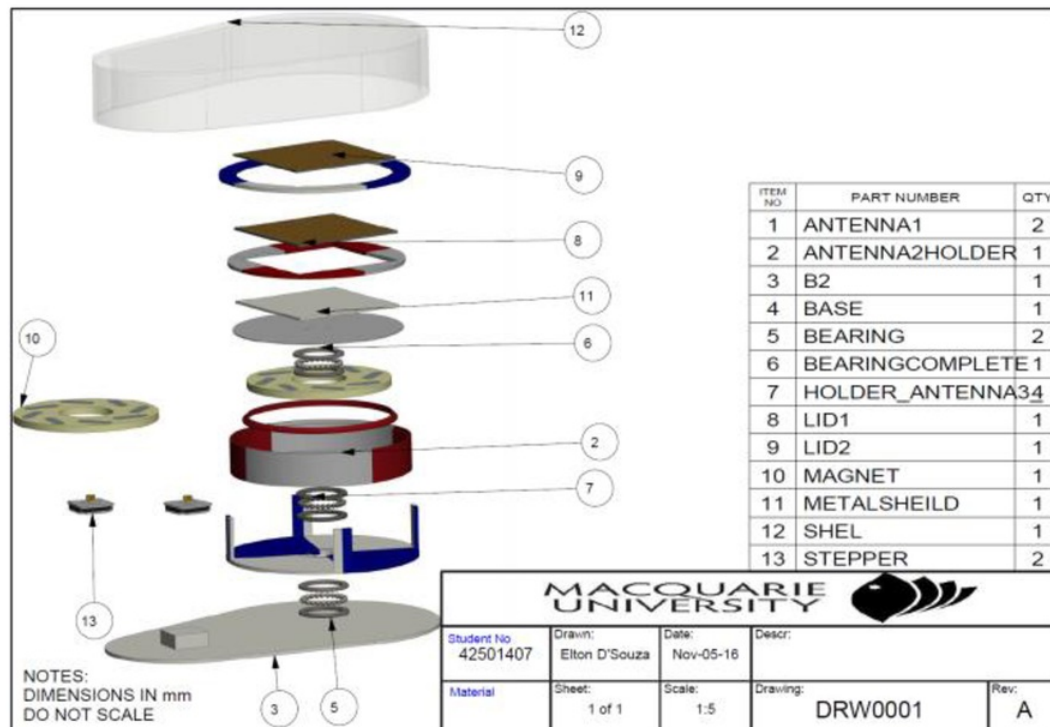


Figure 7: CAD drawing of the existing control system [8].

2.1.3 Material Selection

The chosen materials for this design are:

- Shield and planner holders: both are made of PLA and ABS plastic. These materials are classified as thermoplastic and are very common materials in 3D printing which has been used for this design.
- Thrust ball bearing: metal was the chosen material for the thrust bearing which is fixed in the centre of both inlet and outlet gears.
- Gears: the same metal material used for the thrust bearing.
- Loctite Gel: was used to merge the printed parts together. This is due to the 3D printer being unable to print the whole part.

2.1.4 Systematic Errors

After prototyping the existing rotation system, it was discovered that it had experienced some issues. These issues limited the system operation. These issues include:

- The magnet between the driving gears had a strong magnetic attraction. This led to driving within the metal bearings. As a result of that, the antenna planners was not driven independently as the system requires.
- Due to the above-mentioned issue, the desired rotation speed rate and accuracy were not obtainable.
- The system was designed to operate in a vertical direction only. This is an issue as a main requirement of the antenna application is to be able to operate in both vertical and horizontal directions. The reason for this requirement is to enable it to experience motion in both directions whilst it is operating.
- The system observed a high profile and was heavy. The thickness was due to the design and the weight was due to the magnetic components.
- A high friction occurred in the surrounding areas of the antenna planner holders when they were rotating.

2.1.5 Discussion

The designed system can deliver the required rotation and can be considered successful if there is a testing stage in the project plan. The testing stage is critical to resolving and avoiding these types of errors. This testing stage will be carried out for this project in November 2017. This has been previously mentioned in the Gantt chart in section 1.2.2.

The mentioned issues can be resolved by:

- Choosing another rotation method instead of a magnetic one, considering the weight and thickness.
- Choosing appropriate materials for that system, which will provide the desired stiffness without disrupting the other system functions.
- Supply the system with supporting parts to reduce the friction, increase the speed and enable the system to operate in both vertical and horizontal directions.
- These issues and solutions will be taken into consideration to optimise the existing design.

2.2 Reducing Antenna Positioning Error Research Study

In February 2017, a research study was published by A. A. Mulla and P. N. Vasambekar, explaining how to develop antenna rotation positioning. The aim of the study was to reduce the positioning errors which will enable a better signal transmission. The solution was to correct the rotation speed rate. This was done by applying different methods to adjust the desired speed rate for better positioning. This resulted in a better signal transmission [9].

2.2.1 Positioning an Antenna System Design

In mechanical engineering, to rotate an object there are three different common methods. These methods include driving the object by a chain, belt or gear. Each method has its own set of unique properties for different usages depending on the application need.

In this research study, spur gears were selected for the rotation system. This is because the gears were more accurate in rotating and accuracy. These factors play an important role in antenna positioning system. Besides the accuracy, it does have other advantages such as its availability from suppliers. These can be supplied in different standard sizes and at a low cost.

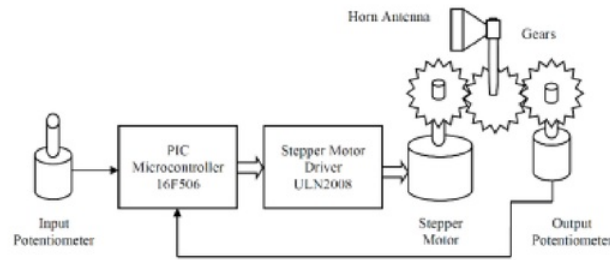


Figure 8: Positioning control system design that operates using an input potentiometer [9].

The above figure shows the positioning control system design that operates using an input potentiometer which sends instructions to the microcontroller. The microcontroller is then able to translate these instructions into the stepper motors, which drive the gears. The gears will also rotate the antenna horn which is fixed in a driven gear. An external power source was used for this system.

2.2.2 Discussion

The experiment followed a procedure of testing the angle and speed from different directions over a number of replicates. The results for reducing the speed rate errors was successfully implemented and developed through this research study. Due to this successful outcome, it was found that the equipment used in this study was suitable for the antenna application and achieved the required rotation accuracy and speed.



Figure 9: Positioning plan of the antenna [9].

It was found that the gears were a good choice for the rotation aspect and could be implemented into our particular study to rotate Macquarie's antenna planner. However, when conducting the research study, the antenna horn was fixed into the driven spur gear in the centre of the gear. Macquarie's planner cannot be fixed from the centre, as this area needs to be clear with no obstructions to ensure efficient transmission.

Another issue in the positioning antenna research was the two driving gears that were fixed through a shaft with motors. The antenna driven gear was fixed from its centre bore with a mounting part.

If a solution was found for these issues, the gears could be used for Macquarie's planner. The solution would need to involve not mounting the antenna driven gear from the centre and leaving the centre clear only for the antenna planner.

The last thing that was noticed with the positioning research study was the gears material consisted of metal. Recall what was stated in the scope of section 1.2.1, conductor or magnetic materials affect the antenna planner transmission. Metals are conductors and cannot be used in the gears driving Macquarie's antenna planner.

2.3 A Cryogenic Rotation System

In January 2016, a review of scientific instruments was published by the American Institute of Physics. The review was about the cryogenic half-wave plate rotation mechanisms. In brief, this rotation system was built to rotate a plate that contains a part which observes a cosmic microwave during a stratospheric balloon flight from the United States in 2015 [10].

The mechanism design approaches were constructed, tested and were found to rotate the plate properly as the system required. The rotation system was designed and reviewed by more than 50 specialized researchers from various mechanical engineering schools. It was made to be operated in motion for an atmospheric environment and to deliver the desired speed rate for the microwave reception. These rotation system requirements are pretty similar to Macquarie's antenna planner rotation system requirements. This citation can be a valuable resource for design development.

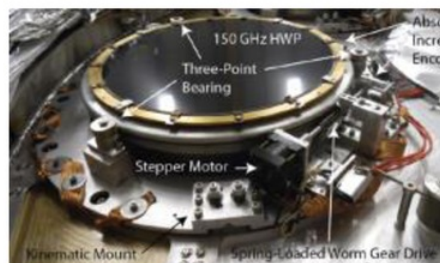


Figure 10: Cryogenic half-wave plate rotation system [10].

2.3.1 Mechansim

As the cryogenic plate is sensitive to microwave receivers, accuracy rotation is the main scope of the system of mechanical approaches. Worm gearing was the solution for the accuracy rotation. The performance of the worm gears enables the return of special helical

teeth shapes. These helical shapes enable the gears to drive with an accuracy that cannot be found in spur gears. It is even more accurate than belt or chain driving methods.

The system used a worm gear which is driven by a stepper motor as shown in the below figure, however, the designers encountered the challenge of matching the driving worm gear with the driven helical teeth. The designers decided that in order to overcome this, they needed to support the system with rollers as is shown in the below figure. The rollers have been placed in symmetric positions around the plate. The function of the rollers is to reduce the friction in the surrounding. In the same time through the rollers, the plate can be positioned. This became the solution for the gears matching challenge.

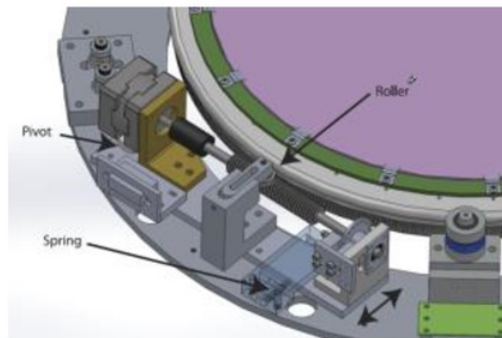


Figure 11: CAD drawing that illustrates the cytogenetic half-wave plate rotation system [10].

2.3.2 Discussion

Worm gears are a good choice for the rotation accuracy. This type of gearing can be used to develop the existing design. Furthermore, rollers play an important role in the system rotation supports. They can be used to reduce the friction, increasing the speed positioning of the plate and even provide overall support to the system enabling it to operate in different directions.

2.4 Wood Thrust Flat Bearing

Ronald Walters is a mechanical engineer with over 20 years of engineering industry experience. He published an article in 2012 about his customised wood thrust flat bearing. The bearing was designed to be rotated by marbles [11]. Ronald experienced the speed rotation rate of different marbles sizes these are shown the in the following figure.



Figure 12: An example of the wood thrust ball bearing experiment [11].

The experiment discovered that the smaller marbles rotate for longer periods of time than the larger marbles. The yellow marble was found to be the smallest and fastest. This marble was then chosen for the designed thrust bearing as the below figure shows. The bearing provided the required effect, of rotating in flexibility and holding the axial load.



Figure 13: Example of the wood thrust bearing experiment using small sized balls [11].

2.4.1 Discussion

Walters customised thrust bearing experiment can be used to develop the existing design. It can be customised if alternate standards were not available and it can be used as a support between the two antenna planner holders. These thrust bearings will work on holding the axial loads, rotate the objects in flexibility, increase the rotation speed and reduce the coefficient of friction. This will result in increasing the system lifetime and qualify it to be the more accurate rotation.

It was found that using marbles made of ceramic material was a good material to use in this project. This is due to the fact that they are an electrical insulator and that their presence will not disrupt the other system elements functionality.

2.5 Overview in The Development of Antenna Control System

In 2016, A.A. Mulla and P.N. Vasambekar published an article reviewing the development of different antenna control systems [7]. The article talks about various systematic errors and the solutions used by the researchers to resolve these errors. The thesis is useful in the way that it provides input in how to improve the knowledge of what an antenna control unit needs to produce a high-quality system.

It is stated that the quality of the antenna is measured by the quality of its signal transmission. To be able to have a better transmission, the control unit that steers the antenna, must be compatible with the antenna transmitter. Size, cost, power, speed, and accuracy are the parameters of the control system. The thesis also outlines some antenna control systems including:

2.5.1 Positioning Antenna Based on Orthogonal Filter

In 2010, S. Nikolic et al. designed an antenna positioning system and applied an orthogonal function into the system [12]. The designers used a new method for the antenna control system based on orthogonal filters. These orthogonal filters were used to determine the electromagnetic field magnitude gradient and steer the antenna based on these factors. It was found that the mechanism of the control system was experienced by the designers and validated in terms of efficiency, speed, and accuracy.

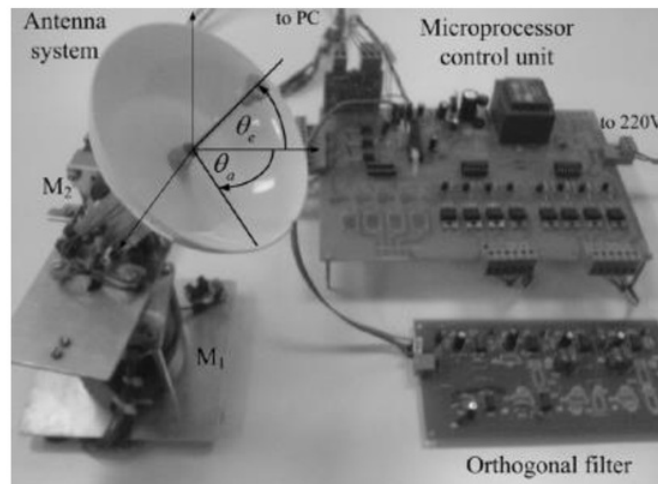


Figure 14: The overall control system showing the two different gears axes [12].

The above figure shows the control system which consists of an orthogonal filter, which can be classified as a sensor, a microcontroller, and two stepper motors. On the left side of the figure, there are the two stepper motors that control the antenna from two axes. The first stepper motor (M1) which is fixed vertically, rotates the flat base that holds the antenna, from the centre and in a horizontal direction from 0 to 360°. While the other stepper motor (M2) which is fixed horizontally, rotates the antenna itself in a vertical direction from 0° to 180° [12].

2.5.2 Poisoning Using FLC and PID Controllers

In 2012, H. Okumus, E. Sahin, and O. Akyazi developed the antenna control system using a fuzzy logic controller (FLC) and proportional integral derivative (PID) [13]. These two controllers were found to improve the antenna transmission. In 2013, the designers had developed their system by supplying it with a self-tuning fuzzy logic controller (STFLC) this greatly improved the transmission. Both of these systems have the same control unit which consists of a potentiometer, power amplifier, motor and gears as shown in the below figure.

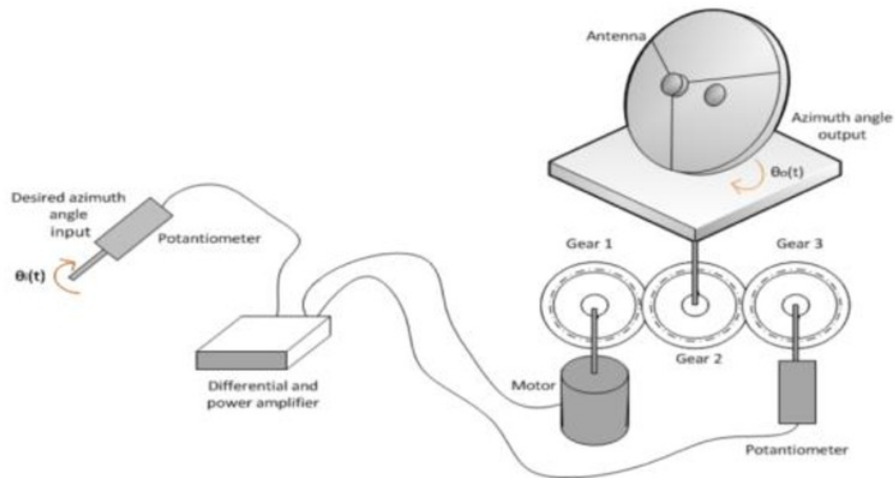


Figure 15: Diagram explains the positioning system by FLC and PID [13].

The potentiometer gives instructions to the amplifier to translate it to the motor. The DC servo motor is used to drive the spur gears and a potentiometer is used to control the driving direction. Three gears were used to be able to control the direction of the antenna [13].

2.5.3 Full Remote Controlled Positioning

In 2015, E. Alhasan and A. Alzubaidi designed a fast antenna control system that enabled the ability to position the antenna beam by a remote controller [14]. It is a challenging issue to steer an antenna beam by a remote. However, the designers developed this system in minimal time and without any difficulties. The system is designed for satellite dish antenna purposes and it consists of a stepper motor that drives the three antenna axes (elevation, polarisation, and azimuth) as the following figure (figure12) shows.

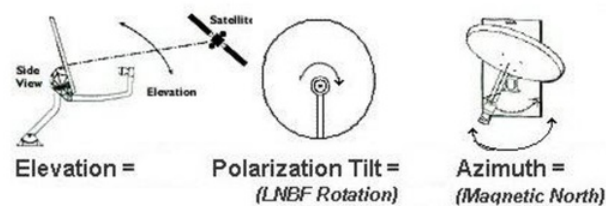


Figure 16: Rotation of elevation, polarisation, and azimuth axes [17].

The results of the system design prove that steering an antenna beam from three different axes can achieve the desired speed by using stepper motors [17].

Chapter 3

Methodology and Approaches

As the literature review in chapter two clarifies, the control system needs to describe the mechanisms of all of the different antenna applications. This review expands the imagination and helps to obtain a solution which reduced complexity.

A solution was obtained after reviewing these different systems. The solution base components are outlined in the following dot points:

- Battery: internal power source.
- Microcontroller: motor controlled by inputs.
- Stepper motors: to drive the gears.
- Gears: to rotate the antenna holders.
- Bearing: to support the rotation system.
- Rollers: to support the antenna holder rotation.
- Shield: a cover to support the system components and protect them.

A complete antenna control system can be built using the above-outlined components. The chosen components can also be used to resolve the existing antenna systemic errors. However, the components need to be in a specific design. This design requires further study. The component functionality is demonstrated in the following subsections. Furthermore, each subsection explains how the design needs to be and clarifies the approaches used to accomplish a successful design.

3.1 Planner Holder

To mount and rotate the antenna planner, a support part required. Therefore, Macquarie's' antenna planner required a holder to be supported.

A holder must be designed in a certain shape that allows us to be able to mount the planner and connect it to the whole part with the driving system. It should also consist of a groove shape for the bearings placement. The preferred shape for the entire holder design is circular, where it can be rotated more accurately than any other shapes.

In designing stage, the holder must be designed first before the other system parts can be. Based on the dimensions and weight of the designed holder, a calculation can be made to determine the required torque. After this step, the gears can be designed.

3.2 Gears

After figuring out the required torque required to rotate the antenna planner holder, gears can be designed to deliver that desired torque [16]. As mentioned in the previous section,

the planner holder has to be the first part of the design, where differences in the designs of the gears deliver a different torque. This is why the required torque must be present before designing the gears.

Gears are the preferred driving method to develop this rotation system. It can be either a worm gearing system or a spur gearing system. Both of these systems deliver the desired rotation, however, the driving gear system needs to be designed to deliver the calculated torque. Through the gears driving system, the antenna planner holder can be directed.

3.3 Bearings

After designing the driving gear system, the total weight of the driving system including the holder part can be calculated. Based on that total weight, the bearing can be designed to support that load.

Thrust ball bearings are the preferred bearing for the planner holders. Thrust bearing functions do not shrink when supporting the axial load, nor do they reduce the friction that may lead to an increase in the rotation speed rate and ultimately, the holders' lifetime. In addition, thrust bearing can be used to support the system so that it can operate in motion and in different horizontal and vertical directions. A thrust bearing would need to be designed in a way that would support the application, enabling it to operate in motion. This design must be studied from different angles to make sure it is free of errors.

3.4 Rollers

Rollers can be designed whenever the driving system is completed. They can be either be standard if this option is available or they can be designed based on the planner holder teeth dimensions.

An important element of the system, and enables the support of the planner holder. This is required as the holder is not mounted like the other parts are. Furthermore, the holder will not be able to rotate freely without the support of the rollers.

3.5 Motors

After designing the holder, driving gears and rollers, the total torque can be calculated. Based on the total torque, the stepper motor, which supplies this torque can be specified. A Stepper motor is the preferred motor to be used in this system. Its function is to serve the gears with the desired torque. Stepper motors have an added advantage of a low cost, low weight and provide a high torque, which is desirable in this instance. The number of motors can be determined based on the designed driving system.

3.6 Microcontroller

A microcontroller can be decided upon after specifying the chosen stepper motor or motors. A microcontroller is an essential part of the system, that monitors the stepper motor. It has

the advantage of being low cost and can be programmed by a several computer software programs such as Arduino. A microcontroller can control the stepper motor by translating its program to the motors.

3.7 Power Source

An internal power source will be used for the system. A battery will be the chosen power source for this project. The power source can be specified after choosing the stepper motor and microcontroller, which requires the chosen power source to be able to operate effectively.

3.8 Shield

The shield is the last part of the system to be designed. The shape of the shield, which consists of a cover and a base, can be designed after planning the entirety of the system. The shield function is to shrink the system components together and to protect them from environmental impacts. The preferred material for a shield is plastic.

Chapter 4

Concept Development

This chapter covers the concept development stage, that branches out to include the concepts generation, combining and improving the concepts, producing the final concept, testing the final concept and setting the final concept specifications. Concepts generation is basically brainstorming a system design that follows an approach to meet the antenna planner system requirements [17][18]. The generated concepts are provided in the following sections 4.1 and 4.2.

After generating the concepts, we considered improving them by combining the concepts features together where possible. From here, the final concept (section 4.3) was produced. This final concept passes a stage of testing which is provided in section 4.4 and finally, the concept specifications are set in section 4.5.

4.1 First Concept

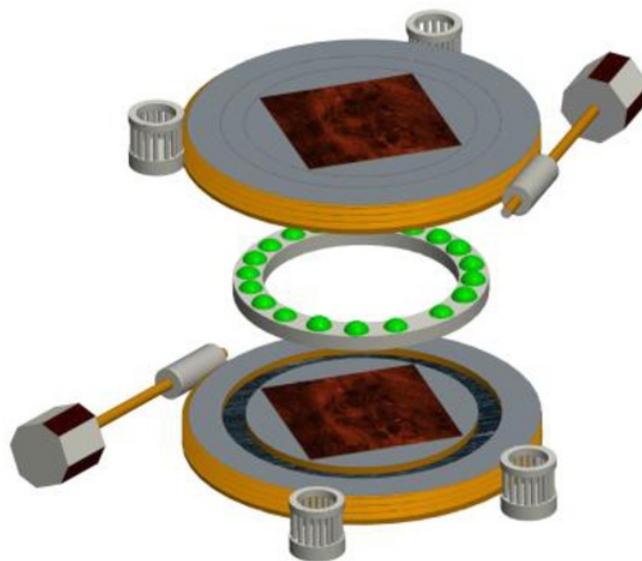


Figure 17: First concept design.

The above figure shows the first system design. The design consists of two circular planar holders that are surrounded by a metallic helical tooth and grooved from both the bottom of the top holder and from the top of the bottom holder. The centre of the holders is designed to mount directly to the antenna planner. Two metallic worm gears are fixed horizontally to drive the holders. In the other side, there are two rollers facing each worm gear and positioned symmetrically. One standard thrust ball bearing has been designed to be positioned between the holders with steel balls. Finally, two stepper motors are used to supply the gears with the desired torque.

After providing the initial design to the supervisor and the co-supervisor, a couple of issues were found in the design. These included:

- The material used for the gearing and ball bearing.
- High amounts of friction.

The first issue was with the chosen materials for the designed gearing. The driving worm gear and the drive holder are both made of metals that are high electrical conductors. The research associates, who are experts in the antenna applications, noted that the design consisting of one ball bearing and gearing will disrupt the antenna transmission function [19][20][21]. The conductor material is designed to not be close to the antenna.

The other issue is friction. Which occurred between the top holder and the shield as well as between the bottom holder and the base. Therefore, another design may be required to resolve these issues.

4.2 Second Concept

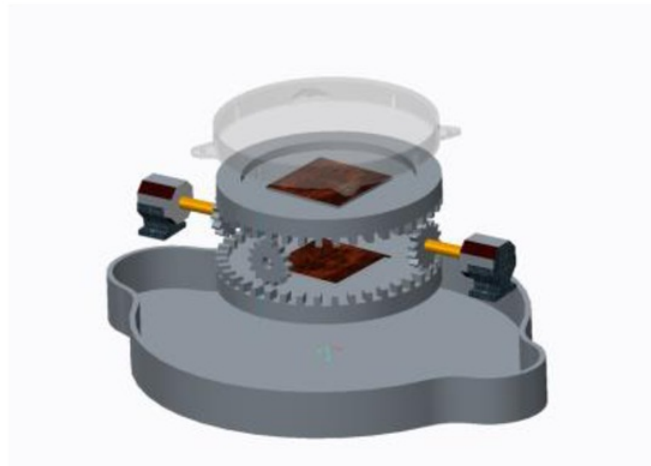


Figure 18: Second design concept.

The second concept, shown in the above figure, is designed in an innovative way. The gearing system, which consists of four spur gears, used to drive two holders that are surrounded with teeth indentations. The gearing idea is designed to drive the system whilst at the same time working as a bearing function. Furthermore, the chosen material for the holder and the gears were insulator plastics. The reason behind the use of a spur gear instead for the worm gear goes back to the helical tooth design difficulty.

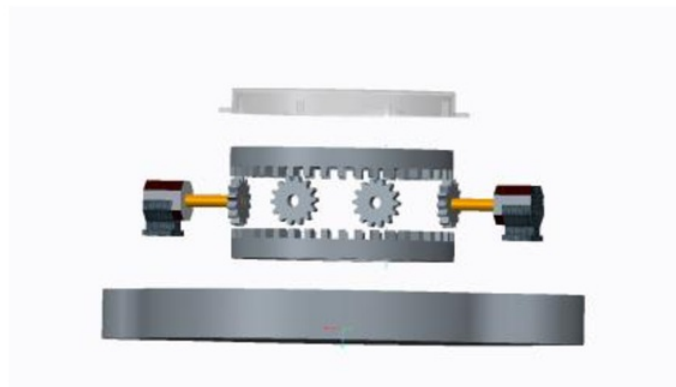


Figure 19: Front view for the second design concept.

The associates noted that there were two major issues in the second concept, including:

- Holders rotation.
- Friction.

The first issue was involved with the holders' rotation. It was found that they could not rotate independently. For example, the designed system cannot rotate the top holder and leave the bottom one fixed in at the same time. The other issue is the same as what was found in the previous concept. The friction issue between the holders and the shield. Therefore, this design still needs to be improved before it can be granted.

4.3 Final Concept

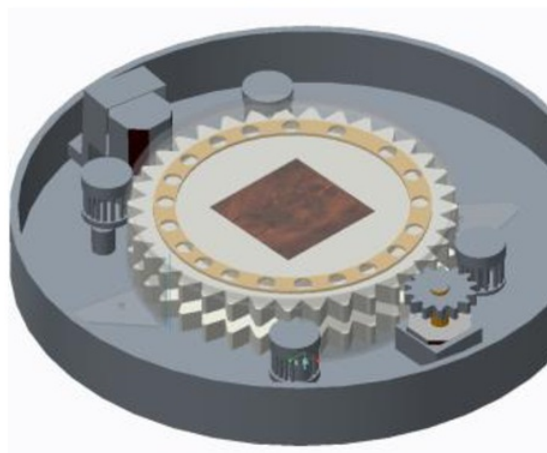


Figure 20: Final concept design.

The final design consisted of two plastic planner holders produced from the centre with a part to mount the antenna planner on. The plastic holders are surrounded with spur tooth

indentations and are grooved from both the bottom and top sides as the following figure shows.

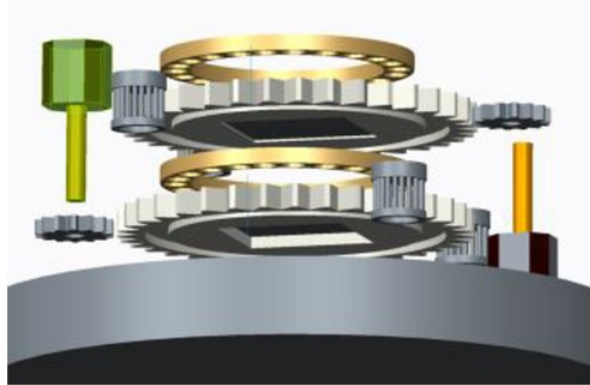


Figure 21: View for the final concept design shows the bearings and the bottom groove.

Three thrust ball bearings support the system and their balls are made of insulating ceramic. One bearing will be between the holders whilst the other bearings will be on the top of the top holder and in the bottom of the bottom holder.

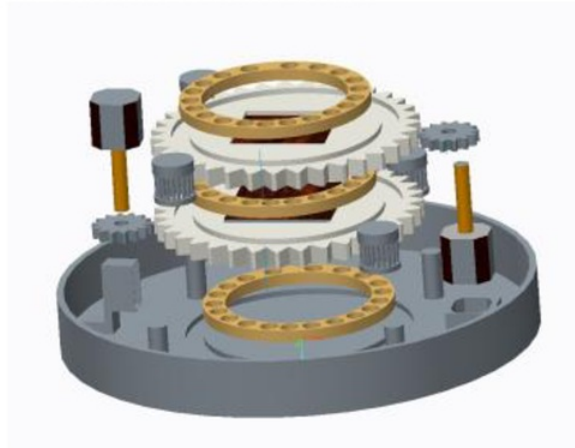


Figure 22: View for the final concept design shows the gearing system.

Each holder is driven by a plastic spur gear. Each driving spur gear is connected vertically with a stepper motor. Two plastic rollers are placed facing each driving gear and positioned in a symmetric fashion.

The two bearings in this concept have solved the friction error which occurred between the holders and the shield. Furthermore, by adding these extra bearings the system can operate in different horizontal and vertical directions. Insulator plastic material has been used to avoid disrupting the antenna transmission function. In addition, plastic gears have the advantage of corrosion resistance, cost-effectiveness, a lightweight and low coefficient of friction [22][23][24][25].

4.4 Concept Testing

The purpose of the testing stage is to determine whether the final concept is ready to use and does what is supposed to, or if it needs to be redesigned. As the only authorized people to supervise the work are the research supervisor and the research associate, the testing stage for this project has been supervised by them.

Producing a system that has been designed based on the idea of operating without crashing, has a higher probability of failure and systemic errors in its overall outcome. Therefore, implementing a test of the design is required before the simulation or analysis stage can be carried out. However, the test will require a detailed and specific input to ensure success [26][27][28].

The design input consists of the dimension of the parts, which controls the system operation, especially the rotation speed rate. The desired speed rate for Macquarie planner antenna system is not less than 180 angular degrees per second. Therefore, the components dimension will be supplied from standard catalogues as a source for the input. Alternative publications on similar projects that have used plastic gears can be called upon as a comparison for what to be expected and how to better the project based on past results.

4.4.1 Rotating Speed Rate Speed

The speed rate measured by the designed planner holder rotation speed. The main role suggests that the planner is the gearing system. If the gears are driving the planner with flexible, accurate and high-speed rotation, then the desired speed rate will be obtained. Speed and accuracy can be obtained if the gear teeth are designed to deliver the desired speed, and the torque supplier is available. However, the chosen material for this gearing design is plastic. This means we need to make sure that the large plastic planner holder can afford to support a high torque and stand for a long lifetime. The limitation of plastic gears relative to the metal gears, can afford a high torque, however, system temperature needs to be taken into consideration in order to reduce the effects on the material. The solution for this issue can be determined by reading the materials data sheet which shows how much the material can resist the temperature [29].

In some research papers, the engineers stated their results when using a plastic based material design [15]. Their results involved the plastic gears operating a basic equation which consisted of the load and some other factors. The paper concluded that by applying the value of the appropriate factors to this equation, the design can consist of a larger plastic gear, which in turn affords a high torque.

From here, the rotating speed rate test can be success, however, there are other elements that affect the rotation flexibility and a friction test is required to be carried out [30][31].

4.4.2 Friction Test

In the designed system, friction probably occurs between the gears and supported rollers, between bearings and the planner groove, and between shield or guard and bearings. A

dynamic test was applied for friction testing [32][33][34]. This has been tested by making an initial prototype for the design [35][36].

Initial design prototype was made by research associate Muhammad Usman. The prototype was fabricated in METS which is located in Macquarie University and are specialized in fabricating and prototyping student projects. The prototype consists of the same idea of two driving gears and two driven gears hold the antenna planner. In addition, the prototype consists of 4 supported gears that are the same as the driving gears, positioned symmetrically and fixed with a grooved bearing in the middle to do the roller function.

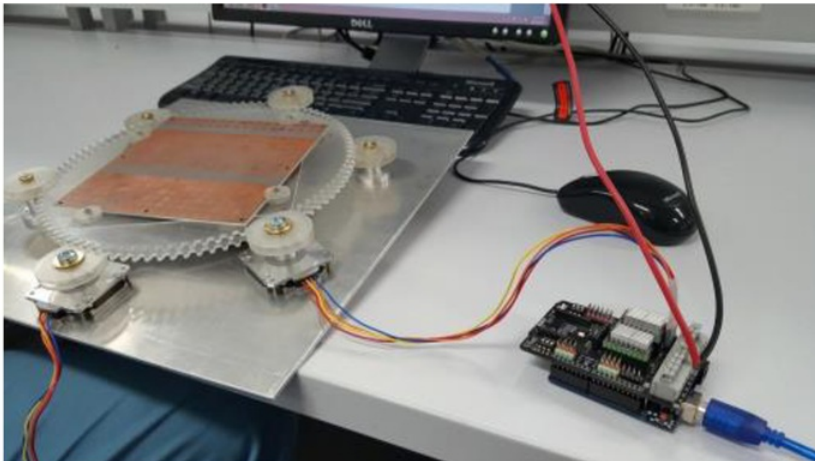


Figure 23: Dynamically testing the final concept in an initial prototype.

The driven planner holder gears were rotating at a speed of $96rpm$, which is rotated 360° per 1.66 second. The speed is positive and the supported roller gears were found to be protecting the driven gears from slipping. However, three errors were noticed and caused noise in the operation. These include:

- The first error was in the gears tooth mesh, which was designed without following the standard spur gear teeth design [37][38]. Therefore, the gears were creating a noise when operating. At the end of the test the tooth was found to be deformed and damaged in a short timeframe.
- The second error was found in the driven gears itself. It was found that they were moving very little whilst operating. The reason for this goes back to the tooth mesh and also to the positioning centroid distance which seems was not accurately calculated [39][40].
- The third error was with the plastic parts which were fixed on each roller and the driving gears to hold the driven gears [41][42]. They were holding the driven gears which are light loads however, they still caused friction and noise.

4.4.3 Supplier Test

Gears need a torque supplier in order to function correctly. In the designed system, a torque is provided to the gears by the stepper motors which are controlled by a microcontroller and supported with an internal power source [43][44]. Stepper motors are available from

suppliers in a range of different varieties, holding a different torque that drives a larger system than the designed one.

Each stepper motor needs a microcontroller and a power source [45]. The stepper motor specifications are provided by the suppliers with the information of the required microcontroller type and the battery voltage [46]. Torque suppliers are available and can supply the gears with the required torque. The previous testing section used the existing design motor and microcontroller which provide a positive speed and they are granted to be used for this research design.

4.5 Final Concept Specifications

Before doing any calculations for the system components, target specifications need to be set. The testing stage clarified the components that needed to be analysed and rectified [47]. The final concept specifications including the needed calculations are summarised in the following dot points:

- Smooth gearing rotation without any noise. Therefore, worm gear will be replacing the spur gear design as they are more gradual engagement teeth in meshing to resolve the occurred noise in the final design initial prototype testing, plus the roller will hold the driven planner gears in an addition parts instead of the tooth itself as it is very complicated to fix a driven spur gear horizontally from its tooth and without any shaft attached in the bore [16].
- Thrust bearing to hold the axial loads and reduce the occurred friction [48].

Chapter 5

Engineering Analysis

An engineering analysis is the part of the project which specializes the engineering project from normal work [49][50]. It is done by a high level of calculations not just gluing and attaching parts which are designed based on an estimated sizes. This chapter covers the engineering analysis which is implanted for each assembly to produce a unique mechanism. The application assemblies are bearing cage, driven planner holder gear, driving gear, motor holder, shaft holder, bearing point and guard or a shield.

The analysis consists a calculation for each assembly dimensions taking in consideration the other assemblies specifications [51][52].

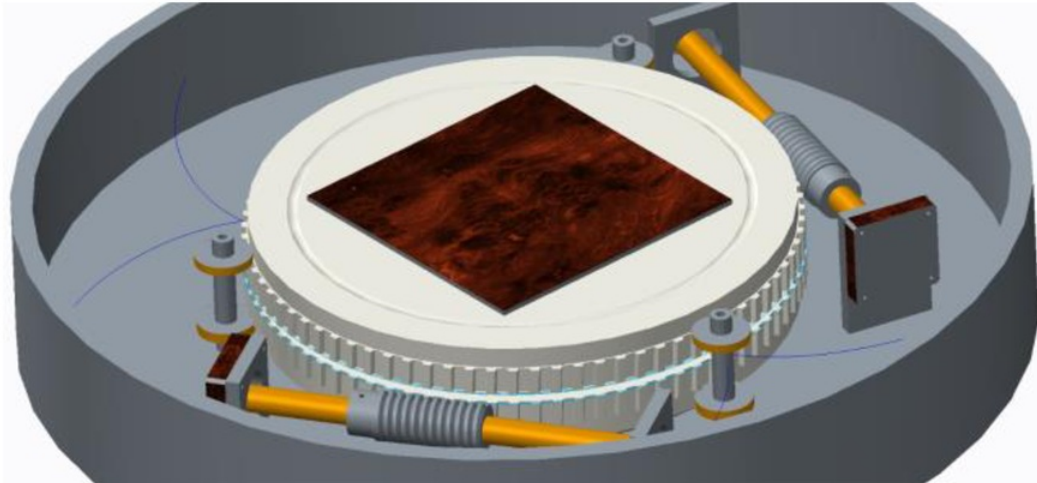


Figure 24: Complete mechanism design for the next generation of Macquarie antenna application.

5.1 Bearing Cage

Recall what was mentioned in the methodology section, the chosen bearing type to hold the axial loads was discovered to be the thrust ball bearing. The standard sizes of large or wide thrust bearings are designed for holding higher loads. The standard size for the inner diameter of which is needed for the system are designed for heavy-duty use and comes with a very heavy weight, thickness and are expensive. Therefore, the only solution is to

design a thrust bearing. Thrust bearings consist of three parts including the rolling element, a cage to hold the elements and raceways [53][54].

5.1.1 Rolling Element

The rolling element for the thrust bearing can be either a ball or roller. Ball bearings are made to carry a lighter weight load than the roller bearings [55][56]. As the loads in this particular antenna application are not heavy, the rolling element balls were chosen. 40 bearing balls were purchased from a VXB supplier as they will be enough to hold the system axial loads. The ball material is Ceramic Si₃N₄ which is non-conductive and does not distribute the antenna radiation. The ball size is 8.731mm and it is considered to be a suitable size to resist the axial loads [57].



Figure 25: Ceramic bearing ball [58].

5.1.2 Cage

The inner diameter of the thrust bearing is 257mm, which requires around 200 balls to operate. As the ceramic balls are expensive, a cage or ring can be used to minimise the number of balls and can still hold the applied axial loads.



Figure 26: Cage design.

The way to design a thrust ball bearing has yet to be published, therefore, a self-study was conducted and the design supervised by an application engineer (George Zeman) who works in SKF which is classified as one of the best global bearing organisations.

The cage material is made from ABS plastic and is a good mix with the ceramic ball. It can operate smoothly with an oil lubrication. ABS plastic material sheet which is attached in appendix A shows the material data. The requirement for a good bearing material is to have a good resistance for the estimated temperature (up to 50°C) which will be experienced during the operation, have a yield strength which can support the applied loads and resist corrosion. The cage consists of an inner diameter of 255mm and outer diameter of 285mm. The cages are rounded with a 1.5 radius. These wide and round dimensions support the cage and make it hard to break.

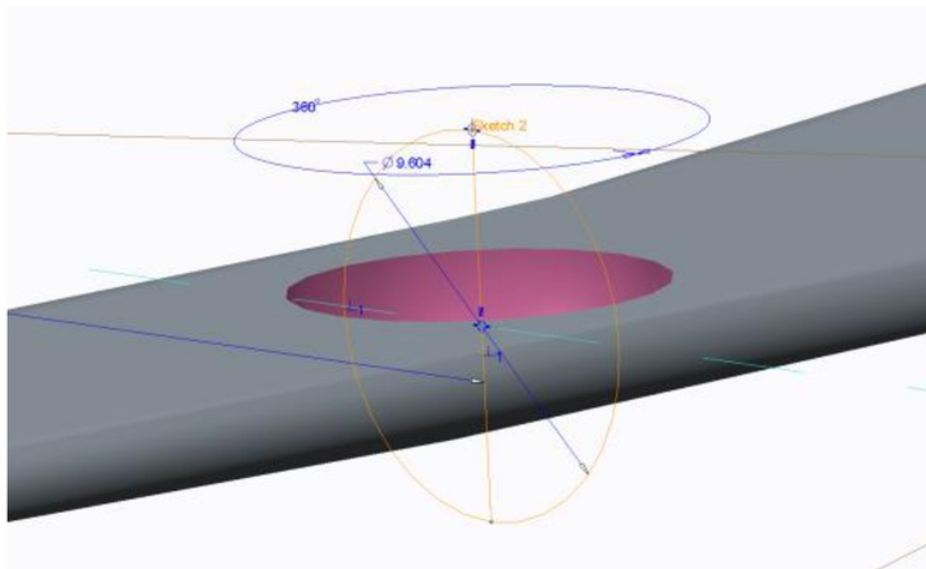


Figure 27: The designed cage bore dimension.

The ceramic ball will be fitted by pushing it into the cage bore. The bore size needed has to be 10% bigger than the actual ball size which is 8.731mm . Therefore, the bore size will be $8.731 + (8.731 \times 0.1) = 9.6041\text{mm}$. Engineer Zeman mentioned that the cage bore needed to be a bit bigger than the ball size and he granted the 9.6041mm . The raceway will be grooved on the guard and the antenna planner gear has to be grooved with a radius of $\cong 4.8\text{mm}$, making sure to leave room between the raceway and the cage to avoid the parts coming in contact with each other. The designed cage thickness is 3mm .

A technique is added to the designed cage to support positioning the cage height as the below figure shows. The extra parts size has a dimension of half the ceramic ball. This size will fix the cage exactly in the middle of the ceramic ball instead of falling on the base as the designed ball bore is bigger than the actual ceramic bearing ball. Four parts is designed on one side only and the reason is more parts will allow a bit more friction as they are fixed.

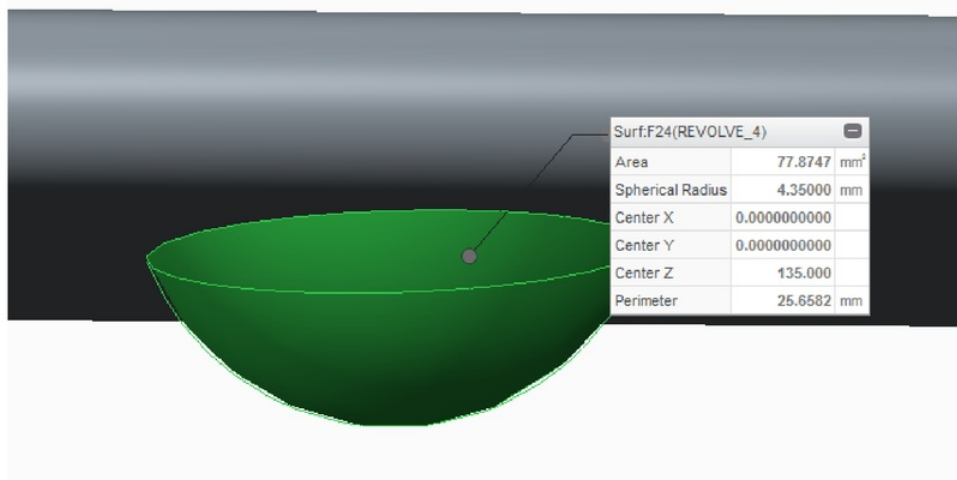


Figure 28: The cage support part for positioning the height.

5.1.3 Raceway

The raceway will be a groove on the Acetal plastic antenna holders and the ABS plastic shield components based on the rolling element size and oil will be used for lubrication to increase the rolling speed. To make sure that the raceway will not deform, a bearing stress analysis was used for both raceways materials [59][60]. Shown in the following:

- ∴ each cage have 11 balls and total weight of 85gram.
- ∴ both driven gears have a total weight of 4.915kilogra.
- ∴ the axiel force on the bottom shield raceway which have a higher loads than the other raceway between the gears = 5kilogram of total load \times 9.81gravity $\cong 49\text{ N}$.

By taking a contact area between one bearing ball and raceway = 0.3mm^2 ,

- ∴ total contact area for one bearing cage will equal to $11 \times 0.3 = 3.3\text{mm}^2$.

From here we can find actual yield stress for the application which should be less than the normal ABS and Acetal plastics yield stress which is given in the data sheet in appendix A and B:

$$\sigma_{act} = \frac{\text{Axial force}}{\text{Total contact area}} \times \text{Factor of safety} = \frac{49}{3.3} \times 2 \cong 29.7 \text{MPa} [61][62].$$

$\therefore (\sigma_{act} = 29.7 \text{Mpa}) < (\sigma_{plastic} = 65 \text{Mpa})$
 $\therefore (\sigma_{act} = 29.7 \text{Mpa}) < (\sigma_{plastic} = 44.8 \text{Mpa})$
 \therefore The raceways analysis is positive and showed that no deformation will occur.

The calculated raceway depth is 1.3mm to avoid crashing the cage into the raceway.

5.1.4 Specifications

Final bearing specifications are detailed in the following table:

Table 3: Designed bearing specifications.

Bearing Type	Thrust Ball Bearing
Cage Material	ABS Plastic
Rolling Element	Balls
Rolling Element Material	Ceramic
Inner Diameter	Ø257mm
Outer Diameter	Ø283mm
Cage Height	3mm
Cage Ball Bore	Ø9.6041mm
Ball Size	Ø8.73mm
Raceway Groove Radius	4.8mm

5.2 Driving Gear

Gears are used in many mechanism applications from the simple can opener to the more complex plane carriers. Comparing gears with other rotary drivers of belts and chains, they are more capable in terms of power transmission rating [63][64].

The driving worm gear is known as a worm screw or worm wheel [65]. It is the part which will drive and rotate the driven gear which holds the antenna planner. The worm screw consists of one tooth that is designed in a shape that allows it to rotate around in a single direction for ever with no end. The chosen material for the driving gear is metal as it is the preferred material that matches with the plastic driven gear. In the gearing industry, all the driving worm screw materials need to be stronger than the driven worm gear. The reason for this is to avoid the gear tooth from seizing, which can be caused by the temperature and torque that occurs after long operation [66][67]. This is because the driving gear is a much smaller size than the driven one which means it takes much more revolutions than the driven gear to rotate one complete round. The chosen metal material is black carbon steel which has a good strength and properties as is shown in the attached data sheet in appendix F.

5.2.1 Worm Screw Calculations

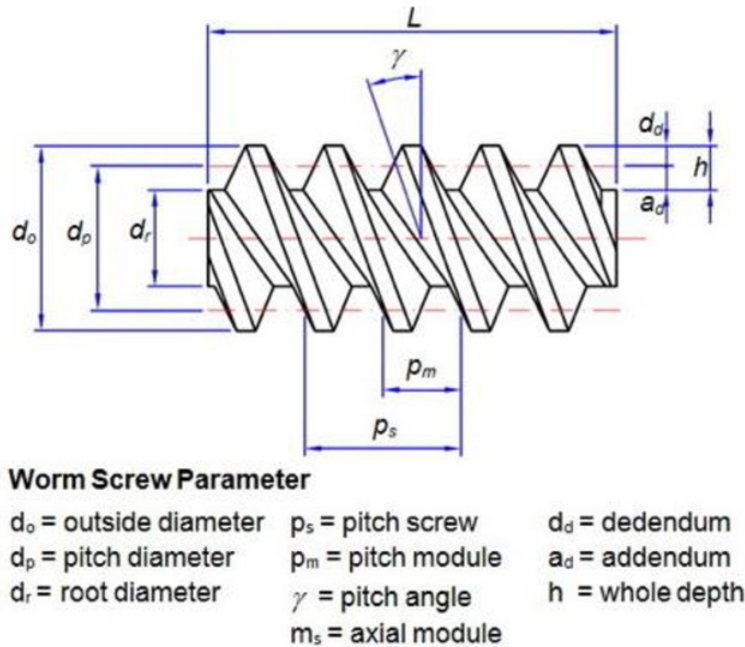


Figure 29: Worm screw parameter [68].

The above figure shows the important parameter of the worm screw which need to calculate and figured in the following calculation to produce the driving gear:

By chosing the pitch module from the standard sizes which is attached
in appendix E (p_m) = 1.25

Addendum (a_d) = p_m = 1.25

Dedendum (d_d) = $1.25 \times p_m = 1.25 \times 1.25 = 1.5625$

Whole depth (h) = $a_d + d_d = 1.25 + 1.5625 = 2.8125$

By choosing a suitable pitch diameter from the standard sizes (d_p) = 25mm

Outer diameter (d_o) = $d_p + 2a_d = 25 + (2 \times 1.25) = 27.5\text{mm}$

The root diameter can be found as (d_r) = $d_o - 2h = 27.5 - (2 \times 2.8125) = 21.875\text{mm}$

To find the pitch angle or the leader angle for helical teeth (γ) = $\sin^{-1} \frac{p_m}{d_p} = \sin^{-1} \frac{1.25}{25}$

$$= 2.865983983^\circ = 2^\circ 51' 57.54''$$

Lenght of the worm screw (L) = $2\sqrt{h \times (D_o - h)}$

$$= 2\sqrt{2.8125 \times (302.876 - 2.8125)} \cong 60\text{mm}$$

Were D_o is the outer diameter of the driven gear which is calculated in section 5.3.2 [69].

One of the screw side will have a shoulder of 15mm long, $\varnothing 20$ outer diameter and pierced from the middle with a 3mm hole for the pin. From here, the calculation for the worm screw is ready and the other calculations are for the manufacturing machining which is explained in the prototyping chapter.

5.2.2 Driving Gear Shaft

A shaft is used in this application to transmit the power or motion from the stepper motor to the gear. There are three properties that are usually a concern in designing shafts. These include the materials properties, geometric layout and the stress and strength. However, as the overall loads of the application are small, there are some properties that will not be a concern [16].

5.2.2.1 Shaft Material

There are very small loads on the driven gear as mentioned in the previous section, this means that the shaft will not resist a high stress load. Therefore, the same metal material will be used for the shaft which is also a common material for shafts in general as it has a good properties as it is provided in appendix F [70].

5.2.2.2 Shaft Geometric

Based on the 21.875mm root diameter which is calculated in the previous section, \therefore a suitable shaft diameter for this worm scrwe is choosen to be 15mm.

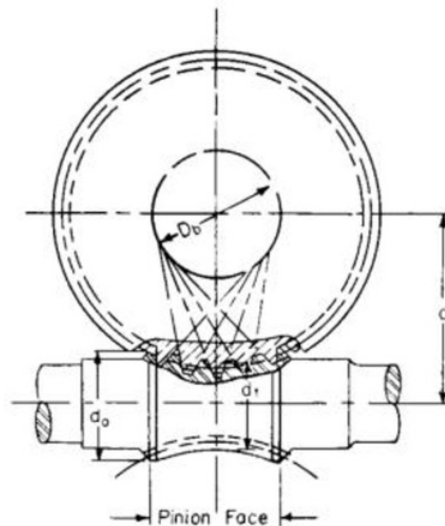


Figure 30: A drawing clarify the centroid of worm gearing system [71].

The shaft which holds the scrwe wheel will be positioning by measuring the centroid distance between the scrwe wheel and the driven gear (C)

$$= \frac{PCD1+PCD2}{2} = \frac{300.376+25}{2} = 162.688mm \quad [71].$$

There are very small axial loads on the shaft components and the parts are light weight. For this light duty, at the end of the shaft a deep groove ball bearing will be attached for smoother rotary.

Shorter shaft length is preferred for power transmission. By using CREO software simulation, the shaft dimension length was found to be 170mm. This dimension was figured out by taking in consideration, leaving room between the shaft holders and the other assemblies to avoid crashing.

5.2.2.3 Shaft Supported Elements

A pin is the technique which is used for torque resistance and to fix the worm screw with the shaft. On the shaft, a 3mm hole is pierced on the length of 70mm. This hole is designed for the roller pin which will be insert through that hole and the other worm screw shoulder hole.

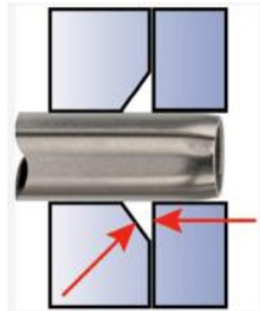


Figure 31: Shows the hollow design pin and how does it fit [72].

The other supported element is called a rigid coupling. This part is designed to connect two shafts together from their ends for the purpose of power transmission. A simple flanged face coupling is needed as the axial loads are very small. One of the coupling pair parts will be designed for the end of the shaft and the other part will be separately designed to fit the fixed motor shaft. 3 M3 bolts and nuts will be used for each pair of coupling parts.

5.2.2.4 Top and Bottom Gear Shaft Holders

The end of the shafts will be received and hold by an ABS plastic shaft holder, which has a high stiff to host the shaft. The shaft holder has a bore of Ø22 and a shoulder at the end of one side of that bore to receive the groove ball bearing which has a Ø12.

The difference between the shaft holder for the top and bottom driven gear are their height as the driving worm screw needs different specific heights to be facing and driving the tooth in a parallel position

5.3 Driven Planner Antenna Holder Gear

The driven gear which holds the antenna planner is consist a helical tooth for the worm gear driving and attached with an edge that is contacting with the supporting bearing points to fix the gear horizontally. The driven gear tooth can be either worm tooth or helical, however, worm tooth cost more to manufacture as it is hard to fabricate and helical tooth which is lower cost can deliver the desire rotation result for the antenna application.

5.3.1 Gear Material

For gear material selection there are some main concentrations includes, gear strength, producibility, cost, weight, noise and corrosion resistance [73]. Plastic is the chosen material for the application driven gear. Their feature comparison with the most common gear material (metals) are in the following:

1. **Producibility:** Injection moulding enables low cost production for plastic and 3D printing for plastic prototyping.
2. **Cost:** In general for large production cost, plastic material ranked as cheaper than metal.
3. **Weight:** plastic is lighter than metal material.
4. **Noise:** can generate a significant noise, however, it depends on the design technique which can be a quiet gear in both materials. In addition, plastic can be operated without lubrication which makes it a preferable feature.
5. **Corrosion resistance:** An advantage of plastic is its higher corrosion resistance, which is more than metals plus it is electric non-conductive.
6. **Strength:** plastic has a disadvantage of lower strength, less chemical and heat resistance than metals.

Plastic gears are preferred for medical equipment industries, toys and electronics application which is antenna application belong to [74]. The chosen plastic for the driven gear is natural Acetal (material data sheet is provided in appendix B). Its main features include high stiffness, very good heat resistance and it's non-conductive. These features are required for the metal driving worm gear [75].

5.3.2 Tooth Calculation

Designing the teeth starts with a basic equations which are published in most of the mechanical fundamental books and then it became more complicated to find the involute for the gear teeth.

In the following calculations, the methods are explained step by step including the involute calculation. The common two standards for the helical tooth calculation are American and English. In this calculation, metric standards are followed to find the tooth numbers.

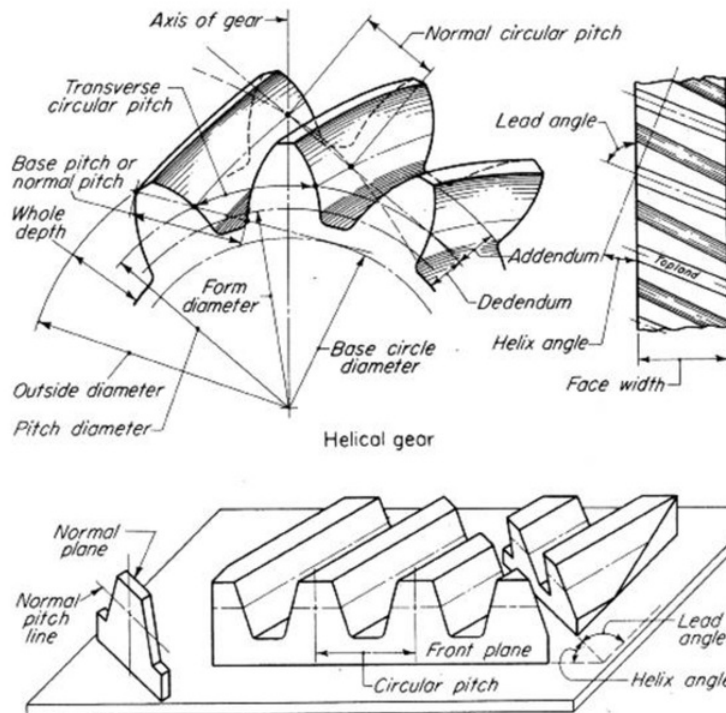


Figure 32: Highlighting the helical tooth parameter [76].

As the application need to be rotate to an angle of 360° , the number of teeth is preferred to be 360 as each teeth rotate is steer to one single degree. However, the pitch diameter will be very large and need to minimise it. By taking 1.5 teeth rotate present each angle, the pitch are acceptable. \therefore Number of teeth for the driven gear (N) = $360 \div 1.5 = 240$ teeth

By chosing the normal module (P_m) = 1.25

calculated helical or leader angle (γ) = 2.865983983°

normal pressure angle as preffered in most gears (ϕ) = 20°

pitch diameter of the driven gear (D_p) = $\frac{P_m \times N}{\cos(\gamma)} = \frac{1.25 \times 240}{\cos(2.865983983)} = 300.376\text{mm}$

outer diameter (D_o) = $D_p + 2P_m = 300.376 + (2 \times 1.25) = 302.876\text{mm}$

$$\text{root diameter } (D_r) = D_p - 2.5p_m = 300.376 - (2.5 \times 1.25) = 297.251\text{mm}$$

$$\text{base circle diameter } (D_b) = D_p \cos \phi = 300.376 \cos(20) = 282.26\text{mm}$$

$$\text{choosen width} = 15\text{mm}$$

$$\text{addendum } (A_d) = p_m = 1.25$$

$$\text{dedendum } (D_d) = 1.25 \times p_m = 1.25 \times 1.25 = 1.5625$$

$$\text{whole depth } (H) = a_d + d_d = 1.25 + 1.5625 = 2.8125 \quad [71].$$

The tooth have an involute curves to maintain a constant angular velocity ratio between the driving worm screw and the driven gear [77]. To calculate the involute for helical angle, the equation is:

$$\text{inv} = \tan(\phi_{deg}) - \phi_{rad} = \tan(20) - 0.349066 = 0.0149 \quad [78].$$

There are three different types of teeth measurement. These measurements are made after manufacturing the gear (it is explained deeply in the prototyping chapter). The types are:

1. Single tooth measurement (not accurate).
2. Span measurement (common and better than the single tooth).
3. Pin size measurement (very accurate but complicated).

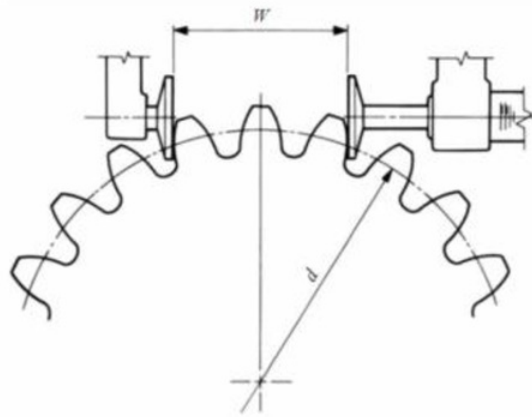


Figure 33: A sample of span measurement over (K) 3 teeth by using a special tool [79].

The used measurement for this calculation is a span measurement. Several equations are used for it and the results are needed to do the measurements:

$$\text{To find the number of teeth which need to be measured } (K) = \frac{\phi \times N}{180 \times \cos(\gamma)^3} + 0.5 =$$

$$\frac{20 \times 240}{180 \times \cos(2.865983983)^3} + 0.5 = 27.26 \cong 27 \text{ teeth}$$

After knowing the number of teeth, need to know the distance between them to be measured (W).

$$\text{By finding the transverse pressure angle } (\phi_t) = \tan^{-1} \frac{\tan \phi}{\cos \gamma} = \tan^{-1} \frac{\tan(20)}{\cos(2.865983983)} =$$

$$20.023^\circ$$

Now (W) can be found $= \cos \phi \times P_m [(k - 0.5)\pi + (inv \times N)] = \cos 20 \times 1.25 [(27 - 0.5)\pi + (0.0149 \times 240)] = 102mm$ [71].

From here, all the driven gear calculations are ready and the manufacturing steps are shown in the prototyping chapter.

5.3.3 Top and Bottom Driven Gears

The top driven gear has a room of $164mm$ square in the middle to hold the antenna planner which has a size of $162mm$ square. Around the planner room it is grooved with a radius of $4.8mm$ as a raceway to receive the bearing balls.

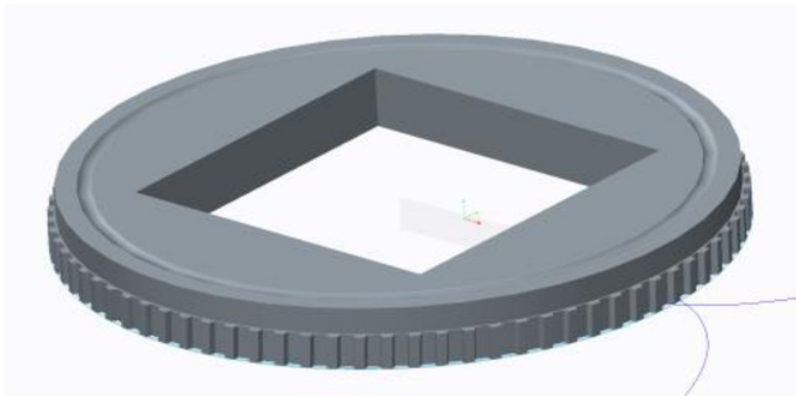


Figure 34: Bottom driven gear.

The top edge is designed to be in contact with the roller bearing points to fix the gear horizontally as there is no shaft to hold it away from the middle. Usually gears do have this ability. The edge has a thickness of $12.5mm$ and a diameter of $296mm$ (which is smaller than the gear root diameter) to leave room and avoid crashing with the driving gear (which has a diameter of $27.5mm$ that calculated in section 5.2) this can affect the smooth rotation. Bottom gears are the same as the top gear design but everything is designed reversed as the bottom gear will be facing the top gear.

5.4 Motor Holder

The motor dimension is provided from the supplier as it is shown in appendix D. The motor holder is designed to host the motor at the provided dimension. The holder has a bore of $22mm$ diameter for the bearing part. It has chamfered angles to save the material and simplify it for easier 3D printing. It also has a rounded fillet to make it stiffer. The material for this part is made from ABS plastic.

There are two different motor holders. The first holder is for the bottom driven gear and it is shorter than the second holder which is designed for the top driven gear. The dimensions are calculated carefully to make sure that the holder hosts the motor and points its shaft into the correct position which will allow it to be parallel with the driven gear tooth.

5.5 Bearing Point

The bearing points are three points around the driven gears. They are positioned around the driven gears symmetrically with 120° between each point ($360^\circ \div 3 = 120^\circ$). Each bearing point has two bearings. One is contacting horizontally with the top driven gear edge and the second one with the bottom driven gear edge. The bearings are fixed on the bearing point shaft by a circlip. This ensures that they are attached on both bearing sides in a standard groove. The used circlips are for the chosen bearing size and followed a standard European circlips specifications as shown in appendix J. There are no equations to calculate the centroid distance for the bearing and the edge, therefore, a long bolt hole was designed to be on the base of the guard to allow space to adjust the distance which fix the driven gear.

5.6 Micro-controller

The same micro-controller which has been used for the existing mechanism will be used to control the new mechanism system. The micro-controller consists of two parts, one is a control that allows for users to program codes and the other part is a driver board which controls the motors directly.



Figure 35: Shows the power provider for the driver board.

The above figure shows the part of the mechanism that provides the driver board with power. Through this power supply which is in Macquarie University labs, the output voltage can be adjusted. In the initial testing, it was noticed that the minimum voltage was required to operate the system. This is 8v. The red and black cables are connected with the driver board, while the controller is connected with the computer by USB cable and run with a power of 5v. The same power source will be used for the new system.

The coding part is not required to be deeply researched at this point in time as the main scope is on the mechanism. Therefore, a simple coding which is provided in appendix C will be used to operate the system. This will be the same as the one which was used for testing the initial design and even the existing design.

There are three identified modes in the codes that can operate the system in three speeds. This is how the initial test will be for the final system. As there is very small axial

loads, no force analysis needed to be calculated for the driven gear and the motors as the simple given codes were able to rotate the driven gear with a speed up to a 360° per 2 second which is the desired speed for the antenna application.

5.7 Guard

The guard design designed to be a circular part that host the whole system. However, for the university researching purpose, the guard will be a normal wood flat sheet to allow a better visually for all the system assemblies.

Chapter 6

Prototyping and Fabrication

This chapter details the process of the application assemblies' construction. There are some assemblies prototyped by 3D printing and some components manufactured by machining in a workshop.

6.1 3D Printing

One of the most common methods used in engineering projects for prototyping is 3D printing. This is because it has the advantages of low costs and ease of modelling [80]. The printer uses common material such as ABS plastic which is available in the university. As presented in the previous sections the advantages of the ABS plastic is its ability to print and prototype the small size supported parts [81].

The process starts with modelling the part through the CREO CAD software and exporting the model with a stereolithographic file type. From here, the component is ready to be printed by plotting the stereolithographic file into the 3D printer. As mentioned in the previous chapter, the assembly dimensions are calculated and analysed through CREO Parametric software which provides the opportunity to visualise the system design and measure the dimension. For example, to leave room between the components, which is much easier than doing it on paper. A detailed manufacturing drawing for each model is present in the following subsections to clarify the assemblies dimension.

6.1.1 Bearing Cage

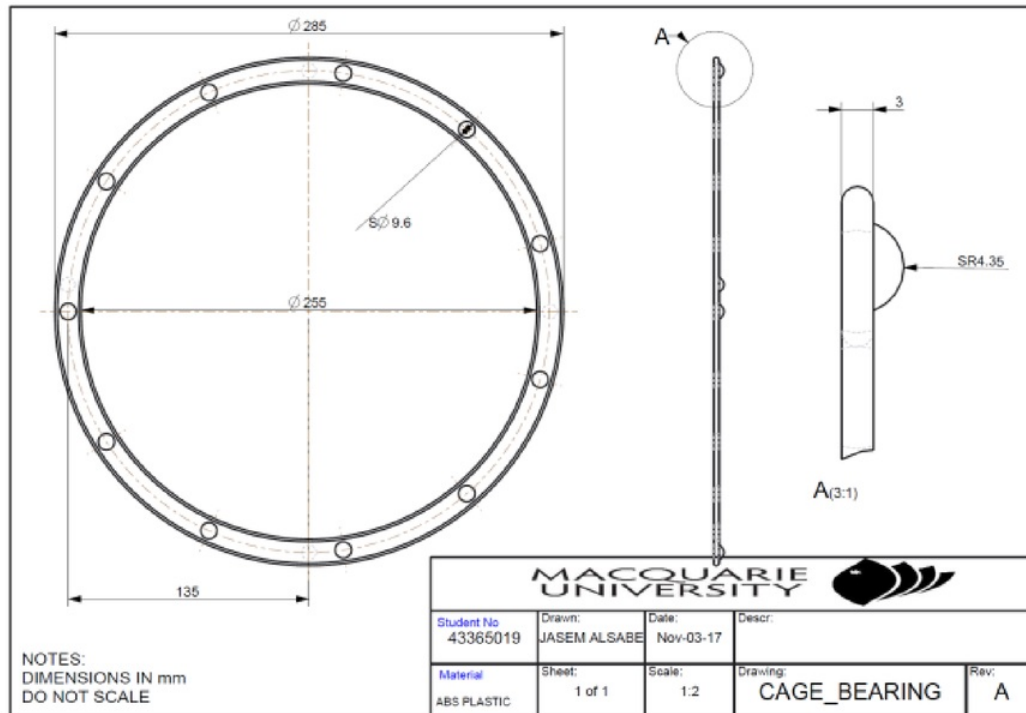


Figure 36: Manufacturing drawing of the bearing cage.

The bearing cage is designed with a thickness of 3mm. 11 ball bores are situated around the cage with a distance of 135mm from the centre. Two cages are printed, one to fit between the gears and the other is located below the bottom gear. A part is added in one of the cage sides with size of 4.35mm which is the half size of the ceramic bearing ball.

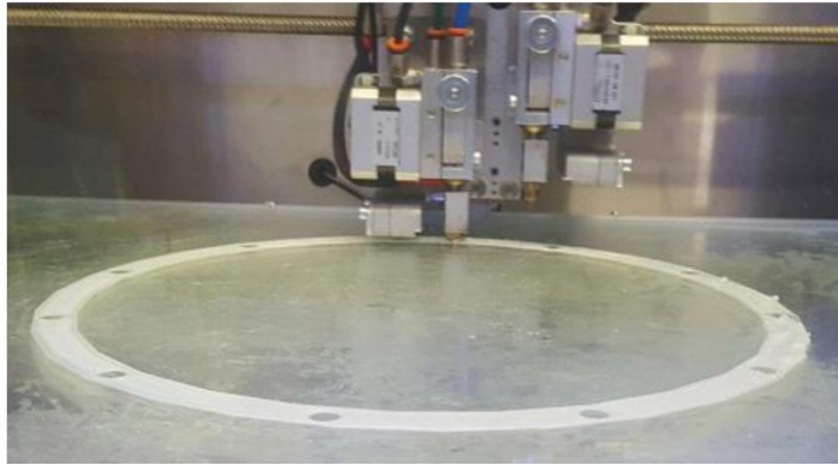


Figure 37: Printing the bearing by 3D printing.

6.1.2 Shaft Holder

There are two shaft holders, one for the top one and one for the bottom.

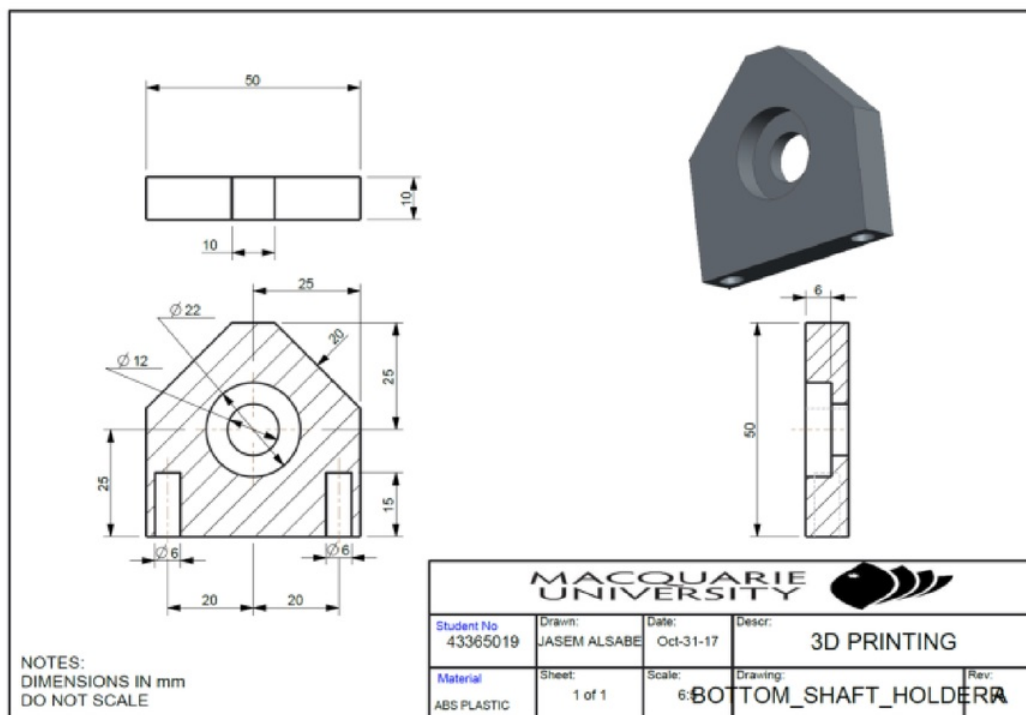


Figure 38: Manufacturing drawing for the bottom gear shaft holder.

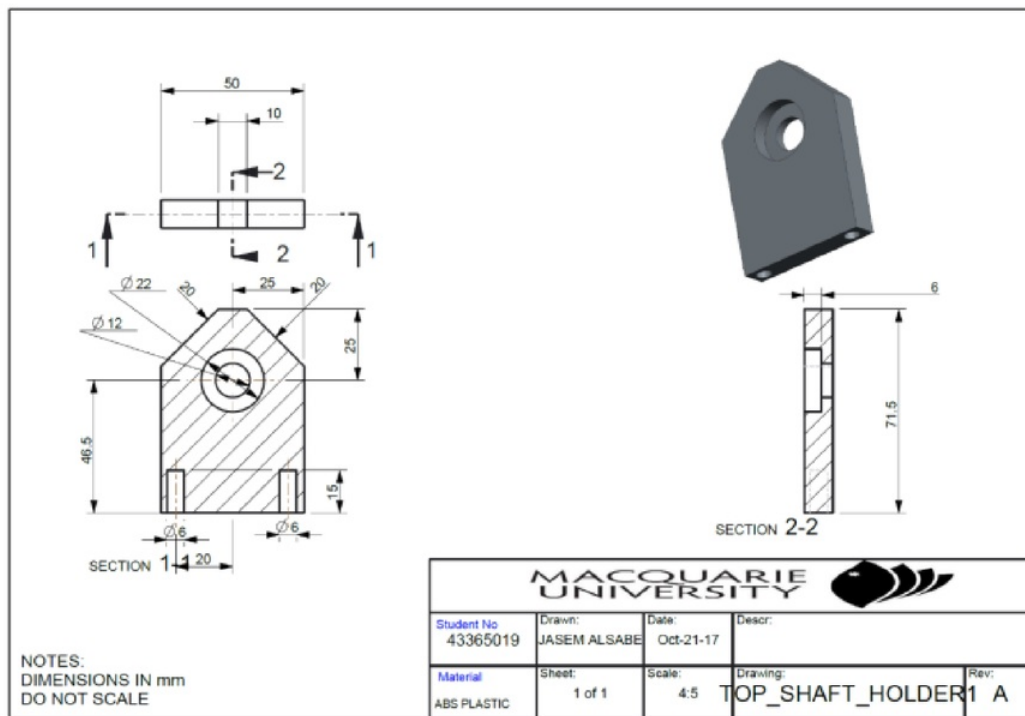


Figure 39: Manufacturing drawing for the top gear shaft holder.

The shaft holders are designed using a simple method as they will not hold high axial loads. The parts are chamfered to save materials. The parts bore is $\varnothing 22$ to host the bearing and there is a shoulder with a $\varnothing 12$ for the shaft. This design is to fit the shaft bearing into the holder. For the M6 bolts, the screw hole standard size for the metal base is 6×1.4 , but for the ABS plastic holder base, a bigger number is used for the M6 bolt size as $6 \times 2.5 = 15\text{mm}$. The 3D printer will print the part without the screw hole and after that, the female thread is cut using a handle tap. The drill size is chosen to be 5mm to fit the M6 tap based on the standard sizes as it is shown in appendix I.



Figure 40: Handle tap.

6.1.3 Motor Holder

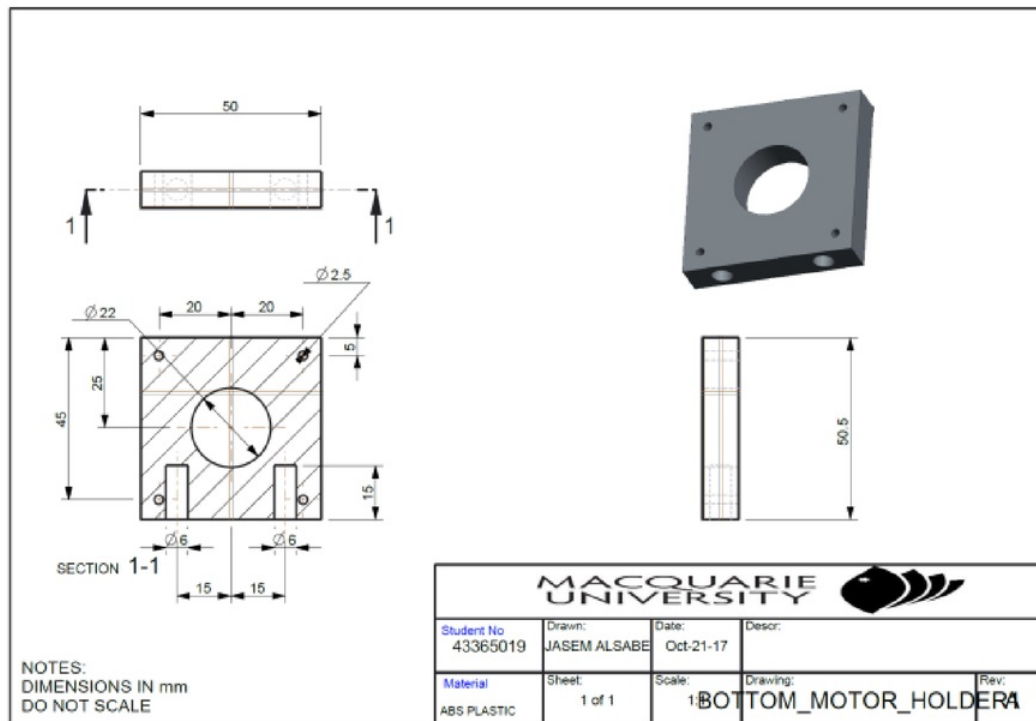


Figure 41: Manufacturing drawing for the bottom gear motor holder.

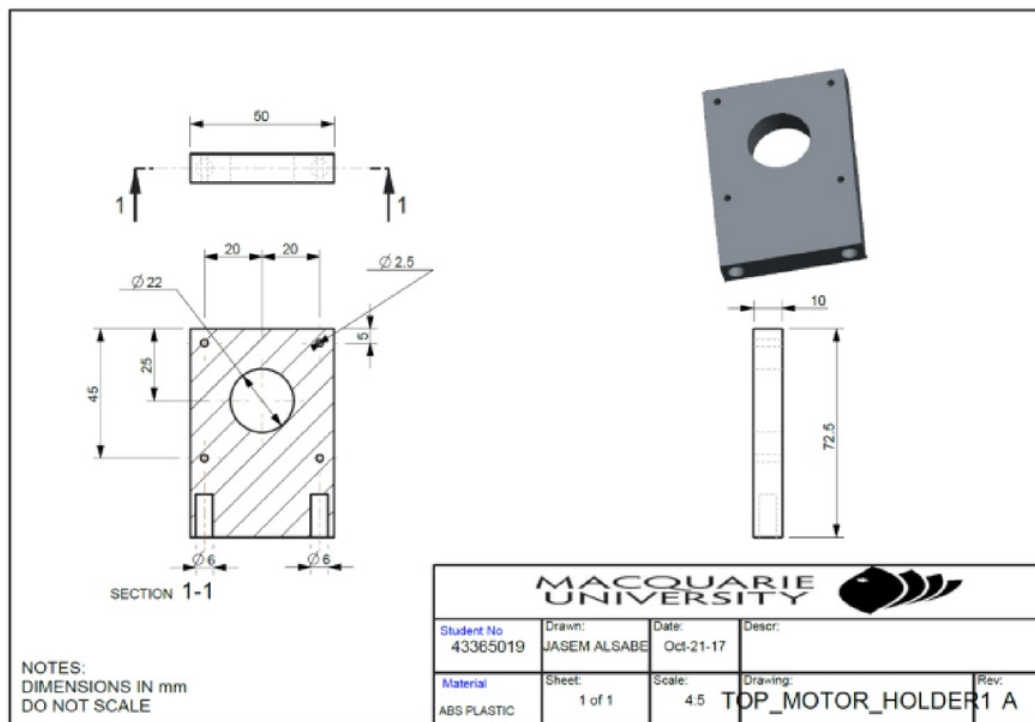


Figure 42: Manufacturing drawing for the top gear motor holder.

The motor holder design has a bore of $\varnothing 22$, but it does not have any shoulder support like the shaft holders do. One side of the shoulder support is enough for this light duty system. The screw hole has the same dimensions as the shaft holder process and is followed by the thread cutting.

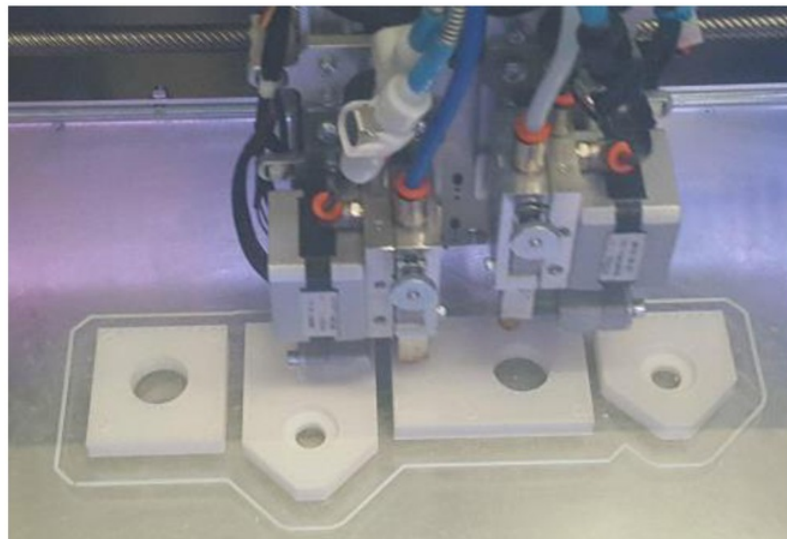


Figure 43: Printing the supported parts by a 3D printer.

6.2 Workshop Manufacturing

There are some components like the gears tooth that is required to have a smooth finish. Although the 3D printing can prototype the gears shape and results with accurate dimensions. However, the prototype tooth cannot be smooth as it is required. Therefore, the best choice is to manufacture the gears by machining which will result in a smooth tooth for better operation.

The process starts with modelling the gears through CREO and producing manufacturer drawings, which are known as the mechanical engineers language. Through these drawings, the technical engineer can understand the shape of the assembly and the dimensions which need to be manufactured. Each gear manufacturer drawing is present in the following subsection and the manufacturing procedure is explained.

6.2.1 Driving Worm Screw

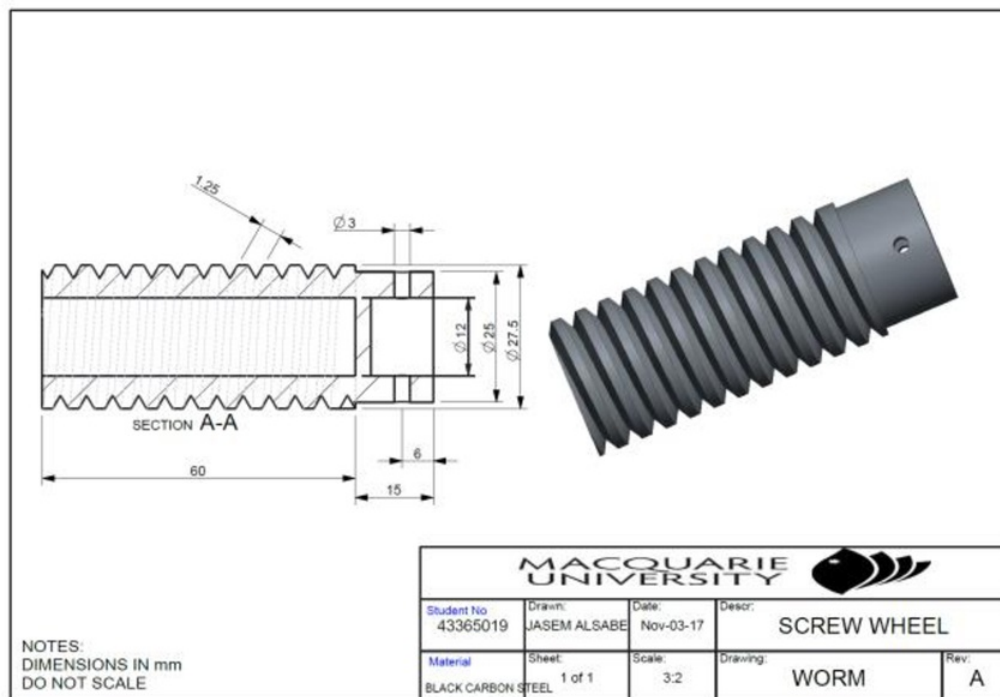


Figure 44: Manufacturing drawing of the worm gear.

As mentioned in Chapter 5 the driving screw wheel material is made of black carbon. A $\phi 30$ rod of black carbon at a length of 250mm is used to make the driving wheel. The size needs to be bigger than the target wheel outer diameter of 27.5mm and longer than the total length of both wheels and their pin arms which is counted to be 150mm. The reason for taking a

longer length is for a machining reason. As the threaded milling machine requires a gap of 100mm between the tooth and the machine chock to avoid crashing while operating.

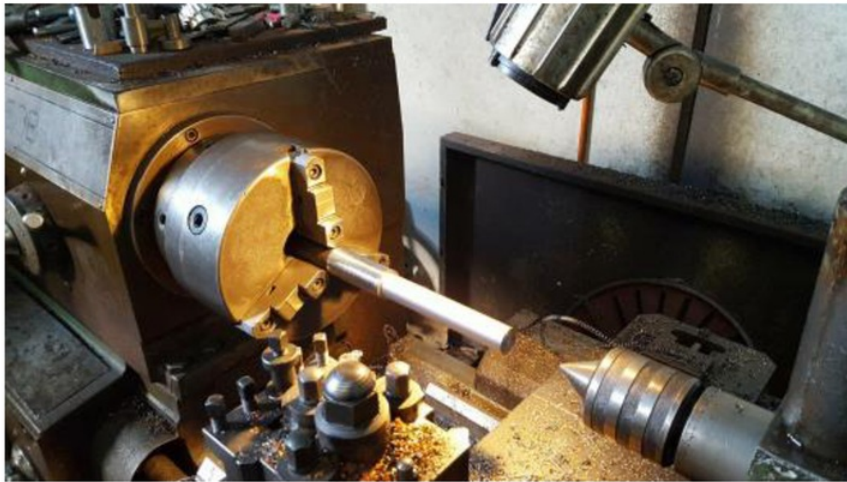


Figure 45: Cutting the rod to 27.5mm diameter by turning machine with a three jaw chock.

By using the turning machine which is shown in the above figure, the rod diameter will be cut from 30mm to 27.5mm after setting the lathe tools and the machine cutting diameter. 165mm long parts have been cut to leave a bit of a gap for the tooth cutter tool, as the wheel tooth length is 150mm.

After turning the rod, the next step is to cut the wheel tooth by using the threaded milling machine. However, before using the machine a few measurements for finding the axial lead, gear ratio, cutter tip width and changing the gears is required by using the standard equations as follow:

$$\text{Axial Lead} = (p_m)\pi \div \cos(\gamma) = (1.25)\pi \div \cos(2.865983983) = 3.9319\text{mm}$$

$$\text{Changing Gear Ratio (i)} = \text{Axial Lead in inch} \div 4 = 0.154799213 \div 4 = 0.386998$$

By plotting this ratio to the gear finder tool, the chosen generated gears option is 21 – 104 – 23

– 120 as it is shown in appendix G. Therefore, the changing gear for the machin is

$$= \frac{21 \times 23}{104 \times 120} \times 4 = 0.0387 = \text{Lead.}$$

$$\begin{aligned} \text{Cutter Tip Width} &= \frac{p_m \times \pi}{2} - (2 \times \tan(\emptyset) \times p_m \times \text{standard screw wheel addendum}) = \\ &= \frac{1.25 \times \pi}{2} - (2 \times \tan(20) \times 1.25 \times 1.2) = 0.91526\text{mm} \quad [71][82]. \end{aligned}$$

After finding the measurement, everything is ready to use the machine by setting the helical cutting angle and the cutting depth which is calculated in chapter 5, and setting the gears as was figured above. Before starting to cut the tooth, the rod diameter needs to be measured by using a Vernier tool as it is shown in the below figure.

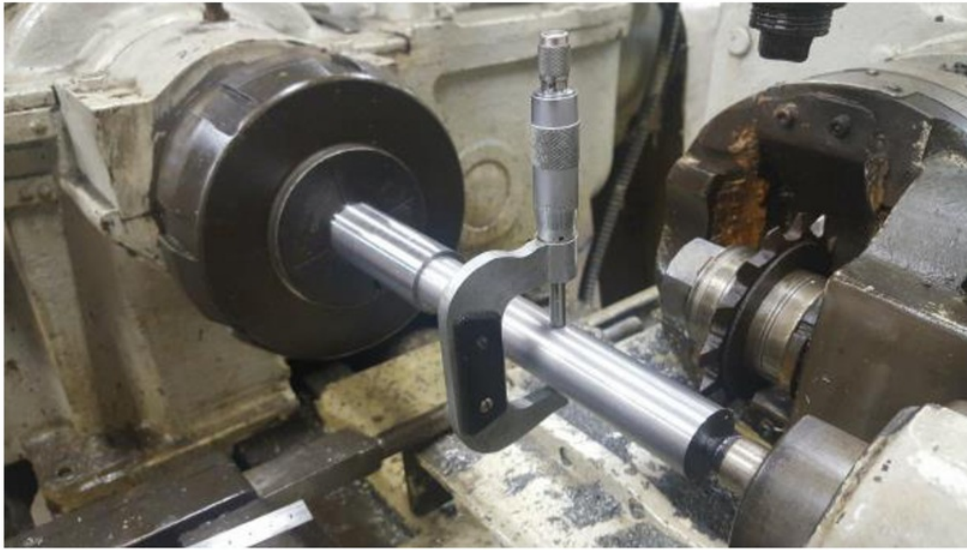


Figure 46: Measuring the rod diameter by using vernier tooling.

The tooth measurement in the wheel is different from the driven gear which was explained in chapter 5. For the screw wheel, the tooth measurement is done for a single tooth only and was done by using a gear tooth Vernier.

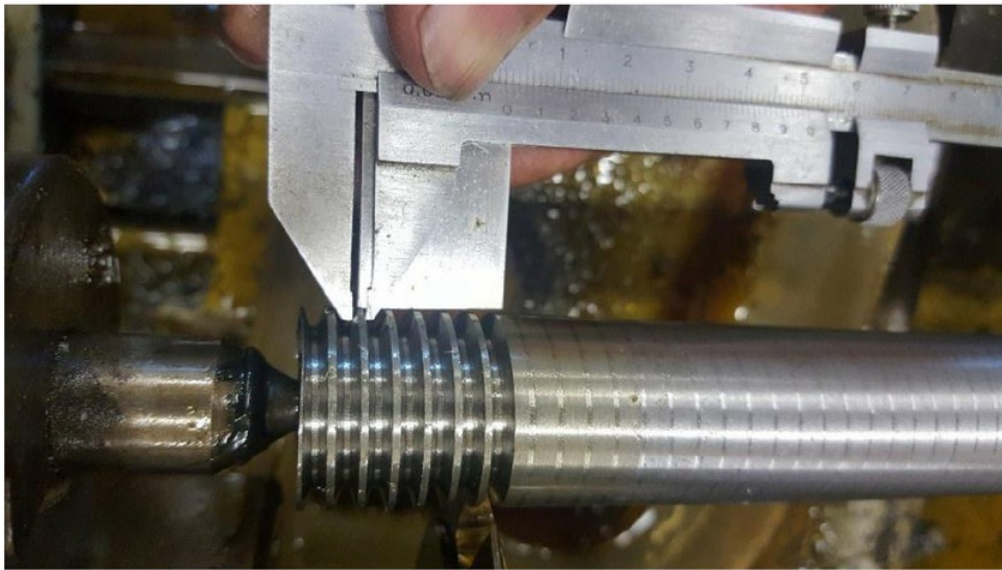


Figure 47: Measuring a single screw wheel teeth by a tooth vernier tool.

After cutting a couple of teeth, a measurement for a single tooth is done as is shown in the above figure. The measurement shows tooth width. This should provide a result as follows:

$$\text{Teeth thickness} = \frac{(p_m)\pi}{2} = \frac{(1.25)\pi}{2} = 1.96\text{mm.}$$

If the measurement was the same, the cutting can continue. If it was different, the cutting depth needs to be changed.



Figure 48: Screw wheel tooth cutting by a threaded milling machining.

An oil is used while the machine is in operation to equalize the material temperature as they are hot whilst the machine is cutting.

There is a feature in the machine where it can be set to a final cutting length, at which point it will stop. After cutting it to 150mm in length, the rod needs to be cut into two halves by using the parting off cutter in the lathe machine. Each half has a length of 75mm. Each half will have a shoulder of 15mm which is made by turning it through the lathe machine. In the same lathe machine, the screw wheels will be drilled firstly with a 7mm drill and then 11.7mm drill and finally with H7 tolerance for more accurate bore to finish the host's 12mm shaft. The drilling should be started using a small drill and gradually increasing in size as it cannot be suddenly drilled with a large size. This can result in a high temperature and may break the drill part. It is also extremely dangerous. From here, the final touches are completed for the screw wheels by grinding the tooth to make them smooth using the grinding machine.

6.2.2 Driven Gear

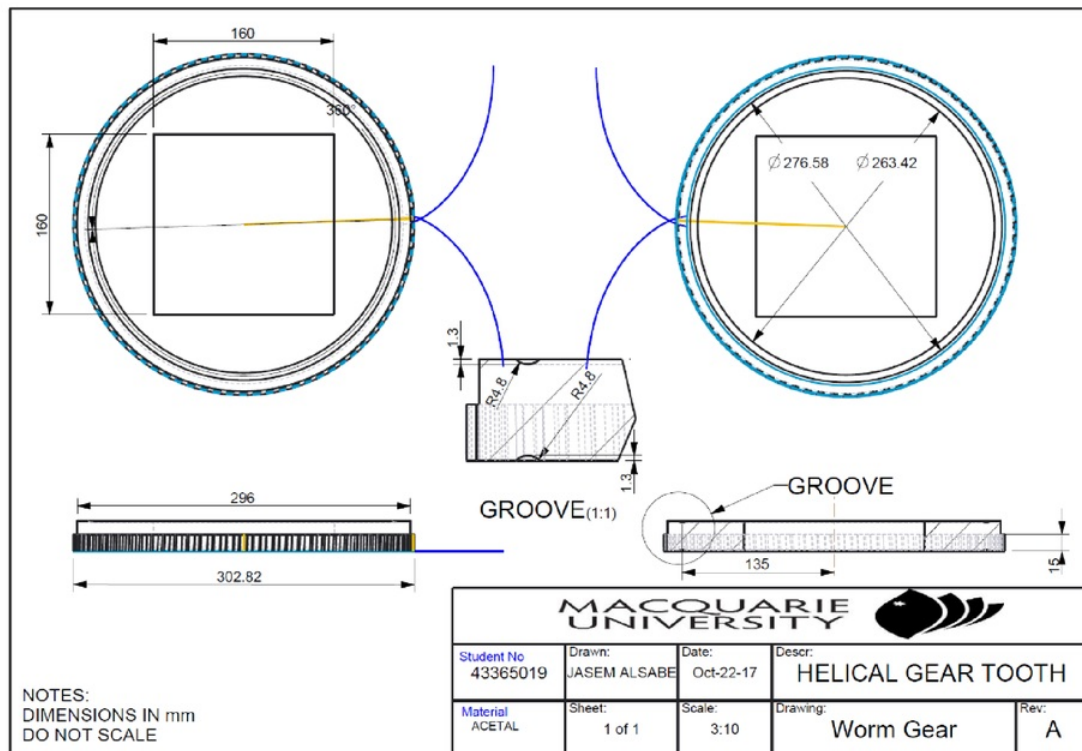


Figure 49: Manufacturing drawing for the driven gears.

The driven gear is made of Acetal plastic material which is sold by suppliers as a circular sheet. The chosen diameter of the previous gear is bit bigger from the targets dimensions. Each purchased disk sheet had a size of $\varnothing 310$ and 30mm thickness which is a bit bigger than the $\varnothing 302$ outer diameter and the 27.5 total thickness of the driven gear.

The process to cut the driven gears begins with turning the disk face to remove the wrinkles. However, the disk has a diameter of $\varnothing 310$ which is very large and this needs to be fixed before turning on the machine with 8 jaws chock as the below figure shows.



Figure 50: Fixing the Acetal disk in the turning machine by using 8 jaws chock.

After smoothing the disk face, the disk centre needs to be drilled with a bore of 20mm in diameter which is made so as to mount it onto the hobbing machine shaft later on. Then the outer diameter is turned to a $\varnothing 302.88\text{mm}$ with a 15mm thick for the tooth part. After that, the disk thickness is reduced to 27.5mm from the other face. Finally, the outer diameter of the other face is turned to 12.5mm for the bearing edge. Both the bore and the outer diameter should be measured after each cut using the Vernier. The measurements should not rely on the set machine dimensions as this may result in different dimensions. A final touch in the turning machine is chamfering the outer diameter for a better tooth cutting reason.



Figure 51: Measuring after each turning cut is very important using the vernier tool.

After that, to make a raceway for the bearing, a special tool is used. The tool consists of a metal part that is grounded to a 4.8mm radius as the below figure. The disk is grooved by the turning machine, using a special tool and setting the cutting depth to be 1.3mm as calculated in chapter 5. Before grooving the raceway, the disk needs to be fixed the exact

distance from the centre in order to have an accurate cut which is 270mm away and around the centre. To fix it and centre it, a dia inductor tool is used which helps to show the jaws what needs to be tied more to get the perfect centre fix.



Figure 52: Grinding a special tool cutter with a radius of 4.8mm .



Figure 53: Fixing the disk to the centre using the dia indicator tool.

The next stage is cutting the driven gear helical tooth which is cut out using a hobbing machine. Before starting to cut the tooth, there are some measurements that machine requires, which are index calculations and the helical angle which is calculated already in chapter 5 as $2^{\circ}51'57.54''$. Following the same process of the worm wheel changing gear, to find the index calculations which results with a gears of $30 - 50 - 42 - 70$ and a ratio of 0.36 . After finding the index, it is set in the machine as the below figure shows. After setting the index, the helical angle is set by moving the cutter arm on the machine to the required helical angle.

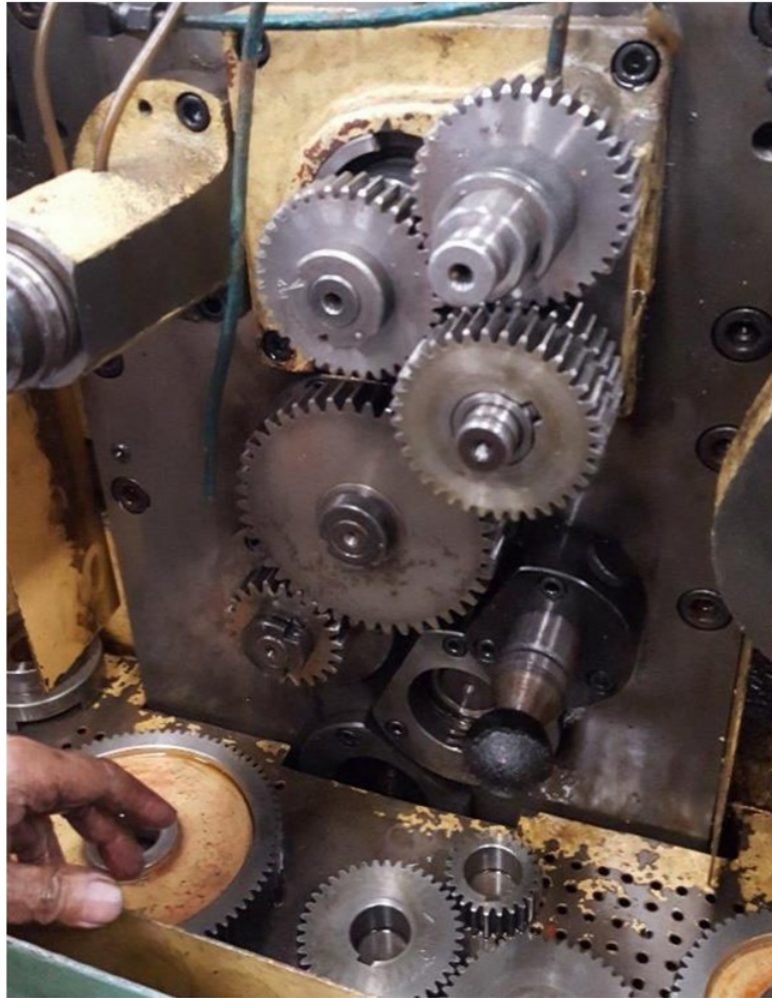


Figure 54: Setting the hobbing machine index.

After setting the helical angle and the index, the cutter hub will be inserted into the machine based on the module number which is chosen to be 1.25. Then the machine is set and ready to operate. The disk is mounted into the hobbing machine, facing each other. This is so that we are able to cut both of them in one go. Loads need to be on both of the disks sides. The reason for this is that whilst cutting them the disk will be bending if one of the sides doesn't had any loads.



Figure 55: Two disk are mounted in in the hobbing machine between loads and the cutter hub is behind them.

After cutting the tooth in the hobbing machine, a square hole will be cut from the centre and will cut a shoulder for it by using the milling machine. Before starting the cut, the square need to be marked based on the manufacturing drawing dimensions. A height gage is used for the square and shoulder dimensions marking.



Figure 56: Marking the cutting dimensions by a height gage.

The cutting process for the square hole is begun with fixing a parallel blocks below the gear and then moving the bit over the marking lines and make sure they are straight for an accurate cutting. Three different cutters is used. The first two cutters are a high speed slot drill, a large one to make the hole and the small one to make the planner shoulder. After that the third cutter is a drill bit which is used to drill a holes in each corner for fixing the planner. The cutting depth need to be small and slow speed as the part size is large and cannot be cut in a high depth suddenly for even a safety reasons.

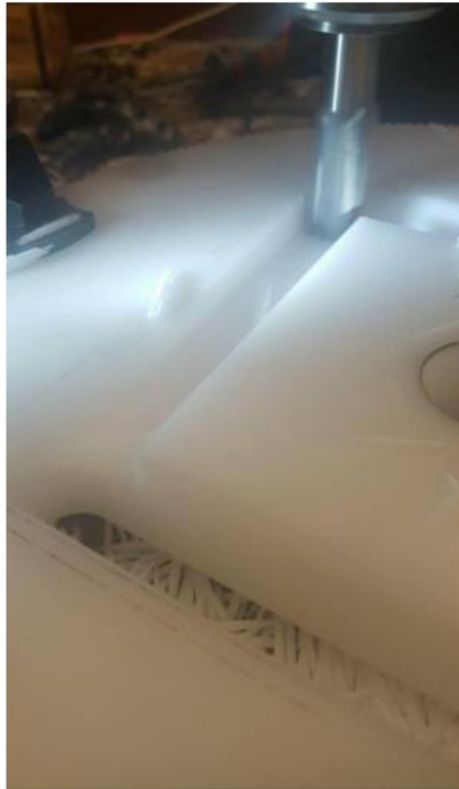


Figure 57: Cutting the gear square hole gradually in a small depth.

From here the machine is ready to cut the tooth. It will stop the cutting automatically as it has been set to do so after cutting a width of 30mm. This is the total width for both of the disks teeth.

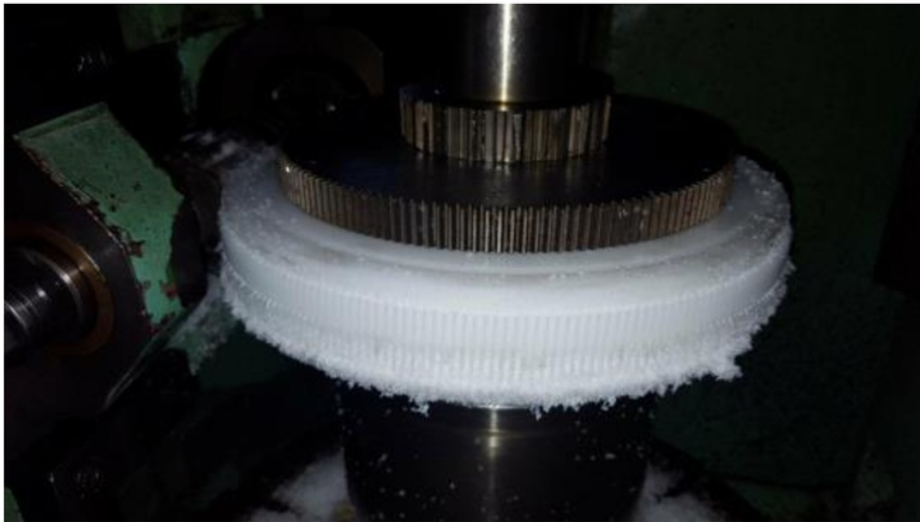


Figure 58: Driven gear tooth shape while cutting them in the hobbing machine.

6.2.3 Bearing Point

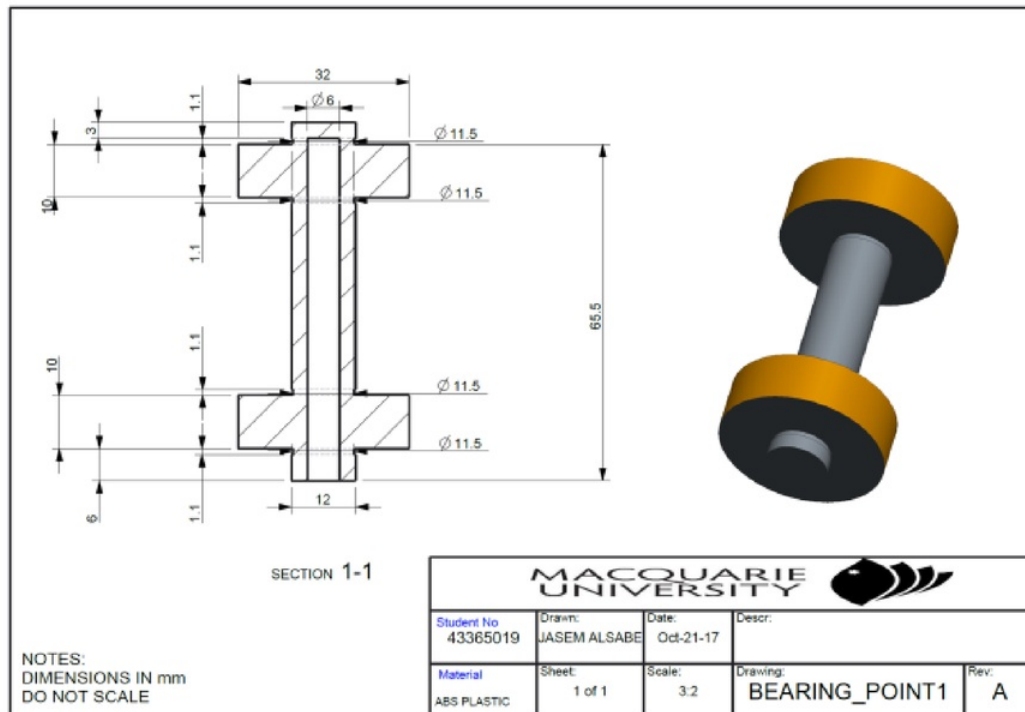


Figure 59: Manufacturing drawing for the bearing point.

After manufacturing the driven gears, the height dimensions need to be measured to see if it is how it has been designed to be or if the results show any differences. If the results are the same as what is shown in the measurements, then there is no need to change the bearing point sizes. If not, the designed sizes need to be changed based on that difference before manufacturing the bearing points.



Figure 60: Putting some bearing balls and taking the heights measurement.

The bearing point rod is made of the same black carbon metal as previously mentioned and has a diameter of $\varnothing 12mm$. The rod is grooved in 4 separate places with a standard circlip groove size created using a lathe tool in the turning machine. Each deep groove bearing will be placed between two grooves which will have their own circlips.



Figure 61: Fitting the deep groove bearing between the circlips.

The rod is designed to have a female thread for M6 bolts. As the material is steel, through the lathe machine the bearing point is drilled from one of the sides for $8.4mm$ length and using a $5.5mm$ tap drill size as the standard size shown in appendix I. M6 bolts are strong enough to hold the horizontal loads even if the system was operating in a different angles which will occur more horizontal loads force.



Figure 62: Bearing points after machining them.

6.2.4 Shaft

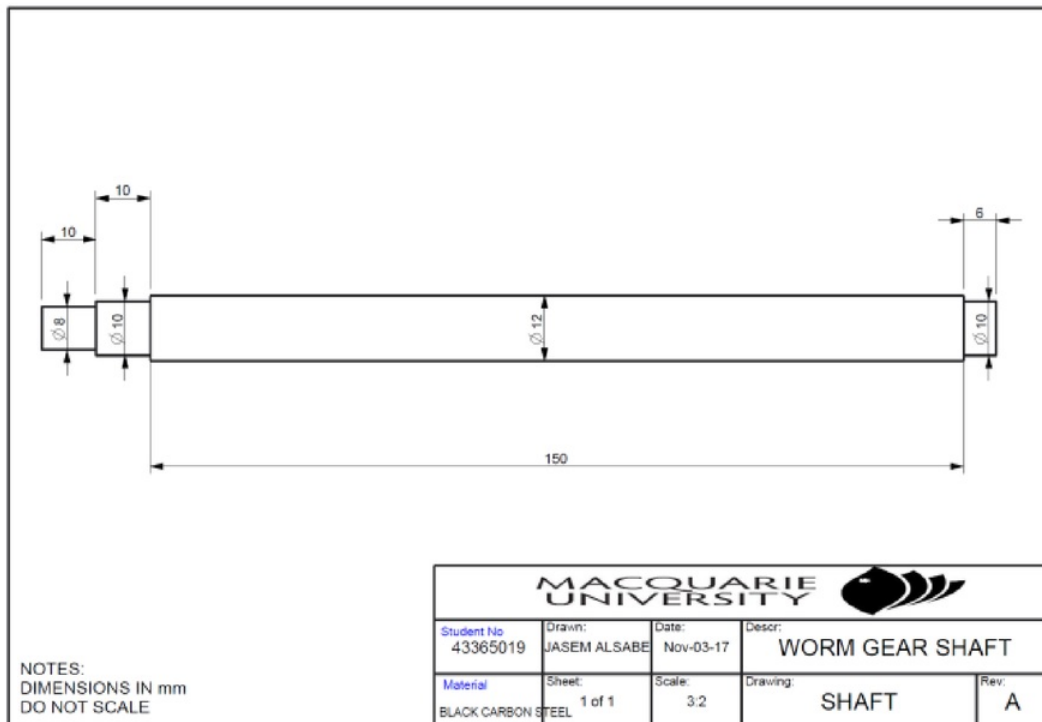


Figure 63: Manufacturing drawing of the shaft.

The shafts will be rotating in the turning machine to a diameter of $\varnothing 12\text{mm}$. Each shaft will be cut using the parting off cutter in the turning machine to a length of 170mm . The shafts will have a coupling part to connect them with the stepper motor shaft. The shafts will be turning in the lathe machine to a diameter of $\varnothing 12\text{mm}$. Each shaft will be cut using the parting off cutter in the lathe machine to a length of 178mm . The whole process of making the shaft is in the lathe machine by turning it as the manufacturing drawing sizes. The $\varnothing 10$ parts are for the bearing fitting and the $\varnothing 8$ is for the coupling part fitting.

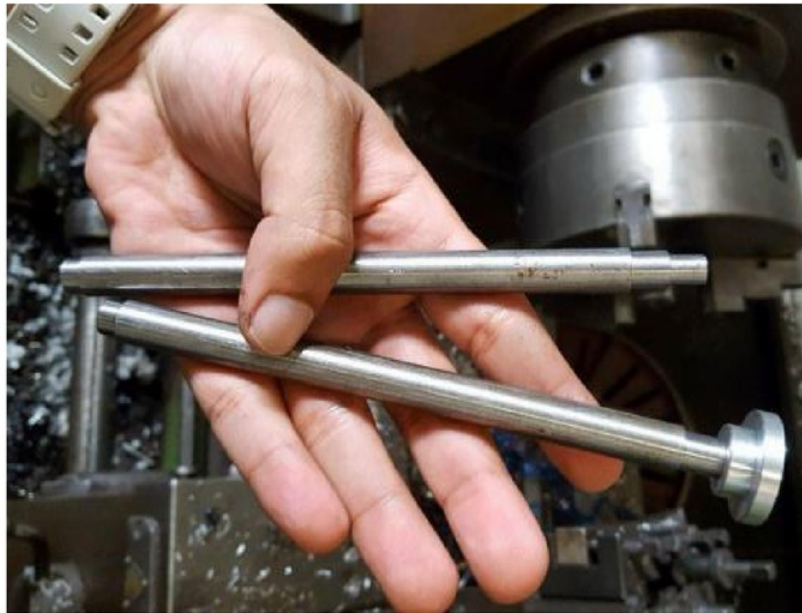


Figure 64: Final shape for the shaft after machining it.

After machining the shaft, the worm wheels need to be fixed in the middle by making sure that distance between the wheel tooth and the bearing are the same in both sides. Then using a 4mm drill bit in the milling machine, a hole is drilled for the rollers pins size 4mm. Which they call it 4mm but its real size is 4.2mm and the reason is to be fixed hardly to connect the worm wheel with the shaft.



Figure 65: Fixing the roller pin in the worm wheel shaft.

6.2.5 Coupling

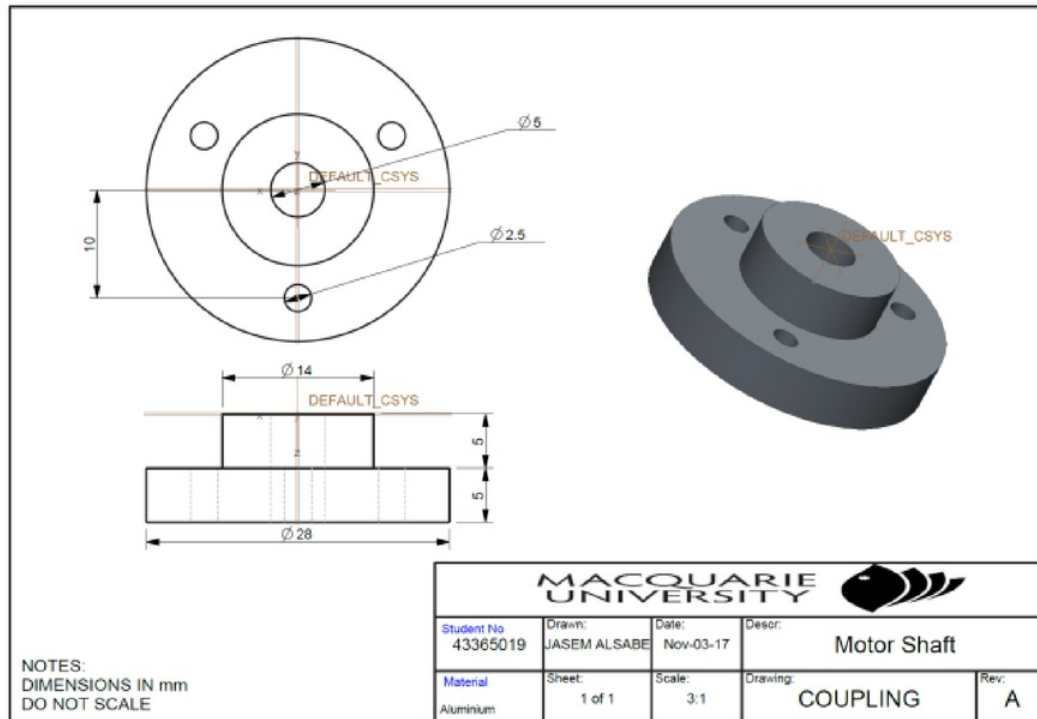


Figure 66: Manufacturing drawing of the motor shaft coupling part.

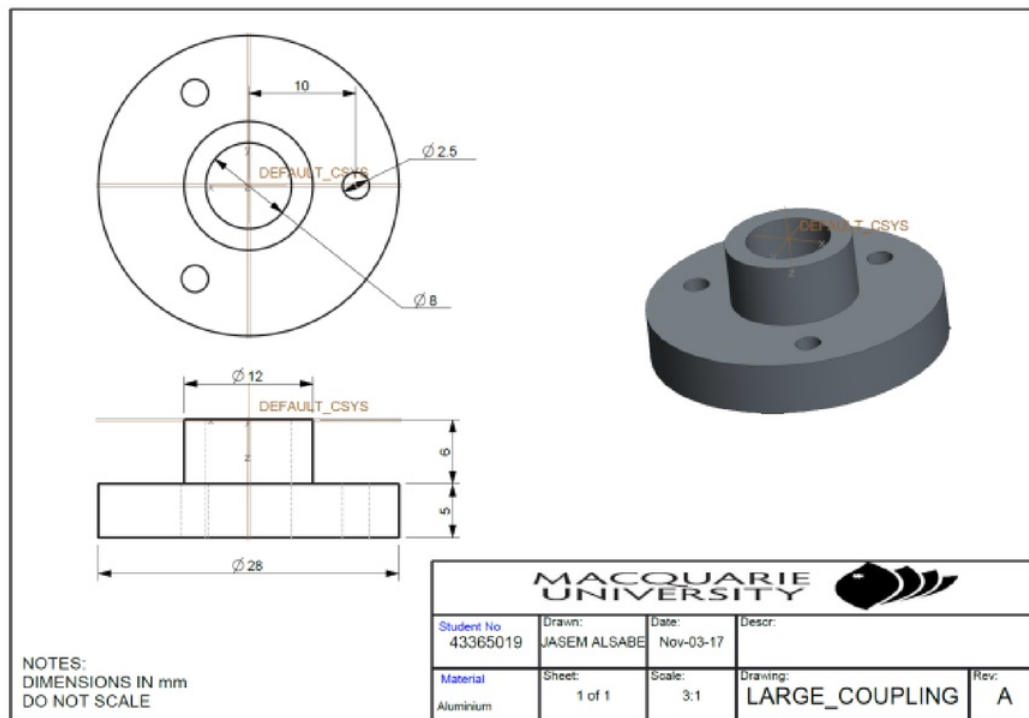


Figure 67: Manufacturing drawing of the shaft coupling part.

Each shaft is designed to have a pair of coupling part to connect the worm gear shaft with the stepper motor fixed shaft. The coupling part material is chosen to be aluminium which is light and had an enough stiffness for coupling. The manufacturing process began with the lathe machine by using parting off cutter to cut 4 pieces from a $\varnothing 28$ aluminium rod. A pair is cut by 10mm and the other pair by 10mm. After that the parts will be turning with the same machine following the given dimensions in the above manufacturing drawing.

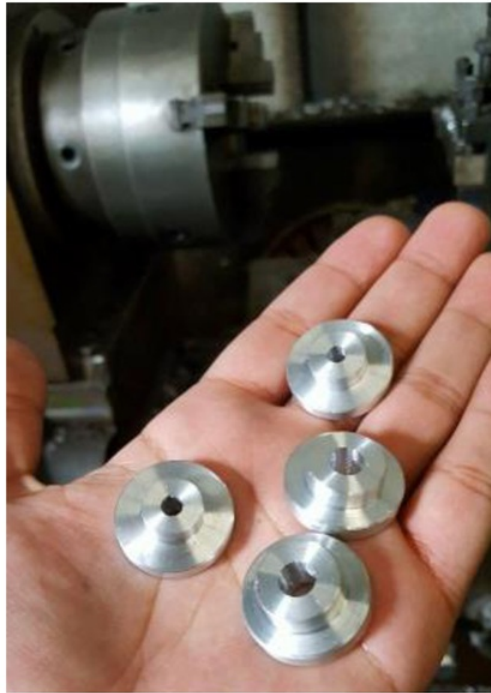


Figure 68: The coupling parts shape after lathe machining.

After that the pin holes need to be drilled. Before drilling them, the pin need to be measured by the micrometre which showed a result of 2.1mm . Therefore, a drill bit of 2.1mm is the suitable size for drilling the pins holes.



Figure 69: Measuring the drill bit by a micrometer to drill an accurate hole size.

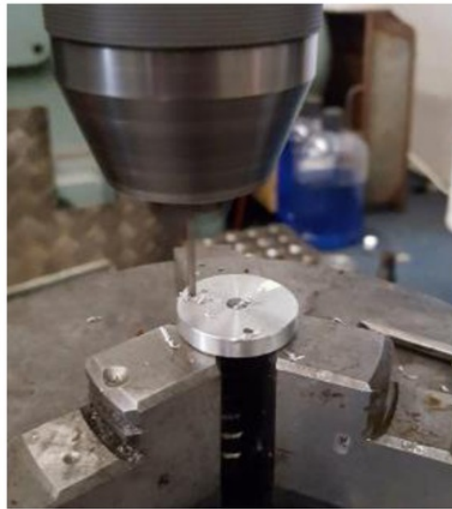


Figure 70: Drilling the pin holes by fixing the coupling with three jaws.

The drilling need to be gradually pushing and gently to avoid braking the small sized bit. Three holes are drilled by leaving a distance of 120° angle between them. If the coupling part need to be fixed in a place which is out of room same as what is going with on here, the pin can be grounded and fixing the shape as the need. After that the pins is fitted in the drilled holes of the coupling component by using a pin punch and it need to be gluing the pins a little bit. LOCTITE which is designed for bonding a cylindrical aluminium fitting parts is the suggested product to do this job as shown in appendix H.



Figure 71: Grounding the pin head to avoid crashing it with the supported components.

For fitting the coupling parts on the fixed motor shaft, a hole of 3.3mm drilled and tapped by a $M4$ handle tap to host the $M4$ grub screw. By adjusting this grub screw the small coupling part will be connected with the fixed motor shaft. The same thing is done for the large coupling part but with a 4.3mm drill bit and tapping the thread with $M5$ handle tap.

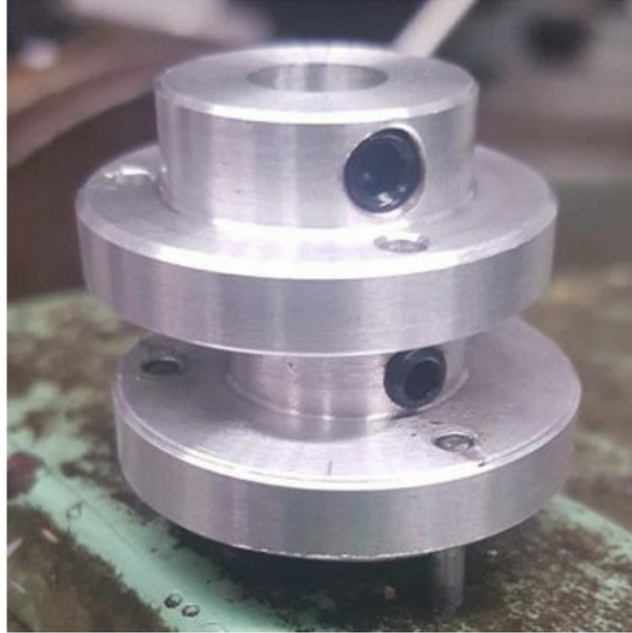


Figure 72: Fixing the grub screw in the small coupling parts.

6.2.6 Guard

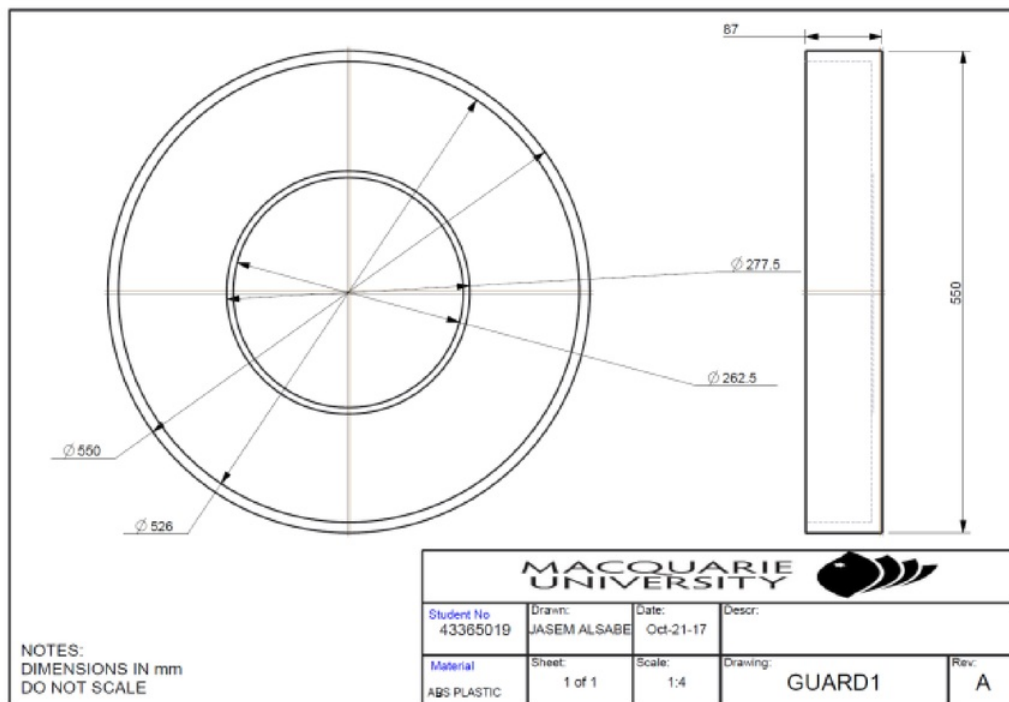


Figure 73: Manufacturing drawing for the guard.

The designed guard is for the future work, as it is mentioned in the previous chapter that guard will be only a flat sheet of 550mm square to host the system for a better project visibility.

Chapter 7

Testing and Refinement

This chapter covers the testing and refinement stage of the project, which begins with testing the prototype assemblies and the whole application. First step is to refine the prototype in case any issues occur. Secondly, testing each assembly directly after it is completely manufactured. The final testing is then carried out for the complete application operation.

7.1 3D Printer Dimension Issue

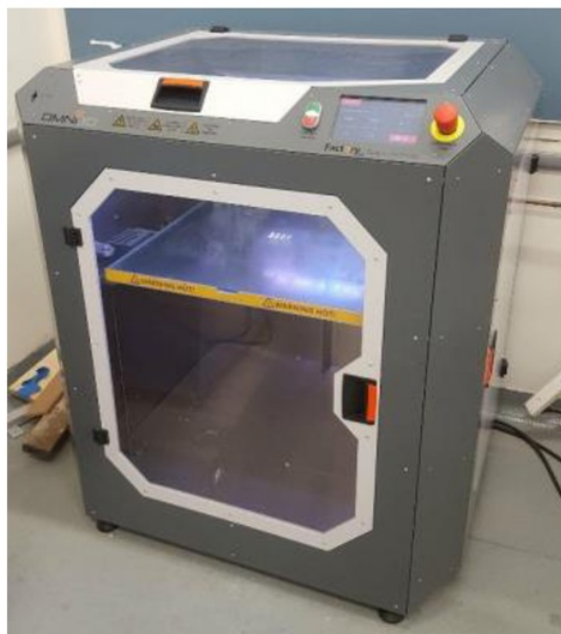


Figure 74: Macquarie University 3D printer.

After printing the systems supported parts which have been fabricated with the above 3D printer, the parts were found to be slightly smaller in dimension than the designed

file indicated it would be. It was noticed after measuring them using the vernier that the difference was more than 2.2mm which is considered to be a very significant difference. The holes of the supported parts are designed to host the bearing of the shaft. This shaft needs to be facing the gear at an accurate height. The 2.2mm difference will change this driving point which in turn will affect the overall functioning of the driving system. This problem has been contributed to the printer itself or with the printing inputs which was carried out by the person who is responsible for that printer. Regardless, the hole diameter can be increased in different ways like polishing. After much testing it was found that the methods that would generally be used to fix these parts was not an accurate way to fix this issue, mostly due to time constraints.

The issue was finally resolved by machining the supported parts to save time and get accurate dimensions. The chosen material for the parts is black nylon. It is a stiff and suitable material for supporting the shaft and motor as the material data sheet shows in appendix K. The machining process began in the lathe machine by turning the $\text{Ø}100\text{mm}$ black nylon disk to a $\text{Ø}60\text{mm}$ which is slightly bigger than the parts size. After that a hole of $\text{Ø}12\text{mm}$ was drilled into the centre of the disk this was made to fit the shaft size of $\text{Ø}12\text{mm}$. The next stage is using a lathe cutter to increase the size of the hole to $\text{Ø}21.5\text{mm}$ to host the $\text{Ø}22\text{mm}$ bearing size. The nylon material can expand easily not like the metals, which helped in this instance. These holes were cut off in a depth of 6mm which is the width of the standard bearing. This exact same lathe cut was also required to be carried out for the other face of the disk. Finally we used the parting cut off tool to cut the disk into two pieces.



Figure 75: Drilling a hole to host the shaft, in the left side the parting cut off tool.

After cutting the parts into a pairs, the circular parts were cut off into a square shape by using the high speed lathe cutter in the milling machine. Before cutting each side, the height need to be measured by the height gage tool.



Figure 76: Cutting the supporting parts by a high speed lathe cutter.

Finally, two holes were drilled below each of the parts by using a 5mm bit drill in the same milling machine and tapping them with a 6mm handle tap.



Figure 77: Supporting shaft parts after machining them.

7.2 Bearing Cage Dimension Issue

The bearing part printed with the accurate inner and outer dimensions except for the bore holes which were found to be smaller than the ceramic balls. The issue was resolved by drilling the holes with a drill bit of 9.5mm . After drilling the holes, the balls were then tested. It was found that the balls were passing the holes as the design intended. Refining the bearing ball holes with the drill was successful.

7.3 Complete System Testing

After machining all the system parts, they can be assembled onto the base table. We began this instruction by marking the spots onto the table, that needed to be drilled. We ensured accuracy by measuring them based on the design and making sure of the bearing points and the shaft centroid distance. After that the base was drilled in using the same marked spots. After fitting the bearings and the shafts into their supporting housing parts, they were fixed onto the table using $M6$ bolts and washers.

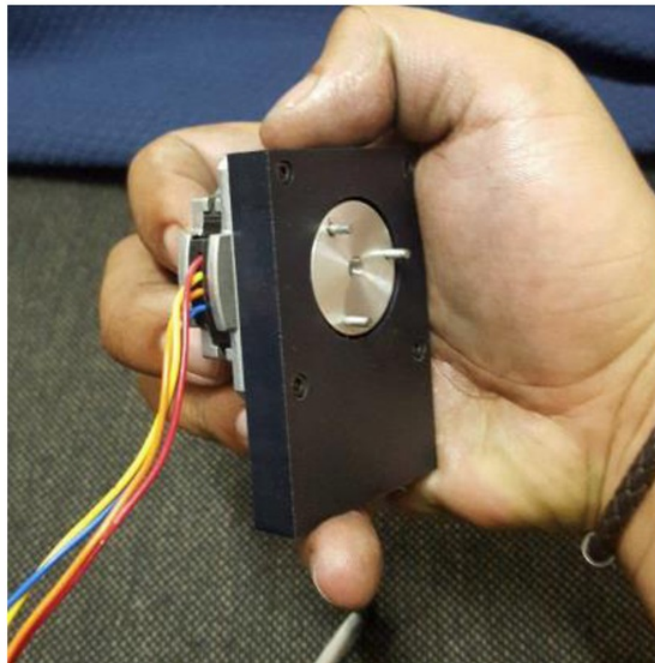


Figure 78: Fixing the motor with the small coupling in the housing part.

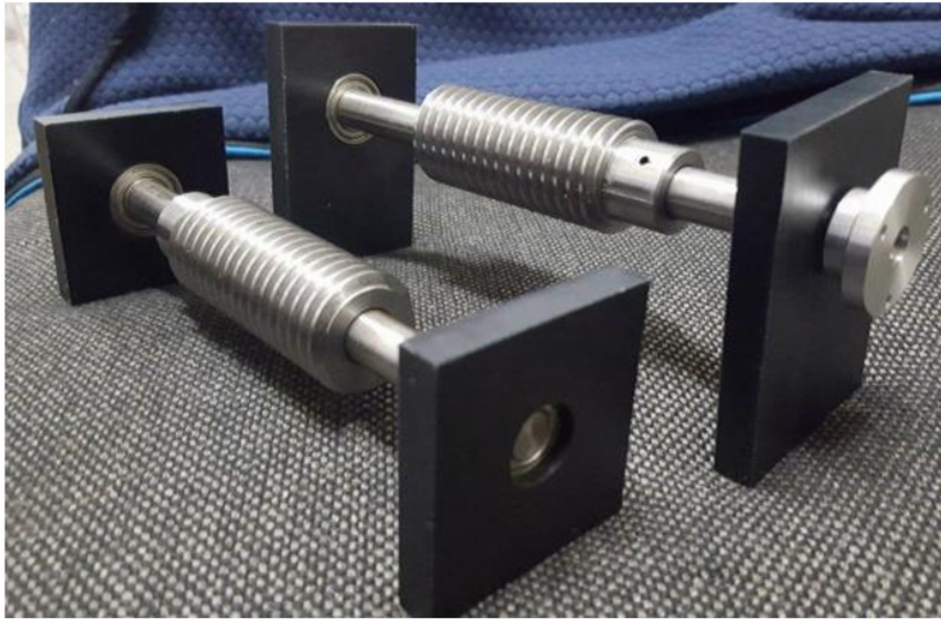


Figure 79: Fixing the shaft and the large coupling in their housing parts.

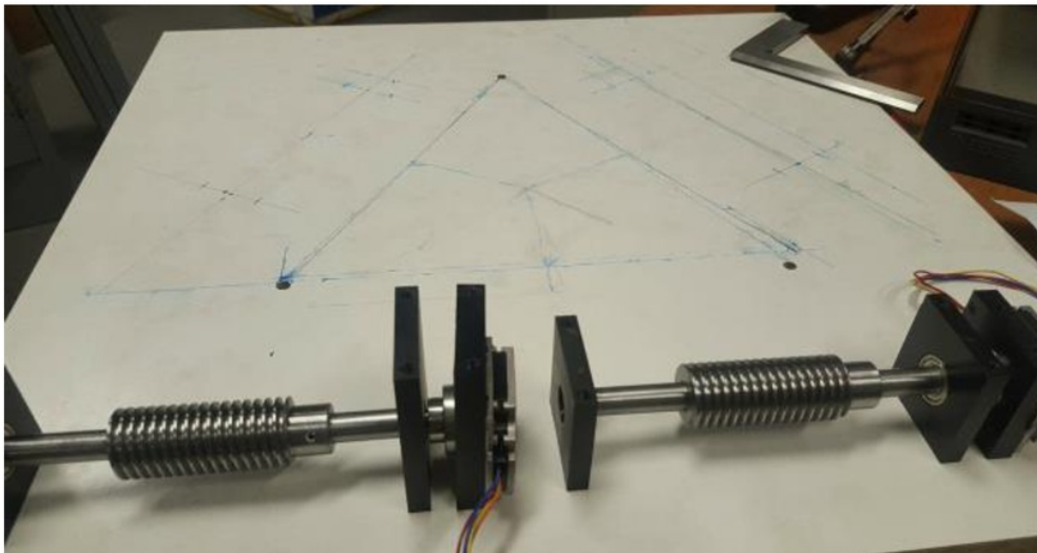


Figure 80: Measuring and marking the drilling spots.

After assembling and checking the centroid worm wheel distance was correct, the system was tested thoroughly by running it repeatedly in the university electronics labs. The antenna planner disks were found to rotate with the desired speed of *47 seconds per 360° revolution*. There was no evidence of any noise occurring between the gears tooth mesh and even in the friction areas. The rotation was very smooth and the only sound was from the ceramic balls rolling which is considered to

be a very positive result. The designed thrust ball bearing and the cage did their specific jobs correctly and the cage was found to be hosting the balls and letting them roll smoothly. The bearing points rollers were rolling all the time and that indicated that their functionality of supporting the gears was working as predicted. The motors in the data sheet show that it ran at 24v. The power supplier that was available in the lab supplied a maximum voltage of 32v. Therefore, both motors cannot be running at the same time as they both require a total voltage of 48v which is more than the maximum voltage available from the power supplier. The table base was moved to an angle of 60 degrees whilst testing the system. The system continued to operate as efficiently as it did when on the stable angle. At this stage, the systematic testing is concluded to be a success without any errors.

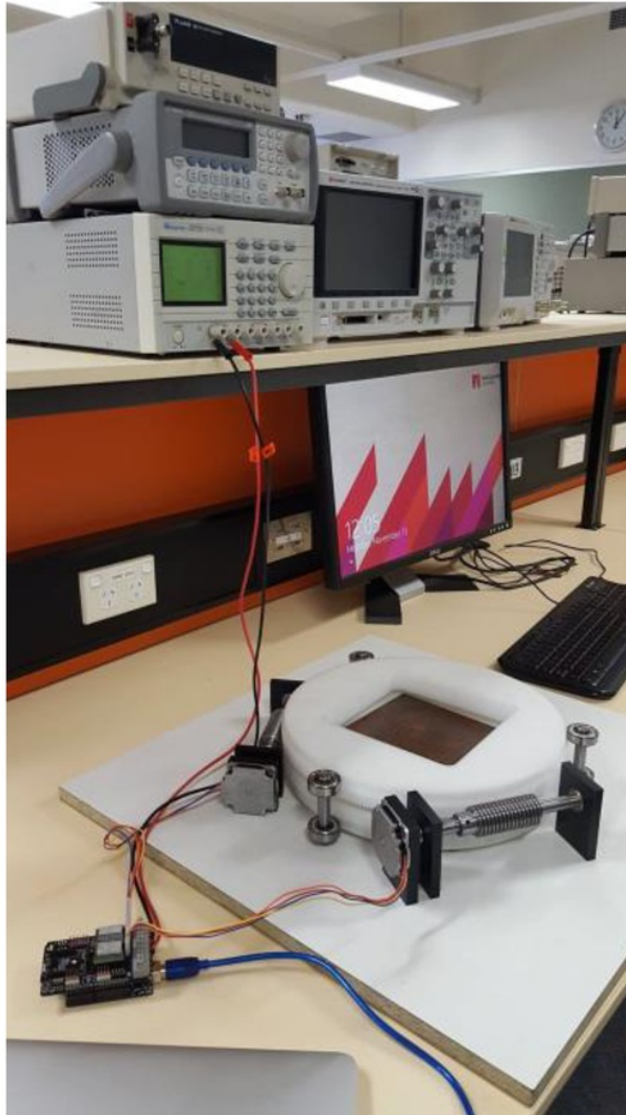


Figure 81: Testing the system in the electronics lab

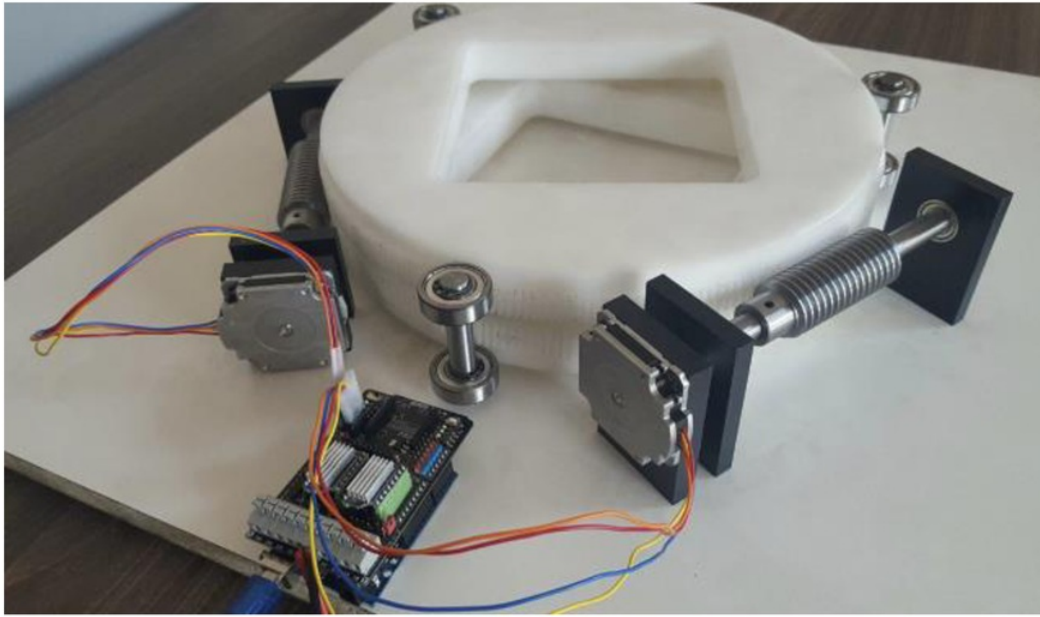


Figure 82: Overall view for the complete system.

Chapter 8

Discussion

The next generation of antenna application development are required to significantly improve its reception capabilities in some regions on earth. This development will provide an invaluable improvement to the function of current internet and mobile phone reception. In order to improve these functions, the university created a brand new planner antenna capable of fulfilling the requirements of reception. Planner plates were created already and now the mechanism for that planner is presented in this thesis. The next stage will be involved making the feed system for that antenna application which required a long period of time to be generated. This mechanism was produced throughout the year of 2017 and has been thoroughly presented in this thesis. The system was designed after developing an understanding of the specifications required for the university antenna planner, and studying serval antenna systems. However, for this specific system, it was an important requirement to do an initial simple prototype prior to the final design. It is useful for testing and finding any issues which had not been accounted for in the initial design.

In the manufacturing stage, it is experienced that it is very important to measure each part before cutting it and measuring it again after each single cut to avoid wasting the time and the budget. The dimensions were very important in the manufacturing stages of this project. High importance was placed on each measurement to ensure that it was being carried out correctly and was accurate. To ensure this, there is a wide range of mechanical measurement tools that were made to produce the accurate desired dimensions.

The antenna gears speed ratio can be increased or decreased by cutting new gears with different tooth calculations. For the worm or helical gears, the factors which change the speed ratio are star type, solar type and planetary type [83]. By changing any of these factors, a faster or slower speed ratio can be used. The current rotating speed can be increased to three second per revelation by replacing the motors and the microcontroller coding. The current rotation accuracy is very high and it is able to rotate through the current stepper motors in an accuracy of 0.375 degree which is very suitable for Macquarie antenna planner. This accuracy achieved duo the gears tooth design. Through the current system, the antenna can be operated in a fixed point after setting the coding by the antenna specialised and the reception can be provided. To make it able to operate while in motion, a feeding system are required to give the orders and the direction to the microcontroller to set that antenna direction and track the satellite while in motion. The assemblies are designed in a way to be ease to assemble to the current table or even any other tables. The components can be removed and fitted easily which add a feature to the mechanical system. The experienced system is able to function in two surfaces, in stable table or in a moving table up to an angle of 60 degree. This feature is duo the design of the system and the chosen materials stiffness and this feature able the system to be used in any antenna

environments in the future work. In addition, the materials resist a temperature of 65 Celsius degree which is a high temperature degree and that is another reason to able the system to operate in different environments. The final system height measured to be less than 70mm and this size is categorised as a low profile comparing with the other similar antenna systems. There is nothing jams between the bottom and the top of the planners and all the elements in that way are used to be non-conductors to avoid disrupting the satellite radiation waves transmission. The final outcome rotation system is unique, quite and flexible.

8.1 Achievements

The target goals of this thesis achieved the predictions thought out prior to commencement of the study. The testing in the previous chapter provided the required evidence to approve the correct functioning of the system. This was approved due to the extensive testing being carried out without experiencing any errors. There were some challenges experienced throughout the testing phases, both before and after designing it.

The main challenge was in eliminating the friction from the system as much as possible. This challenge has been dealt with by designing a complete thrust ball bearing including the cage. These products are not available through suppliers as it is wide, thin and non-conductive. To design a bearing, an intensive study was required to be completed in order to understand it completely. This was carried out because similar studies had not been published in the fundamental mechanical engineering books available to students.

The other challenge was with fixing a driven gear horizontally without any shafts. To overcome this, three bearing points were designed to do this job which led to its successful functioning.

The new antenna mechanism is currently working properly and can be operated for an extended amount of time, in different antenna environments. The specialist antenna planner makers have the ability to set their own input codes and do their own testing as they may need to develop the antenna planner further in the future.

8.1 Costs

The prototype costs are always more expensive than the production costs, the following table shows the prices of the components which can be reduced for production of quantity.

Table 4: Total project cost.

Part	Supplier	Cost
Gears and supporting parts machining	A&A GEAR MAKER	\$1707
Bearing cage	MACUARIE UNIVERSITY	\$150
Ceramic ball for bearings	VXB BALL BEARINGS	\$190
Stepper motors	MACUARIE UNIVERSITY	\$0
Base	MACUARIE UNIVERSITY	\$0
Dual microcontroller	MACUARIE UNIVERSITY	\$0
Bolts	MACUARIE UNIVERSITY	\$0
Washers and Grub screws	LM FASTENERS PTY LTD	\$18
10 deep groove bearings and Circlips	STATEWIDE BEARINGS	\$56.5
Acetal material	CUT TO SIZE PLASTICS	\$278
Total Cost (\$AUD)		\$2249.5

Chapter 9

Conclusions

This thesis presents the new mechanism development within Macquarie University antenna planner. The thesis introduced a background about the general antenna system and the new antenna technology planner which was made by the university. The introduction consists the whole plan and stages for the development during the year. After that a summarise of different related systems was shown and discussed including the university existing mechanism. Then, the system was developed by studying the existing system, examining the existing errors and incorporating these into different antenna systems. Four concepts were produced, discussed and resolved the systemic errors to produce a final design free of systemic errors. The resulted system included a worm gearing system to rotate the antenna planner through a predicted method. In this chapter, a summery and overview for the system is given and a guide of future work for the systems continuous performance.

9.1 Review

In this paper, the thesis addresses a literary review of engineers and researchers who developed the antenna mechanical systems using a range of various methods. After studying the systematic issues, they came across, a new system was designed and tested to produce a mechanism that was free of these errors. The scope was for two performance based results; these include reducing the friction as possible and making a flexible rotation system. A design was produced for the new system and all of the manufacturing processes have been stated in detail in the above thesis report. The results of the gearing system proved to be a success. It delivered the required system based on the application specifications needed. A system that rotates gears by a stepper motor with an accurate rotation angle. The design included a bearing cage designed specially to hold the driven gears. The bearing idea was required to hold the axial loads and to it operate with a non-conduct ceramic balls to avoid disrupting the antenna planner radiation signals. In addition, there are three bearing points around the system. This bearing set is designed to hold the driven gears horizontally and protect them from the possibility of slipping. The driving wheel is supported with a deep groove bearing to reduce the friction of the rotation, increase the speed and hold the shaft loads.

9.2 Future Work

This new system has been built for long term usage. However, there is always the requirement for continuously updated technology within the current antenna application

environment. This is to ensure it has the ability to keep up with technology advancements and to add on extra features that the system may require in the future. This chapter introduces some extra features that can be added to the application, however, each feature requires a further period of time to study and ensure they are the correct methods to progress the antenna in the future.

9.2.1 Feedback System

A feedback system is used in almost all current established antennas systems. Its function is to track the satellite and improve the tracking system [84]. Sensors are used to operate the feedback system and can be added to the system by a connection with a micro-controller chip [85].

9.2.2 Accurate Angle Rotation

The motor has a 1.8 step angle which means 200 steps per revolution. The driving worm gear is attached with the motor shaft count as a single tooth only and the driven gear as 240 teeth. Therefore, the step ratio can be calculated as:

$\frac{1}{\text{motor steps}} \times \text{number of the driven gear teeth} = \frac{1}{200} \times 240 = \frac{1}{48000}$, which is very positive for the speed and accuracy.

The mechanism is designed to rotate in a very accurate angle through the worm gear. To have this accurate angle rotation, a requirement is setting the correct microcontroller input codes which provides a set of instructions to rotate the planner driven gear to these angles. In the input codes, by setting the frequency, it can control the motor rotation which enables accurate positioning of the antenna planner to its required accurate angles [86].

9.2.3 Stability

As the application functionality is to provide an internet and mobile reception directly from the satellite, it can be either used on top of cars, planes, trains or boats. However, the motion of these transports is not always in the same horizontal angles. They may move in a different angle to what is currently acceptable, for example when a plane takes off or lands it will be moving in a different angle direction.

The present system is designed to be fixed onto a base, which will be moving with the same transport body. This might affect the system operation as it is designed to operate in a limit of angles. To increase the angle limitation, a stability base system can be used instead of the fixed base [87] [88]. In addition, a third bearing is required for this type of system, the balls and a spare cage are also available already. Furthermore, drilling a hole on the driven gear can save the gear weight which in turn can reduce the loads and the forces enabling it to have an easier rotation and increase the angle limitation.

9.2.4 Guard

The guard design is attached in the prototyping chapter and the material of that guard can be chosen based on its different environment requirements.

Appendix A

ABS Material Data Sheet [89]

ABS Material Data Sheet


Physical Properties	Metric	English	Comments
Density	1.04 g/cc	0.0376 lb/in ³	Grade Count = 3
Melt Flow	18 - 23 g/10 min	18 - 23 g/10 min	Average = 21.3 g/10 min; Grade Count = 3
Mechanical Properties			
Hardness, Rockwell R	103 - 112	103 - 112	Average = 110; Grade Count = 3
Tensile Strength, Yield	42.5 - 44.8 MPa	6160 - 6500 psi	Average = 44 MPa; Grade Count = 3
Elongation at Break	23 - 25 %	23 - 25 %	Average = 24.3%; Grade Count = 3
Flexural Modulus	2.25 - 2.28 GPa	326 - 331 ksi	Average = 2.3 GPa; Grade Count = 3
Flexural Yield Strength	60.6 - 73.1 MPa	8790 - 10600 psi	Average = 68.9 MPa; Grade Count = 3
Izod Impact, Notched	2.46 - 2.94 J/cm	4.61 - 5.51 ft-lb/in	Average = 2.8 J/cm; Grade Count = 3
Electrical Properties			
Arc Resistance	120 sec	120 sec	Grade Count=1
Comparative Tracking Index	600 V	600 V	Grade Count=1
Hot Wire Ignition, HWI	15 sec	15 sec	Grade Count = 1
High Amp Arc Ignition, HAI	120 arcs	120 arcs	Grade Count = 1
High Voltage Arc-Tracking Rate, HVTR	25 mm/min	0.984 in/min	Grade Count = 1
Thermal Properties			
Maximum Service Temperature, Air	88 - 89 °C	190 - 192 °F	Average = 88.7°C; Grade Count = 3
Deflection Temperature at 1.8 MPa (264 psi)	88 - 89 °C	190 - 192 °F	Average = 88.7°C; Grade Count=3
Vicat Softening Point	100 °C	212 °F	Grade Count = 1
Flammability, UL94	HB	HB	Grade Count = 3

Appendix B

Acetal Material Data Sheet [90]

WS Hampshire Inc.

Over 100 Years of Non-Metallic Material Fabrication



ACETAL

Acetal is the common name for a family of thermoplastics with the chemical name "PolyOxy-Methylene". Acetal is available in a general purpose copolymer grade, a homopolymer version (Delrin®), and several filled grades. Acetal provides high strength and stiffness, enhanced dimensional stability, and is easy to machine. As a semi-crystalline material, acetal is characterized by a low coefficient of friction and good wear, high strength, stiffness, dimensional stability, very low moisture absorption, good wear and abrasion resistance and a wide range chemical resistance.

ACETAL GRADES

ACETAL COPOLYMER (unfilled)

The copolymer grade offers excellent performance at a slightly lower cost than Delrin®. Acetal copolymer may exhibit center line porosity, but porosity-free material is available. Certain grades are FDA, USDA, NSF, Canada AG and 3-A Dairy compliant. Low stress levels and high strength assure flatness and dimensional stability up to a maximum continuous service temperature of 180°F (80°C). Acetal copolymers are available in a wide variety of colors, including **RED, ORANGE, YELLOW, GREEN, BLUE, VIOLET, BLACK, WHITE & NATURAL**.

DELIRIN® (unfilled)

Delrin® acetal homopolymer offers slightly higher mechanical properties than acetal copolymer, but may contain a low density center (also known as "center line porosity") especially in large cross-sections. The homopolymer also gives slightly less chemical resistance than copolymer acetal. For example, Delrin® is ideal for small diameter, thin-walled bushings that benefit from the additional strength and rigidity of homopolymer acetal. Delrin® is available **BLACK & NATURAL** colors.

NOTE: In 2002, DuPont Company discontinued production of Delrin® II 550SA resin ... this has been replaced by Delrin® 511P.

DELIRIN® AF (PTFE-filled)

This material is manufactured from Delrin® homopolymer resin which has been uniformly filled with a dispersion of PTFE fibers. Delrin® AF is a unique thermoplastic material for use in moving parts in which low friction and long wear life are important. It retains 90% of the mechanical strength of unfilled acetal homopolymer, while offering very low friction and almost no "slip-stick" behavior. Delrin® AF is **BROWN** in color.

TYPICAL PROPERTIES OF ACETALS

ASTM or UL test	Property	Acetal Copolymer	Delrin® Homopolymer	Delrin® AF PTFE-filled
PHYSICAL				
D792	Density (lb/in³) (g/cm³)	0.051 1.41	0.051 1.41	0.054 1.5
D570	Water Absorption, 24 hrs (%)	0.2	0.2	0.2
MECHANICAL				
D638	Tensile Strength (psi)	9,500	11,000	8,000
D638	Tensile Modulus (psi)	400,000	450,000	435,000
D638	Tensile Elongation at Break (%)	30	30	15
D790	Flexural Strength (psi)	12,000	13,000	12,000
D790	Flexural Modulus (psi)	400,000	450,000	435,000
D695	Compressive Strength (psi)	15,000	16,000	16,000
D695	Compressive Modulus (psi)	400,000	450,000	350,000
D785	Hardness, Rockwell	M88 / R120	M89 / R122	M85 / R115
D256	IZOD Impact Notched (ft-lb/in)	1	1	0.7
THERMAL				
D696	Coefficient of Linear Thermal Expansion (x 10⁻⁴ in./in./°F)	5.4	4.7	5
D648	Heat Deflection Temp (°F / °C) at 264 psi	220 / 104	250 / 121	244 / 118
D3418	Melting Point Temp (°F / °C)	335 / 168	347 / 175	347 / 175
-	Max Operating Temp (°F / °C)	180 / 82	180 / 82	180 / 82
C177	Thermal Conductivity (BTU-in/ft²-hr-°F) (x 10⁻⁴ cal/cm-sec-°C)	1.6 5.5	2.5 8.6	-
UL94	Flammability Rating	HB	HB	HB
ELECTRICAL				
D149	Dielectric Strength (V/mil) short time, 1/8" thick	420	450	400
D150	Dielectric Constant at 1 MHz	3.8	3.7	3.1
D150	Dissipation Factor at 1 MHz	0.005	0.005	0.01
D257	Volume Resistivity (ohm-cm) at 50% RH	1015	1015	3.0 x 10¹¹

NOTE: The information contained herein are typical values intended for reference and comparison purposes only. They should NOT be used as a basis for design specifications or quality control. Contact us for manufacturers' complete material property datasheets.

All values at 73°F (23°C) unless otherwise noted. DELRIN is a registered trademark of DuPont

Appendix C

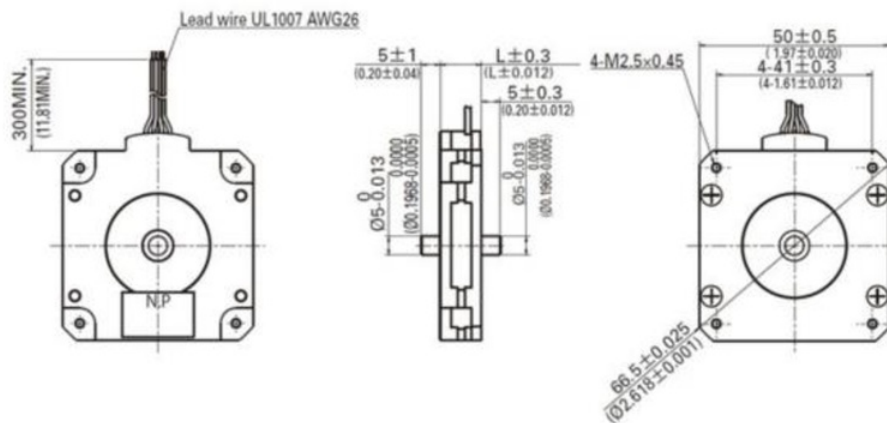
Arduino Codes [91]

```
/*
This sample code is for testing the 2 stepper motors
The rotation velocity can be adjusted by the code switch
Microcontroller: Arduino UNO
*/

int M1dirpin = 7; //Motor X direction pin
int M1steppin = 6; //Motor X step pin
int M1en=8; //Motor X enable pin
int M2dirpin = 4; //Motor Y direction pin
int M2steppin = 5; //Motor Y step pin
int M2en=12; //Motor Y enable pin
void setup()
{
  pinMode(M1dirpin,OUTPUT);
  pinMode(M1steppin,OUTPUT);
  pinMode(M1en,OUTPUT);
  pinMode(M2dirpin,OUTPUT);
  pinMode(M2steppin,OUTPUT);
  pinMode(M2en,OUTPUT);
  digitalWrite(M1en,LOW); // Low Level Enable
  digitalWrite(M2en,LOW); // Low Level Enable
}
void loop()
{
  int j;
  delayMicroseconds(2);
  digitalWrite(M1dirpin,LOW);
  digitalWrite(M2dirpin,LOW);
  for(j=0;j<=5000;j++){
    digitalWrite(M1steppin,LOW);
    digitalWrite(M2steppin,LOW);
    delayMicroseconds(2);
    digitalWrite(M1steppin,HIGH); //Rising step
    digitalWrite(M2steppin,HIGH);
    delay(1);}
}
```

Appendix D

Stepper Motor Dimensions [92]



Appendix E


Standard Module Sizes [16]

NORMAL MODULES	
millimetres	
1st choice	2nd choice*
1	1.125
1.25	1.375
1.5	1.75
2	2.25
2.5	2.75
3	3.5
4	4.5
5	5.5
6	(6.5)
	7
8	9
10	11
12	14
16	18
20	22
25	28
32	36
40	45
50	

Recommended module for gears (Australian standards)

Appendix F

Black Carbon Steel Material Data Sheet [93]

**Atlas
Specialty
Metals**

Atlas 1045

Medium Tensile Carbon Steel Bar 1045

Colour code: Jade Green

Introduction
Atlas 1045 is a fully killed plain carbon steel product containing nominally 0.45% carbon. This grade was formerly designated as K1045. Atlas 1045 is supplied based on it meeting specified chemical composition requirements only.

Related Specifications
Bar in grade 1045 is supplied in accordance with the requirements of JIS J4051 grade S45C and/or AS1442 grade 1045 in the case of black bar, and AS1443 grade 1045 in the case of bright (cold finished) bar.

Chemical Composition*Specification values in %*

C	Si	Mn	P	S
0.43-0.50	0.10 - 0.35	0.60-0.90	≤ 0.040	≤ 0.040

Conditions of Supply – Typical Mechanical Properties
Atlas 1045 is not guaranteed to meet any specified minimum mechanical properties and the values in the table below reflect typical properties only. These values reflect grade D6 (AS 1443) for cold drawn sections, grade T6 (AS 1443) for turned and polished and grade 6 (AS 1442) for rolled (black) sections. Brinell Hardness (HB) is not specified in these standards.

Condition	Diameter (mm)	Tensile Strength (MPa)	Yield Stress (MPa)	Elongation (% in 50mm)	Hardness (HB)
Cold Drawn	Up to 16mm inclusive	690 min	540 min	8 min	207 min
	>16mm to 38mm incl	650 min	510 min	8 min	195 min
	>38mm to 80mm incl	640 min	500 min	9 min	190 min
As rolled / Turned and Polished	All sizes to 260mm	600 min	300 min	14 min	179 min

Atlas 1045 Bright Bar can be supplied as D6 or T6 (or equivalent) with guaranteed mechanical properties on special order request. Atlas 1045 Black Bar can be supplied in the normalised condition with guaranteed mechanical properties on special order request.

Revised April 20061 of 4

W www.atlasmetals.com.au | Technical Assistance | E tech@atlasmetals.com.au

Appendix G

Gear Finder Tool [94]

Gear Finder

<i>Ratio Gears</i>	<i>Actual Ratio</i>	<i>Ratio Error</i>
21 / 104 x 23 / 120	0.038701923077	0.000002033524
21 / 114 x 25 / 119	0.038699690402	0.000000199151

2 of 2 gear sets have been shown

Enter Gear Ratio here --> 0.0386998895532480525

Appendix H

Loctite Data Sheet [95]



Technical Data Sheet

LOCTITE® 680™

(TDS for the new formulation of LOCTITE® 680™) September 2013

PRODUCT DESCRIPTION

LOCTITE® 680™ provides the following product characteristics:

Technology	Acrylic
Chemical Type	Methacrylate ester
Appearance (uncured)	Green liquid ^{MS}
Fluorescence	Positive under UV light ^{MS}
Components	One component - requires no mixing
Viscosity	Medium
Cure	Anaerobic
Secondary Cure	Activator
Application	Retaining
Strength	High

LOCTITE® 680™ is designed for the bonding of cylindrical fitting parts, particularly where low viscosity is required. The product cures when confined in the absence of air between close fitting metal surfaces and prevents loosening and leakage from shock and vibration. LOCTITE® 680™ provides robust curing performance. It not only works on active metals (e.g. mild steel) but also on passive substrates such as stainless steel and plated surfaces. The product offers high temperature performance and oil tolerance. It tolerates minor surface contaminations from various oils, such as cutting, lubrication, anti-corrosion and protection fluids.

This Technical Data Sheet is valid for LOCTITE® 680™ manufactured from the dates outlined in the "Manufacturing Date Reference" section.

NSF International
Certified to ANSI/NSF Standard 61 for use in commercial and residential potable water systems not exceeding 82° C. **Note:** This is a regional approval. Please contact your local Technical Service Center for more information and clarification.

TYPICAL PROPERTIES OF UNCURED MATERIAL

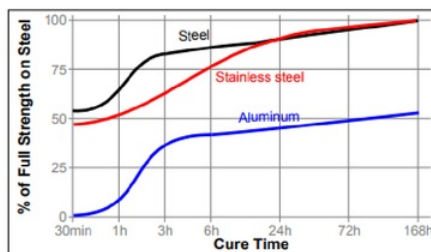
Specific Gravity @ 25 °C	1.1
Viscosity, Brookfield - RVT, 25 °C, mPa-s (cP): Spindle 3, speed 20 rpm,	750 to 1,750 ^{MS}
Viscosity, Cone & Plate, 25 °C, mPa-s (cP):	
Shear rate 129 s ⁻¹	650 to 1,850

Flash Point - See MSDS

TYPICAL CURING PERFORMANCE

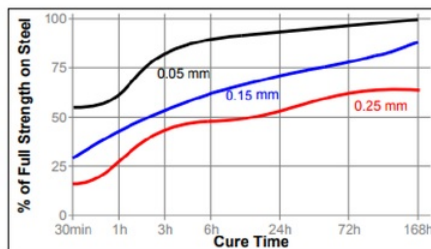
Cure Speed vs. Substrate

The rate of cure will depend on the substrate used. The graph below shows the shear strength developed with time on steel pins and collars compared to different materials and tested according to ISO 10123.



Cure Speed vs. Bond Gap

The rate of cure will depend on the bondline gap. The following graph shows shear strength developed with time on steel pins and collars at different controlled gaps and tested according to ISO 10123.



Appendix I

Metric Tap and Drill Standard Sizes [96]

Metric Tap & Clearance Drill Sizes		Tap Drill				Clearance Drill			
		75% Thread for Aluminum, Brass, & Plastics		50% Thread for Steel, Stainless, & Iron		Close Fit		Standard Fit	
Screw Size (mm)	Thread Pitch (mm)	Drill Size (mm)	Closest American Drill	Drill Size (mm)	Closest American Drill	Drill Size (mm)	Closest American Drill	Drill Size (mm)	Closest American Drill
M1.5	0.35	1.15	56	1.25	55	1.60	1/16	1.65	52
M1.6	0.35	1.25	55	1.35	54	1.70	51	1.75	50
M 1.8	0.35	1.45	53	1.55	1/16	1.90	49	2.00	5/64
M 2	0.45	1.55	1/16	1.70	51	2.10	45	2.20	44
	0.40	1.60	52	1.75	50				
M 2.2	0.45	1.75	50	1.90	48	2.30	3/32	2.40	41
M 2.5	0.45	2.05	46	2.20	44	2.65	37	2.75	7/64
M 3	0.60	2.40	41	2.60	37	3.15	1/8	3.30	30
	0.50	2.50	39	2.70	36				
M 3.5	0.60	2.90	32	3.10	31	3.70	27	3.85	24
M 4	0.75	3.25	30	3.50	28	4.20	19	4.40	17
	0.70	3.30	30	3.50	28				
M 4.5	0.75	3.75	25	4.00	22	4.75	13	5.00	9
M 5	1.00	4.00	21	4.40	11/64	5.25	5	5.50	7/32
	0.90	4.10	20	4.40	17				
	0.80	4.20	19	4.50	16				
M 5.5	0.90	4.60	14	4.90	10	5.80	1	6.10	B
M 6	1.00	5.00	8	5.40	4	6.30	E	6.60	G
	0.75	5.25	4	5.50	7/32				
M 7	1.00	6.00	B	6.40	E	7.40	L	7.70	N
	0.75	6.25	D	6.50	F				
M 8	1.25	6.80	H	7.20	J	8.40	Q	8.80	S
	1.00	7.00	J	7.40	L				
M 9	1.25	7.80	N	8.20	P	9.50	3/8	9.90	25/64
	1.00	8.00	O	8.40	21/64				
M 10	1.50	8.50	R	9.00	T	10.50	Z	11.00	7/16
	1.25	8.80	11/32	9.20	23/64				
	1.00	9.00	T	9.40	U				
M 11	1.50	9.50	3/8	10.00	X	11.60	29/64	12.10	15/32
M 12	1.75	10.30	13/32	10.90	27/64	12.60	1/2	13.20	33/64
	1.50	10.50	Z	11.00	7/16				
	1.25	10.80	27/64	11.20	7/16				
M 14	2.00	12.10	15/32	12.70	1/2	14.75	37/64	15.50	39/64
	1.50	12.50	1/2	13.00	33/64				
	1.25	12.80	1/2	13.20	33/64				
M 15	1.50	13.50	17/32	14.00	35/64	15.75	5/8	16.50	21/32
M 16	2.00	14.00	35/64	14.75	37/64	16.75	21/32	17.50	11/16
	1.50	14.50	37/64	15.00	19/32				
M 17	1.50	15.50	39/64	16.00	5/8	18.00	45/64	18.50	47/64
M 18	2.50	15.50	39/64	16.50	41/64	19.00	3/4	20.00	25/32
	2.00	16.00	5/8	16.75	21/32				
	1.50	16.50	21/32	17.00	43/64				
M 19	2.50	16.50	21/32	17.50	11/16	20.00	25/32	21.00	53/64
M 20	2.50	17.50	11/16	18.50	23/32	21.00	53/64	22.00	55/64
	2.00	18.00	45/64	18.50	47/64				
	1.50	18.50	47/64	19.00	3/4				



the premier source of parts and accessories for mini lathes and mini mills

LittleMachineShop.com • (800) 981-9663

Circlip Standard Sizes [97]

STANDARD EXTERNAL CIRCLIPS EUROPEAN SPECIFICATIONS

D1400 INCORPORATING DIN 471 & BS3673 Pt.4

All dimensions in mm

Circlip on shaft

Circlip in groove

Lug for sizes 3 to 9 mm

Alternative lug for sizes 4-8 mm

Most sizes over 185 mm are without lugs

Beam configuration on some larger sizes

Size printed in blue are preferred sizes

† Thrust load calculations see pages 9 & 10

SIZE CODE	Shaft				Groove (G)				Circlip (F)												Wt. (kg)	TcT (N)	TgT (N)
	S	G	Tol.	W	Tol.	n (mm)	a	Tol.	Tol.	C	C1	L	b	h	h (mm)								
9000	3	2.8	+0.00	0.50	0.50	0.3	0.10	0.40	2.7	7.0	6.6	1.9	0.8	1.0	0.02	1170	150						
0040	4	3.2	+0.00	0.50	0.50	0.3	0.10	0.40	2.7	-0.04	8.6	8.2	2.2	0.9	1.0	0.03	1600	190					
0050	5	4.8	+0.00	0.70	0.70	0.3	0.10	0.40	4.7	-0.15	10.3	9.8	2.5	1.1	1.0	0.06	2500	100					
0060	6	5.7	+0.048	0.80	0.80	0.6	0.15	0.70	8.6		11.7	11.1	2.7	1.3	1.2	0.13	4100	240					
0070	7	6.7		0.90	0.90	0.6	0.15	0.80	6.5		13.5	12.8	3.1	1.4	1.2	0.18	5600	400					
0080	8	7.5	+0.00	0.90	0.90	0.6	0.20	0.80	7.4	-0.06	14.7	14.0	3.2	1.5	1.2	0.20	6200	600					
0090	9	8.6	0.06	1.10	1.10	0.8	0.20	1.00	8.4	-0.18	16.0	15.2	3.3	1.7	1.2	0.32	8800	680					
0100	10	9.6		1.10	1.10	0.8	0.20	1.00	9.3		17.0	16.2	3.3	1.8	1.5	0.40	9700	750					
0110	11	10.5		1.10	1.10	0.8	0.25	1.00	10.2		18.0	17.1	3.3	1.8	1.5	0.41	10700	1040					
0120	12	11.5		1.10	1.10	0.8	0.25	1.00	11.0		19.0	18.1	3.2	1.8	1.7	0.45	11700	1130					
0130	13	12.4		1.10	1.10	0.9	0.30	1.00	11.9	+0.10	20.2	19.2	3.4	2.0	1.7	0.52	12700	1470					
0140	14	13.4		1.10	1.10	0.9	0.30	1.00	12.9	-0.36	21.4	20.4	3.5	2.1	1.7	0.56	13600	1580					
0150	15	14.3	+0.00	1.10	1.10	1.1	0.35	1.00	13.8		22.6	21.6	3.6	2.2	1.7	0.62	14600	1980					
0160	16	15.2	-0.11	1.10	1.10	1.2	0.40	1.00	14.7		23.8	22.6	3.7	2.2	1.7	0.68	15600	2410					
0170	17	16.2		1.10	1.10	1.2	0.45	1.00	15.7		25.0	23.8	3.8	2.3	1.7	0.77	16600	2580					
0180	18	17.0		1.30	1.30	1.5	0.50	1.20	16.5		26.2	24.8	3.9	2.4	2.0	0.99	17600	3290					
0190	19	18.0		1.30	1.30	1.5	0.50	1.20	17.5		27.2	25.8	4.0	2.5	2.0	1.10	22200	3580					
0200	20	19.0	+0.00	1.30	1.30	1.5	0.60	1.20	18.5		28.4	27.0	4.0	2.6	2.0	1.18	24800	3770					
0210	21	20.0		1.30	1.30	1.5	0.60	1.20	19.5	+0.13	29.6	28.2	4.1	2.7	2.0	1.26	25400	4000					
0220	22	21.0	-0.13	1.30	1.30	1.5	0.60	1.20	20.5	-0.42	30.8	29.4	4.2	2.8	2.0	1.36	26700	4190					
0230	23	22.0		1.30	1.30	1.5	0.65	1.20	21.5		32.0	30.6	4.3	2.9	2.0	1.54	26900	4340					
0240	24	22.9		1.30	1.30	1.7	0.65	1.20	22.2		33.2	31.7	4.4	3.0	2.0	1.52	28000	4980					
0250	25	23.9	+0.00	1.30	1.30	1.7	0.65	1.20	23.2		34.2	32.7	4.4	3.0	2.0	1.70	29200	5180					
0260	26	24.9	+0.00	1.30	1.30	1.7	0.65	1.20	24.2		35.5	33.9	4.5	3.1	2.0	1.76	30400	5390					
0270	27	25.6	-0.21	1.30	1.30	2.1	0.70	1.20	24.9	+0.21	36.7	34.8	4.6	3.1	2.0	1.89	31800	5730					
0280	28	26.6	+0.14	1.60	1.60	2.1	0.70	1.50	25.9	-0.42	37.9	36.0	4.7	3.2	2.0	2.47	40900	7390					
0290	29	27.6		1.60	1.60	2.1	0.70	1.50	26.9		39.1	37.2	4.8	3.4	2.0	2.75	42400	7860					
0300	30	28.6		1.60	1.60	2.1	0.70	1.50	27.9		40.5	38.6	5.0	3.5	2.0	2.50	43800	7520					
0310	31	29.6		1.60	1.60	2.6	0.85	1.50	29.6		43.0	40.7	5.2	3.6	2.5	3.02	46700	10300					
0320	32	30.3		1.60	1.60	2.6	0.85	1.50	30.5		44.0	41.7	5.2	3.7	2.5	3.30	48200	10600					
0330	33	31.3		1.60	1.60	2.6	0.85	1.50	31.5	+0.25	45.4	43.1	5.4	3.8	2.5	3.72	49700	10900					
0340	34	32.3	-0.50	1.60	1.60	3.0	1.00	1.50	32.2		46.8	44.2	5.6	3.9	2.5	3.78	51100	13200					
0350	35	33.0		1.85	1.85	3.0	1.00	1.75	33.2		48.5	45.2	5.6	4.0	2.5	4.09	51400	13860					
0360	36	34.0		1.85	1.85	3.0	1.00	1.75	34.2		50.2	47.6	5.8	4.2	2.5	4.58	54800	14300					
0370	37	35.0		1.85	1.85	3.0	1.00	1.75	35.2		52.6	49.5	6.0	4.5	2.5	5.54	56600	18800					
0400	40	37.5	+0.00	1.85	1.85	3.8	1.25	1.75	38.5		55.7	52.5	6.5	5.0	2.5	5.99	58600	19800					
0420	42	39.5	-0.25	1.85	1.85	3.8	1.25	1.75	41.5		59.1	55.9	6.7	5.0	2.5	6.75	63700	21200					
0430	43	40.5		1.85	1.85	3.8	1.25	1.75	42.5	+0.35	60.1	56.9	6.7	5.0	2.5	7.24	68100	21700					
0440	44	41.5		1.85	1.85	3.8	1.25	1.75	43.5	-0.30	61.3	58.1	6.8	5.0	2.5	7.30	68600	22100					
0470	47	44.5		1.85	1.85	3.8	1.25	1.75	45.5		62.5	59.3	6.9	5.0	2.5	7.51	67900	22800					
0480	48	45.5		1.85	1.85	3.8	1.25	1.75	46.5		64.5	60.8	6.9	5.5	2.5	8.88	80300	26300					
0500	50	47.0		2.15	2.15	4.5	1.50	2.00	47.8		66.0	63.0	7.0	5.5	2.5	9.53	84100	28400					
0520	52	49.0		2.15	2.15	4.5	1.50	2.00	48.8		68.5	65.2	7.1	5.5	2.5	10.35	87400	30500					
0540	54	51.0		2.15	2.15	4.5	1.50	2.00	50.8		70.2	66.4	7.2	5.5	2.5	10.41	88000	31100					
0560	56	52.0		2.15	2.15	4.5	1.50	2.00	51.8		71.8	67.8	7.3	5.5	2.5	10.50	89000	31700					
0580	58	53.0	+0.00	2.15	2.15	4.5	1.50	2.00	52.8	+0.46	73.6	69.0	7.3	5.5	2.5	12.47	93900	32800					
0600	60	55.0	-0.30	2.15	2.15	4.5	1.50	2.00	53.8	-1.10	75.6	71.8	7.4	5.8	2.5	13.89	97100	33600					
0620	62	59.0		2.15	2.15	4.5	1.50	2.00	57.8		77.8	74.0	7.5	6.0	2.5	12.36	100000	35100					
0630	63	60.0		2.15	2.15	4.5	1.50	2.00	58.8		79.0	75.2	7.6	6.2	2.5	13.10	102000	35600					
0650	65	62.0		2.09	2.09	4.5	1.50	2.50	60.8		81.1	77.6	7.6	6.3	3.0	20.44	131000	36600					

Standard material - carbon spring steel. Standard finish - phosphate and oil.

Appendix K

Black Nylon Material Data Sheet [98]



Material	TECAMID 66 GF15 FRT black		Main features
Fillers	glass fiber/flame retardant (halogen free)		→ Good heat deflection temperature
Chemical designation		PA 66	→ High creep resistance
Density	DIN EN ISO 1183	[g/cm³] 1.30	→ Good slide and wear properties
Mechanical properties			→ Hydrolysis and superheated steam resistant
Compressive Modulus	DIN EN ISO 604	[MPa] 2.660	→ Good wear properties
Compressive Strength at 2%	DIN EN ISO 604	[MPa] 46.9	→ Inherent flame retardant
Compressive Strength at 1%	DIN EN ISO 604	[MPa] 27	→ Very good chemical resistance
Tensile strength at yield	DIN EN ISO 527-2	[MPa] 80	
Tensile Elongation at break	DIN EN ISO 527-2	[%] 3	
Tensile Modulus	DIN EN ISO 527-2	[MPa] 5.500	
Flexural Strength	DIN EN ISO 178	[MPa] 119	
Flexural Modulus	DIN EN ISO 178	[MPa] 4.980	
Charpy Impact	DIN EN ISO 179-1EU	[kJ/m²] n.b.	
Burn test results			
Flammability	Pass/Fail [thickness]		
60-s-vertical Bunsen burner test : FAR 25.853 : 25.853(a) App F Part 1 (a)(1)(i) ABD031 : AITM 2.0002A			Pass (4 mm)
Smoke density ABD031 : AITM 2.0007B			Pass
Toxicity ABD031 : AITM 3.0005			Pass

- Main features**
- Good heat deflection temperature
 - High creep resistance
 - Good slide and wear properties
 - Hydrolysis and superheated steam resistant
 - Good wear properties
 - Inherent flame retardant
 - Very good chemical resistance

Information about exemption from liability and terms and conditions of supply can be found in our material datasheets and in our Stock Shapes catalogue or at www.ensinger-online.com.



Curbell Plastics is a proud supplier of Ensinger materials.











Ensinger GmbH · Rudolf-Diesel-Straße 8 · 71154 Nürtingen · Germany
www.ensinger-online.com

Ensinger Inc · 365 Meadowlands Boulevard · Washington, PA 15301 · USA
www.ensinger-inc.com

Appendix L

Consulting Meetings Form

Consultation Meetings Attendance Form

Week	Date	Comments (If applicable)	Student's Signature	Supervisor's Signature
0	27/7/2017	initial design		<i>Nazmul Huda</i>
1	2/8/2017	Materials		<i>Nazmul Huda</i>
2	8/8/2017	Power supplier		<i>Nazmul Huda</i>
3	19/8/2017	Second design		<i>Nazmul Huda</i>
4	21/8/2017	Radiation effect and third design		<i>Nazmul Huda</i>
5	28/8/2017	Existing design issues		<i>Nazmul Huda</i>
6	9/9/2017	Prograss report		<i>Nazmul Huda</i>
7	14/9/2017	Testing design		<i>Nazmul Huda</i>
8		Mid Break		
9	12/10/2017	Gear calculation		<i>Nazmul Huda</i>
10	17/10/2017	Symmetric positioning		<i>Nazmul Huda</i>
11,12		Prototyping and Testing		

References

- [1]. *Airline IT Trends Survey 2016* | SITA. [online] Available at:
<https://www.sita.aero/resources/type/surveys-reports/airline-it-trends-survey-2016>.
- [2]. Huang, T. T. (2016). The impact of the Internet on global industry: New evidence of Internet measurement. *Research in International Business and Finance*, 37, 93-112.
Retrieved from:
<http://www.sciencedirect.com/science/article/pii/S0275531915300143>.
- [3]. J. Ramsay, "Highlights of antenna history," in *IEEE Antennas and Propagation Society Newsletter*, vol. 23, no. 6, pp. 7-20, December 1981.
URL: <http://ieeexplore.ieee.org/stamp/stamp.jsp?tp=&arnumber=1140989&isnumber=25539>.
- [4]. A look at our history. (n.d.). Retrieved June 18, 2017, from
<https://www.gogoair.com/history>.
- [5]. Virgin Australia Selects Gogo For In-Flight Connectivity (Updated). (2017, August 11).
Retrieved September 18, 2017, from: <http://www.thinkom.com/virgin-australia-selects-gogo-flight-connectivity/>.
- [6]. M. U. Afzal and K. P. Esselle, "Steering the Beam of Medium-to-High Gain Antennas Using Near-Field Phase Transformation," in *IEEE Transactions on Antennas and Propagation*, vol. 65, no. 4, pp. 1680-1690, April 2017.
URL: <http://ieeexplore.ieee.org/stamp/stamp.jsp?tp=&arnumber=7857713&isnumber=7892904>.

- [7]. A.A. Mulla, P.N. Vasambekar, Overview on the development and applications of antenna control systems, In Annual Reviews in Control, Volume 41, 2016, Pages 47-57, ISSN 1367-5788, (<http://www.sciencedirect.com/science/article/pii/S1367578816300153>).
- [8]. D'Souza, E. (2016). *MOTOR-DRIVEN MULTI-ROTATION SYSTEM FOR ANTENNA BEAM STEERING* (Bachelor thesis, Australia, 2016). Sydney: Macquarie University.
- [9]. Mulla, Asif & Vasambekar, Pramod. (2017). Speed Rate Corrected Antenna Azimuth Axis Positioning System. 9. 151-158.
- [10]. S. Bryan, P. Ade, M. Amiri, S. Benton, R. Bihary, J. Bock, . . . B. Crill,. (2016). A cryogenic rotation stage with a large clear aperture for the half-wave plates in the spider instrument. *Review of Scientific Instruments*, 87(1), 014501.
- [11]. R. Walters (2012, September 16). Wood Thrust Bearing - Marbles & Ball Bearings. Retrieved from http://woodgears.ca/reader/walters/thrust_bearing.html.
- [12]. Nikolić, S., Antić, D., Danković, B., Milojković, M., Jovanović, Z., Perić, S. Orthogonal functions applied in antenna positioning (2010) *Advances in Electrical and Computer Engineering*, 10 (4), pp. 35-42.
- [13]. H. I. Okumus, E. Sahin and O. Akyazi, "Antenna azimuth position control with classical PID and fuzzy logic controllers," *2012 International Symposium on Innovations in Intelligent Systems and Applications*, Trabzon, 2012, pp. 1-5. URL: <http://ieeexplore.ieee.org/stamp/stamp.jsp?tp=&arnumber=6247049&isnumber=6246930>.
- [14]. Alhasan, E.A.G.M., Alzubaidi, A.J. A design of software driver for a satellite dish antenna positioning system (2015) *IOSR J. Eng.*, 5 (1), pp. 42-44.
- [15]. Designing Plastic Gears and General Considerations of Plastic Gearing. (n.d.). Retrieved July 18, 2017, from <http://www.sdp-si.com/Plastic/design-of-plastic-gears.php>.

- [16]. S. Cheng, "Mechanical stress analysis and gears system design", *ILearn*, 2016.
[Online].Available:
http://ilearn.mq.edu.au/pluginfile.php/43365019/mod_resource/content/1/Mech23_week8.pdf.
- [17]. Kossiakoff, A., W. Sweet, S. Seymour, and S. Biemer, May 2011, *Systems Engineering: Principles and Practice*, 2nd Ed., Hoboken, N.J., John Wiley & Sons, Inc.
- [18]. Air Force Policy Directive 10-28, April 17, 2012, Air Force Concept Development and Experimentation.
- [19]. C. A. Balanis, *Antenna theory analysis and design*, John Wiley, c1997.
- [20]. G. Quintero and A. Skrivervik, "Analysis of planar UWB elliptical dipoles fed by a coplanar stripline," in *IEEE International Conference on Ultra-Wideband, ICUWB 2008*,., Hannover, Germany, 10-12, 2008.
- [21]. P. Dhenge and P. S. Ashtankar, "Effect of different substrate material on the radiation characteristics of the UWB antenna," *2013 International Conference on Communication and Signal Processing*, Melmaruvathur, 2013, pp. 971-976.
- [22]. 6. Jiachun Li and Haipeng Gao, "The exploration and research of plastic gear design and manufacturing theory," *International Conference on Advanced Technology of Design and Manufacture (ATDM 2010)*, Beijing, 2010, pp. 214-218.
- [23]. Z. Youchen, "Research on mechanism of vibration damping of involute cylindrical plastic gears," *2011 International Conference on Electronics, Communications and Control (ICECC)*, Ningbo, 2011, pp. 2790-2792.
- [24]. J. Li, H. Gao and X. Ynag, "The Research of Plastic Gear Tooth Tip Modification and Rack Tool Root Modification," *2010 International Conference on Digital Manufacturing & Automation*, ChangSha, 2010, pp. 778-781.

- [25]. Designing Plastic Gears and General Considerations of Plastic Gearing. (n.d.). Retrieved September 14, 2017, from <http://www.sdp-si.com/Plastic/design-of-plastic-gears.php>.
- [26]. Celine, G. (2009). Multi-Antenna Techniques Require Thorough Testing Solutions. *Electronic Design*, 57(18), 36-41.
- [27]. Jianxin Yu, Huifeng Tan, Jianzheng Wei, Dynamic Testing of an Inflatable Wrap-rib Reflector Antenna, In *Procedia Engineering*, Volume 199, 2017, Pages 483-488, ISSN 1877-7058, <https://doi.org/10.1016/j.proeng.2017.09.053>.
(<http://www.sciencedirect.com/science/article/pii/S1877705817334835>)
- [28]. J. Vikstedt, "Test challenges of smart antenna systems," *2017 IEEE International Symposium on Electromagnetic Compatibility & Signal/Power Integrity (EMCSI)*, Washington, DC, 2017, pp. 1-47. doi: 10.1109/ISEMC.2017.8078068.
- [29]. Guo Yang, Yu Zhong, & Zte Corporation. (2011).
- [30]. Errichello, R. (1992). *Friction, lubrication, and wear of gears*. (Vol. 18).
- [31]. A.C. Rao, Gear friction coefficients and forces, In *Wear*, Volume 53, Issue 1, 1979, Pages 87-93, ISSN 0043-1648.
- [32]. Schwartz, A. (1998). Friction testing. *Air Transport World*, 12.
- [33]. Zhang Dan, Duan Baoyan, Huang Jin, MA Yanling, & Xidian University. (2010).
- [34]. G. List, G. Sutter, J.J. Arnoux, and A. Molinari, "Study of Friction and Wear Mechanisms at High Sliding Speed," *Mechanics of Materials*, 2014. [View at Publisher](#) · [View at Google Scholar](#).
- [35]. What's the difference between prototype and initial samples? (n.d.). Retrieved September 15, 2017, from <https://elsmar.com/Forums/apqp-and-ppap/46555-whats-difference-prototype-initial-samples.html>.

- [36]. Anjoran, R. (2015, August 29). The Importance of Prototype Build before Production - Part 8. Retrieved September 15, 2017, from <https://qualityinspection.org/prototype-build-china/>.
- [37]. Ma, Hui, Feng, Mengjiao, Li, Zhanwei, Feng, Ranjiao, & Wen, Bangchun. (2017). Time-varying mesh characteristics of a spur gear pair considering the tip-fillet and friction. *Meccanica*, 52(7), 1695-1709.
- [38]. Yang Luo, Natalie Baddour, Ming Liang, Effects of gear center distance variation on time varying mesh stiffness of a spur gear pair, In Engineering Failure Analysis, Volume 75, 2017, Pages 37-53, ISSN 1350-6307, <https://doi.org/10.1016/j.engfailanal.2017.01.015>.
- [39]. Hofmann, E., & Getriebebau-NORD Schlicht + Kuechenmeister G.M.B.H. & CO. (1984).
- [40]. Bendix Aviation Corporation. (1947).
- [41]. Friction-free bearing. (2003). *Materials Today*, 6(3), 10.
- [42]. Gubanov Sergej Mikhajlovich, Zjuzin Aleksandr Vasil'Evich, Kolomiets Ehduard Dmitrievich, Reshetnikov Vjacheslav Vital'Evich, Filin Igor' Aleksandrovich, & Otkrytoe Aktsionernoe Obshchestvo "Sibirskij Khimicheskij Kombinat". (2011).
- [43]. Torque Stepper Motor. (2014). *Product Design & Development*, 69(9), 25.
- [44]. William Edward Schmitz, & Westinghouse Electric Corporation. (1985).
- [45]. Prasad, S.A. Hari, Kariyappa, B.S., Nagaraj, R., & Thakur, S.K. (2009). Micro controller based Ac power controller. *Wireless Sensor Network (WSN)*, 1(2), 76.
- [46]. Anonymous. (2004). Microcontroller. *Wireless Design & Development*, 12(10), 42.

- [47]. Mark T. MacLean-Blevins, 7 - Final detailed design, In *Plastics Design Library*, William Andrew Publishing, 2018, Pages 197-223, *Designing Successful Products with Plastics*, ISBN 9780323445016, <https://doi.org/10.1016/B978-0-323-44501-6.00007-6>.
- [48]. Ochi Shinya, & Koyo Seiko CO Ltd. (2006).
- [49]. International Society for Boundary Elements. (1989). *Engineering Analysis with Boundary Elements*.
- [50]. Zheng Li, J., SpringerLink, & SpringerLINK ebooks - Engineering. (2015). *CAD, 3D Modeling, Engineering Analysis, and Prototype Experimentation : Industrial and Research Applications / by Jeremy Zheng Li*.
- [51]. Janoski, & Luke, Thomas, David E. (2013). *Assembly*. 6-7.
- [52]. Arena, V. (2010). *Assembly*. 85-88.
- [53]. Messerschmidt Rainer, Van Der Knokke Henri, & Schaeffler Technologies AG & CO. Kg. (2012).
- [54]. Schaefer; James R, & The United States Of America As Represented The Secretary Of The Air Force. (1983).
- [55]. Ito Naoko, Tsutsui Hideyuki, & Ntn Toyo Bearing CO., Ltd. (2011).
- [56]. Wang Qiao, Hu Bing, Liu Shengyu, Shi Jianguo, Liu Qing, LI Nongzhang, & Hunan Guanghui Bearing Manufacture CO., Ltd. (2011).
- [57]. Houpert, L., & Chevalier, F. (2012). Rolling bearing stress based life--Part I: Calculation model.(Author abstract)(Report). *Journal of Tribology*, 134(2), 02113/1-02113/13.
- [58]. VXB Bearings Online Store The Ball Bearing Supplier & Distributor. (n.d.). Retrieved from <http://www.vxb.com/>.

- [59]. Marek Kryne, Jacek Selejdak, & Stanislaw Borkowski. (2012). THE QUALITY OF MATERIALS APPLIED FOR SLEWING BEARING RACEWAY – TECHNICAL PAPER. *Materiálové Inžinierstvo*, 19(4), 157-163.
- [60]. Houpert, L., & Chevalier, F. (2012). Rolling bearing stress based life--Part I: Calculation model.(Author abstract)(Report). *Journal of Tribology*, 134(2), 02113/1-02113/13.
- [61]. Bearing. (n.d.). Retrieved November 06, 2017, from <http://www.skf.com/au>.
- [62]. American Society of Mechanical Engineers. (1919). *Mechanical Engineering*.
- [63]. Blagin, E., Dovgyallo, A., & Uglanov, D. (2017). Mechanical Engineering. *MATEC Web of Conferences*, 108, MATEC Web of Conferences, Vol.108.
- [64]. Jelaska, D. (2012). *Gears and gear drives*. Oxford: Wiley-Blackwell.
- [65]. Du Zibin, & Erzhong Group Heavy Equipment CO., Ltd. (2009).
- [66]. Conyngham, M. (1999). Metallurgical aspects to be considered in gear and shaft design. *Gear Technology (USA)*, 16(2), 49-55.
- [67]. Shigley, J. E. (2006). *Standard handbook of machine design*. Norwich, NY: Knovel.
- [68]. Worm Gear Design: Gear Parameter and Description Worm Gear Design: Gear Param... (n.d.). Retrieved from <https://plus.google.com/+UjangHermanuloh79/posts/5p57V69xcqN>.
- [69]. Mott, R. L., Vavrek, E. M., & Wang, J. (2018). *Machine elements in mechanical design*. NY, NY: Pearson.
- [70]. Shigley, J. E. (2006). *Standard handbook of machine design*. Norwich, NY: Knovel.
- [71]. Marks, L. S., Sadegh, A. M., Avallone, E. A., & Baumeister, T. (2007). *Marks standard handbook for mechanical engineers*. New York etc.: McGraw-Hill Professional Publishing.
- [72]. How to Properly Pin a Shaft and Hub Assembly. (2014, July 11). Retrieved from <http://www.designworldonline.com/properly-pin-shaft-hub-assembly>.
- [73]. Milani, A., & Shanian, S. (2006). Gear material selection with uncertain and incomplete data. Material performance indices and decision aid model. *International Journal of Mechanics and Materials in Design*, 3(3), 209-222.
- [74]. Chao Huiyan, Luo Dacheng, & Ningbo Polaris Technology CO., Ltd. (2009).
- [75]. Yu, W., Mechefske, C., & Timusk, K. (2017). Effects of tooth plastic inclination deformation due to spatial cracks on the dynamic features of a gear system. *Nonlinear Dynamics*, 87(4), 2643-2659.
- [76]. Shigley, J. E. (2006). *Standard handbook of machine design*. Norwich, NY: Knovel.

- [77]. Retrieved from <http://nptel.ac.in/courses/Webcourse-contents/IIT-Delhi/Kinematics%20of%20Machine/site/gear/gear03.htm>.
- [78]. Involute Gear Profile | KHK Gears. (n.d.). Retrieved from http://khkgears.net/new/gear_knowledge/gear_technical_reference/involute_gear_profile.html.
- [79]. KHK Gears. (n.d.). Retrieved from <http://khkgears.net/gear-knowledge/gear-technical-reference/tooth-thickness/>.
- [80]. Majumdar, Budhaditya, Baer, David, Chakraborty, Sudipta, Esselle, Karu P, Heimlich, Michael, & Macquarie University. Department of Engineering. (2016). Advantages and limitations of 3D printing a dual-ridged horn antenna.
- [81]. Weng, Wang, Senthil, & Wu. (2016). Mechanical and thermal properties of ABS/montmorillonite nanocomposites for fused deposition modeling 3D printing. *Materials & Design*, 102, 276-283.
- [82]. Tooth Thickness. (n.d.). Retrieved November 06, 2017, from <http://khkgears.net/gear-knowledge/gear-technical-reference/tooth-thickness>.
- [83]. Gear Types and Characteristics | KHK Gears. (n.d.). Retrieved from <http://khkgears.net/gear-knowledge/abcs-gears-b/gear-types-characteristics>.
- [84]. Harrison Robert M, Ahmed Mansoor, Cai Zhijun, & Motorola, Inc. (2008).
- [85]. Bon-Ju Gu, Wang-Hoon Lee, Kazuaki Sawada, Makoto Ishida, Wireless smart sensor with small spiral antenna on Si-substrate, In *Microelectronics Journal*, Volume 42, Issue 9, 2011, Pages 1066-1073, ISSN 0026-2692, <https://doi.org/10.1016/j.mejo.2011.06.009>.
- [86]. Barrett, S., & Synthesis Collection Three. (2010). *Arduino microcontroller processing for everyone! Part II / Steven F. Barrett*. (Synthesis digital library of engineering and computer science). San Rafael, Calif. (1537 Fourth Street, San Rafael, CA 94901 USA): Morgan & Claypool.
- [87]. Wei Zhiling, GAO Xiaoping, & Kunshan Powerstencil CO.,Ltd. (2012).
- [88]. Jury, E. (1965). A modified stability table for linear discrete systems. *Proceedings of the IEEE*, 53(2), 184-185.
- [89]. ABS Plastic. (n.d.). Retrieved from https://www.teststandard.com/data_sheets/ABS_Data_sheet.pdf.
- [90]. Acetal. (n.d.). Retrieved from http://www.wshampshire.com/pdf/acetal_grades.pdf.

- [91]. Arduino. (2017, August 28). Retrieved from <https://arduino.isonprime.com/2017/08/28/control-the-stepper-motor-with-bluetooth-7-steps-with-pictures/>.
- [92]. Pololu - Sanyo Pancake Stepper Motor: Bipolar, 200 Steps/Rev, 50×11mm, 4.5V, 1 A/Phase. (n.d.). Retrieved from <https://www.pololu.com/product/2297>.
- [93]. Carboon Steel Material. (n.d.). Retrieved from <http://www.atlassteels.com.au/documents/Atlas1045.pdf>.
- [94]. Gear Finder. (n.d.). Retrieved from <https://quickgear.bizland.com/id23.html>.
- [95]. Loctite. (n.d.). Retrieved from http://www.loctite.tw/twc/content_data/327273_UPGRADE680EN.pdf.
- [96]. Tab Standards. (n.d.). Retrieved from <https://littlemachineshop.com/reference/TapDrillSizes.pdf>.
- [97]. Circlips Australia. (n.d.). Retrieved from <http://www.circlips.com.au/contentblank.php?sec=products&sec2=circlips&sec3=d1400>
- [98]. Retrieved from <https://www.curbellplastics.com/Research-Solutions/Technical-Resources/Technical-Resources/TECAMID-66-GF15-FRT-Black-Nylon-Data-Sheet>.